Oligosaccharide-Mediated Targeting of Dendritic Cells and the Development of Carbohydrate Microarrays

by

Eddie William Adams

B.S., Biotechnology (1995)
Rochester Institute of Technology

Submitted to the Department of Chemistry in partial fulfillment of the requirements for the degree of

Doctor of Philosophy

at the
Massachusetts Institute of Technology
February, 2005

Signature of Author Signature Redacted

Department of Chemistry
January 17, 2005

Certified By Signature Redacted

Peter H. Seeberger
Visiting Professor of Chemistry, MIT
Professor of Chemistry, ETH Zurich, CH
Thesis Supervisor

Accepted By Signature Redacted

Robert W. Field
Professor of Chemistry
Chairman, Departmental Committee on Graduate Students

This doctoral thesis has been examined by a committee of the Department of Chemistry as follows:

Signature Redacted

Professor Daniel S. Kemp_____
Chair

Signature Redacted

Professor Peter H. Seeberger_____
Thesis Supervisor

Signature Redacted

Professor Nir Hacohen_____
Thesis Co-Supervisor

Signature Redacted

Professor Jianzhu Chen_____
Department of Biology

Oligosaccharide-Mediated Targeting of Dendritic Cells and the Development of Carbohydrate Microarrays

by

Eddie William Adams

B.S., Biotechnology (1995)
Rochester Institute of Technology

Submitted to the Department of Chemistry on December in Partial Fulfillment of the Requirements for the Degree of Doctor of Philosophy

ABSTRACT

Bone-marrowed derived dendritic cells (DCs) constitute a critical arm of the immune system capable of polarizing the immune response toward active immunity or tolerance. Successful therapeutic modulation of DC function *in vivo* should create opportunities for more potent, efficacious vaccines and, in setting of autoimmunity, strategies aimed at the limiting the numbers and character of autoreactive T cells.

This thesis describes work aimed at accessing DCs *in vivo* by way of cell-surface carbohydrate binding proteins expressed by these cells. Synthetic oligosaccharides bearing a tri(ethylene glycol) linker with a reactive thiol handle were chemically coupled to model antigens to generate oligosaccharide-antigen conjugates. These conjugates were evaluated for their ability to specifically target DCs *in vitro*. Those oligosaccharide moieties that led to enhanced presentation of model antigen to antigen-specific T cells were evaluated for their ability to access DCs *in vivo* upon subcutaneous immunization and the immunological outcome of DC targeting was studied in detail.

The development of carbohydrate microarrays as tools for the identification of the carbohydrate specificities of carbohydrate-binding proteins (lectins and antibodies) is also described here. High density carbohydrate arrays were generated with synthetic saccharides bearing the aforementioned thiol linker. These arrays were used to study the glycan-dependent interactions of two gp120-binding proteins of immunological consequence, the dendritic cell lectin DC-SIGN and the broadly neutralizing antibody, 2G12, as well as two inhibitors of HIV infection isolated from cyanobacteria, cyanovirin-*N* and scytovirin. The structural diversity of immobilized carbohydrates represented on these arrays enabled the unambiguous characterization of the structural determinants required for gp120 recognition by each of these proteins.

Thesis Supervisor: Peter H. Seeberger
Title: Visiting Professor of Chemistry, MIT
Professor of Chemistry, ETH, Zurich, CH

Thesis Co-Supervisor: Nir Hacohen
Title: Assistant Professor of Medicine,
Harvard Medical School

I know of no more encouraging fact than the unquestionable ability of Man to elevate his life by a conscious endeavor.

Henry David Thoreau

Acknowledgements

This thesis marks the end of a short (but intense) and oddly circuitous journey that began with the seemingly simple desire to do research of my own design. Along the way I have been fortunate to find aid, humor, and inspiration in a number of people who deserve acknowledgement here. I apologize in advance to those whom I neglect to mention.

I would like to thank Peter Seeberger for giving me the opportunity to take molecules made in his lab and apply them to problems in immunology. His motivation to see ideas translated quickly into physical reality pushed Dan Ratner and I to develop several carbohydrate microarray systems in the early days of my thesis research. In addition, Peter exhibited great patience when it became apparent that bridging chemistry and immunology was easier said than done. In all, he has been a generous thesis advisor whose hands-off style of management was a perfect match to my stubborn *leave-me-alone-or-I'll-circulate-that-picture-of-you-riding-an-elephant-in-the-hills-of-India-when-you-were-supposed-to-be-attending-a-conference* style of research.

A significant portion of my thesis research was conducted with the guidance of Dr. Nir Hacohen. Among the instances of my life characterized by luck, meeting Nir ranks high. Nir is a true leader whose curiosity, scientific creativity and powerful intellect will lead his lab to continue accomplishing great things in immunology and genetics. He is extraordinarily generous, uncommonly kind and always good humored. It has been a true joy to work with him over the past two years.

I owe a huge debt of gratitude to Professor Daniel S. Kemp for both the time he spent with me in his capacity as a wonderfully gifted educator as well as for making his lab's resources available to me when this thesis required it. Professor Kemp is a truly inspiring figure and I shall always consider it an honor to have had the opportunity to learn from him.

Much of work contained in this thesis is the product of a very fruitful collaboration with my colleague and friend Dr. Daniel M. Ratner. Dan is a generous, talented individual and a great chemist. He possesses an energy for intellectual endeavor that bespeaks great things to come. I wish to thank him here for all of his research-related assistance, coffee-time, and hundreds of wonderful discussions on all manner of topics during our time together in the Seeberger/Kemp labs.

Thanks to my friend and colleague, Dr. Luís Moita, Portugal's finest immunologist, for many wonderful discussions in the realm of immunology and American political culture during our frequent morning coffee breaks as well as his technical guidance at various points throughout my apprenticeship in the wild world of DCs.

My deepest debt of gratitude is owed to the Adams and the Richey families. Thank you for your constant encouragement and our time together (though often hurried) through the past three years. In particular, I would like to thank my parents who, by never imposing limitations on my pursuits during my formative years, gave me a highly optimistic view of the world that said all things were possible through the determined application of one's will.

And, of course, my Bree: where do I even begin? I love you and thank you for making this journey with me.

This thesis is dedicated to

Bree Richey,

whose many sacrifices and unwavering support through the years made all of this possible.

List of Abbreviations

AIBN	Azobisisobutyronitrile
APC	Antigen Presenting Cell
ASGPR	Asialoglycoprotein Receptor
BSA	Bovine Serum Albumin
CFA	Complete Freund's Adjuvant
CFSE	5-(6)-Carboxyfluorescein Diacetate Succinimidyl Ester
ConA	Concanavalin A
CPM	Counts Per Minute
CRD	Carbohydrate Recognition Domain
CVN	Cyanovirin-N
DC	Dendritic Cell
DC-SIGN	Dendritic Cell Specific ICAM-Grabbing Non-Integrin
EDC	1-Ethyl-3-(3-Dimethylaminopropyl)-Carbodiimide
EDTA	Ethylenediaminetetraacetic acid
EGS	Ethylene-glycol-bis(succinimidylsuccinate
ELISA	Enzyme-Linked Immunosorbant Assay
FITC	Fluorescein Isothiocyanate
3-FL	3-Fucolactose
Flt3	FMS-like tyrosine kinase 3
Gal	Galactose
hr	hour
IFN	Interferon
IL	Interleukin
LPS	Lipopolysaccharide
Man	Mannose
mBSA	mannosylated bovine serum albumin
MHC	Major Histocompatibility Complex
min	Minute(s)
MMR	Macrophage Mannose Receptor

MW	Molecular Weight
NK	Natural Killer Cell
NKT	Natural Killer T Lymphocyte
OVA	Ovalbumin
PBS	Phosphate Buffered Saline
s	Second(s)
siRNA	short-interfering Ribonucleic Acid
SMCC	Succinimidyl-4-(N-maleimidomethyl)cyclohexane-1-carboxylate
TAP	Transporter of Antigenic Peptides
TCEP	Tris(2-Carboxyethyl) Phosphine Hydrochloride
TCR	T Cell Receptor
TLR	Toll-like Receptor
TNF	Tumor Necrosis Factor
Treg	Regulatory T lymphocyte
v	Volume

Table of Contents

Chapter 1

Introduction and Background

1.1 Scope of the Thesis

This thesis is comprised of two related bodies of work, which sought to find novel applications for synthetic carbohydrate structures generated in the Seeberger laboratory. The first area of investigation, the subject of Chapter 2, consisted of the development of carbohydrate microarrays for the identification of carbohydrate-binding proteins and the determination of carbohydrate structural features required for protein-carbohydrate interactions. The second application (Chapter 3) bridged the realm of carbohydrate chemistry with contemporary problems in immunotherapy, with an emphasis on autoimmunity. By taking advantage of the flexibility and precision offered by synthetic chemistry, novel carbohydrate-antigen conjugates were generated and employed to polarize the *in vivo* immune response in the direction of antigen-specific unresponsiveness, also known as immunological tolerance; the ability to induce this state of tailored antigen-specific immunological tolerance could have many therapeutic applications in allergy and autoimmunity.

To provide the appropriate contextual framework for these two areas of investigation, the following sections will (1) discuss carbohydrate-lectin interactions, (2) present carbohydrate microarrays as a screening tool, (3) introduce the biology of dendritic cells (DCs), drawing particular attention to their influence on T lymphocyte responses, (4) highlight the role of C-type lectins in immunology, focusing on DCs in particular and (5) outline a strategy for modulating T cell immune responses based on carbohydrate-mediated targeting of DCs *in vivo*.

1.2 Carbohydrate-Lectin Interactions

The field of glycobiology—that is, the investigation of the role of carbohydrates in biological processes—has witnessed an enormous growth in knowledge in the last fifteen years due to the successful application of genetic techniques[1]. Both the study of congenital disorders of glycosylation in humans[2] and the targeted knock-out of glycosylation-specific genes in mice[3] have revealed unanticipated and crucial roles for glycans in processes as diverse as cell-cell adhesion[4], cell motility,[5] immune regulation[6,7], and signal transduction[8], to name just a few. With an estimated 1% of both the human and mouse genomes dedicated to the production of enzymes involved in the addition, removal and modification of carbohydrate monomers, glycosylation has

emerged as one of the most common post-translational modifications of proteins and late-stage modifications of cellular lipids[1]. With the revolutionary application of small-interfering RNA interference (siRNA)[9] to "knock-down" the expression of genes of interest, it is likely that the roles of predicted glycosyltransferases and glycosidases in cellular physiology—both normal and pathological—will be quickly addressed.

One of the more intriguing concepts to emerge from these productive years of investigation is that glycans, in addition to their long-appreciated functions in forming protective, stabilizing, and organizational barriers, impart physiologically important molecular signatures to proteins and lipids[10,11]. These signatures, often temporally restricted, can influence a protein or lipid's spatial distribution within a cell, the extracellular matrix, or even within the whole organism, and modulate its biomolecular interactions (e.g., protein-protein interactions). For example, in activated T lymphocytes, the differential glycosylation of isoforms of CD45, a receptor-like protein tyrosine phosphatase, by sialylation and O-linked glycosylation leads to differing levels of receptor homodimerization and, in turn, negative regulation of CD45-mediated signaling[8].

As an evolutionary correlate to the diverse repertoire of expressed glycoforms, referred to collectively as an organism's glycome, mammalian genomes encode a large number (> 100) of biochemically diverse carbohydrate-binding proteins, or lectins, capable of recognizing these glycoforms[12]. Lectins are grouped into different classes according to amino acid sequence homology and evolutionary relatedness[13]. Some lectin classes share common carbohydrate monomer specificity, such as mannose-6-phosphate recognition by members of the P-type lectin class, while other class members are highly diverse in their carbohydrate recognition profile; these lectins are grouped solely on the basis of the observed lectin domain(s) in their primary sequence. A glimpse at a sample of some of the known or putative functions attributed to lectins (Figure 1.1) reveals that recognition of the molecular signatures imparted by various glycoforms contributes to numerous physiological processes.

Given this ability to recognize unique carbohydrate signatures and thereby mediate downstream processes, a full appreciation of a lectin's biological role(s) in a particular cell or tissue requires a detailed understanding of which glycans the lectin can recognize, and under which cellular conditions that glycan is present. Once the cognate oligosaccharide has been

Process	Lectin	Class	Natural Ligand
Protein sorting to prelysosomal compartments	Cation-independent Man-6-P receptor	P-type	phosphorylated high-mannose oligosaccharides
Leukocyte homing to tissues during inflammation	P-selectin	C-type	sialyl Lewis X in combination with tyrosine sulfate residues
Cell-cell interactions (between T cells & B cells)	Siglec-2	I-type	α2→6 linked sialic acid residues on unidentified glycoprotein
Induction of apoptotic responses	Galectin-1	S-type	poly-N-acetyl-lactosamine units on developing thymocytes

Figure 1.1 Representative examples of the biological roles fulfilled by mammalian lectins. Absolute verification of these roles has been obtained in many cases by genetic knockout of the lectin and/or the ligand in mice.

identified, various tools (e.g., glycosylation inhibitors, glycosylation-site mutants, siRNA) can be employed to modulate the expression of that glycoform and the downstream consequences of impaired glycan-lectin interactions can be studied. Identification of the cognate glycan, however, is a non-trivial undertaking.

1.3 Carbohydrate Microarrays for Screening Lectin-Carbohydrate Interactions

Historically, the identification of carbohydrate-binding proteins and their natural ligands has been a process marked by serendipity[14]. For instance, in laying the groundwork for a therapeutic treatment of patients with Inclusion Cell Disease, a condition in which there is a failure to sort hydrolytic enzymes to the lysosome due to the absence of a mannose-6-phosphate tag, animals received intravenous injections of mannose-6-phosphate modified lysosomal enzymes[15,16]. The rapid clearance of these enzymes from circulation prompted a series of investigations that uncovered the existence of a mannose-specific receptor in liver sinusoidal

macrophages. Recently, a technique-driven approach to ligand identification coupled genetics and proteomics in an effort to determine the possible physiological ligands of the mannose receptor by analyzing levels of serum glycoproteins in wild-type versus mannose receptor knockout mice[17]. These studies revealed increased levels of several mannose-bearing lysosomal enzymes and serum glycoproteins in the knockout mice compared to the wild-type. As some of these proteins are involved in inflammatory responses, the results suggested a model of glycoprotein clearance by the mannose receptor in which potentially harmful pro-inflammatory glycoproteins are cleared from circulation in order to promote the anti-inflammatory milieu required for tissue repair.

The powerful genetic approach to ligand identification employed by Nussenzweig and colleagues[17] allows one to identify lectin ligands *in vivo* under both steady-state conditions (i.e., in the absence of infection) or after the introduction of pro-inflammatory stimuli, such as a pathogen or bacterial endotoxin. What cannot be gleaned from such an approach, however, are the structural determinants required for ligand-receptor interactions.

A biochemical corollary to these genetic and proteomic approaches that facilitated the determination of key structural features required for lectin-carbohydrate interactions would enhance our understanding of processes mediated by such interactions, as well as aid in the design of inhibitors of these binding events (such as those so actively pursued for the selectins)[18,19], and help establish a catalog of physiologically important glycan signatures. Inspired by the success of DNA microarrays, a number of groups[20-23], including ours[24-27], have begun to explore the microarray platform, and derivatives thereof, as a means of accessing fine structural details of carbohydrate-protein interactions. Akin to DNA microarrays with their high density of immobilized cDNA, carbohydrate microarrays present immobilized saccharides that to be screened against any potential binding protein of interest[28]. Binding events are detected by colorimetric means or by fluorescence. The microarray format offers many advantages over conventional methods, such as microtiter (e.g., ELISA) based systems, for studying such interactions[29]. This includes the ability to screen several thousand binding events in parallel while requiring a minimal amount of analyte and ligand for study – making the most of precious synthetic or naturally procured materials.

Recent advances in the preparation of complex carbohydrates, such as improved synthetic methodologies[30], including the development of an automated solid-phase synthesizer[31], and

advances in *in vitro* enzymatic biosynthetic strategies,[32,33] are making it increasingly possible to obtain milligram quantities of pure, chemically defined oligosaccharides. Combining this synthetic skill with the microarray platform, with its capacity for presenting thousands of distinct molecules per array, allows one to screen any one carbohydrate-binding protein of interest against a diverse library of potential ligands. Such microarray screens not only reveal what carbohydrate is recognized by a particular protein, mannose vs. galactose, for example, but also provide information regarding the importance of geometries imparted by underlying glycosidic linkages and the role of secondary modifications, such as sulfation or amination.

Based on the number of predicted glycosyltransferases in the human and mouse genomes (300) and on the number of known glycans that have been sequenced from proteins and lipids, it is predicted that humans and mice contain approximately 500 distinct glycoforms[1,34]. Given these numbers, it is reasonable to expect that a dedicated, multi-laboratory, synthetic effort converging on a single immobilization chemistry could readily generate arrays representing the major glycoforms found in mammalian systems. A case in point, the Consortium for Functional Glycomics has pooled the resources of a number of laboratories to generate arrays featuring 200+ distinct carbohydrate structures[35].

With the increasing availability of such representative glycan arrays, the identification of lectin ligands will surely accelerate. Indeed, with the combination of genetics, glycan sequencing via mass-spectrometry, and carbohydrate microarrays, the necessary tools are being assembled that will permit elucidation of the functional aspects of the mammalian glycome.

1.4 Dendritic Cells: A Master Switch on the Path to Immunity or Tolerance

While B and T lymphocytes comprise the responding arms of adaptive immunity, providing rapid and highly specific responses to invading pathogens, their ability to respond as well as the nature and timing of their responses are tightly regulated by dendritic cells (DCs)[36]. DCs are bone-marrow derived antigen-presenting cells (APCs) that possess several specialized properties which make them uniquely suited to bridge the innate and adaptive immune systems. Since their identification over 30 years ago[37-39], DCs' ability to stimulate strong T cell immune responses to pathogens and tumors has been studied extensively *in vitro* and *in vivo*. This line of investigation has illuminated how inflammation is initiated at the cellular and molecular levels.

In recent years, however, several *in vivo* studies have made a convincing case that DCs can also carry out the seemingly opposite role of inhibiting effector T cell responses[40]. This latter role, attributed to DCs in the steady state, is thought to be instrumental in regulating the numbers and behavior of autoreactive peripheral (extrathymic) T cells that, if left unchecked, could mount aggressive immune responses against our own tissues. For purposes of clarity, each of these aspects of DC function will be discussed separately below after a brief introduction to DC biology.

1.4.1 Basics of DC Biology

DCs control adaptive immunity by virtue of their ability to capture, process and present antigens to a diverse $CD8^+$ and $CD4^+$ T cell repertoire in the context of class I and class II major histocompatibility complexes (MHC), respectively. Due to their high surface expression levels of MHC-peptide complexes (10-100 times greater than B cells)[41], T cell co-stimulatory molecules,[42] and strong cytokine production,[43]DCs are typically two orders of magnitude more effective as APCs than either macrophages or B cells (the other main APCs of the immune system).[44,45]Furthermore, while macrophages appear to be able to activate memory T cells, DCs alone are unique in their capacity to stimulate the proliferation of naive antigen-specific T cells, thus initiating primary immune responses.

In addition to capacity to stimulate T cells, the *in vivo* distribution of DCs allows them to fulfill a key sentinel function by trafficking between the peripheral tissues of the body and the lymphoid organs where naive T cells are resident until activated in an antigen-specific fashion[46]. DCs are located in almost all of our tissues where, as noted below, they capture and process tissue associated antigens as well as antigens from any invading pathogens. Either as a function of routine turnover or when prompted by infection, DCs will migrate to the local draining lymph nodes and present their antigenic payload to the pool of potential responder cells[47]. As will be discussed below, the phenotypic state of the DCs migrating from peripheral tissues greatly shapes the nature of the ensuing T cell response.

1.4.1.1 Immature DCs: Acquisition of Antigen

Although it is a simplification, it is convenient to speak of the DC lifespan as having three distinct phases: immaturity, maturity, and death. The first phase, the 'immature' stage is characterized by DCs' capacity to actively sample their environment and capture antigens—in the form of soluble proteins and lipids, apoptotic and necrotic cells, and whole pathogens—by way of specialized cell-surface receptors, phagocytosis, and a process known as macropinocytosis, in which large membrane extensions sample the extracellular fluid of the tissues in which DCs are resident[48,49]. Captured antigen enters the endocytic pathway of the cell, is degraded into defined antigenic peptides and delivered to MHC class II-rich compartments to form MHC-peptide complexes. After formation, these complexes are delivered to the cell surface for presentation to T cell antigen receptors (TCRs)[50,51]. In addition to their ability to capture and present antigenic peptides in the context of MHC class II molecules, a subset of DCs, the $CD8\alpha^+$ DC, is unique in its ability to present exogenous antigen in the context of MHC class I molecules to $CD8^+$ T cells[52,53]. This is highly significant in that it allows one cell type to access both the $CD4^+$ and $CD8^+$ arms of the T cell response. In addition to these antigen-handling properties, it is also important to note that immature DCs express low levels of T cell co-stimulatory molecules, such as CD40, and CD86, and low levels adhesive molecules, such as CD54, that promote the formation of DC-T cell interactions.

1.4.1.2 Mature DCs: Becoming 'Nature's Adjuvant'

Once an immature DC has acquired antigen it can either remain in the immature state, in which case it remains a poor stimulator of T cell activation, or it can undergo a profound series of genetic and phenotypic changes—broadly referred to as 'maturation'—that give it the aforementioned capacity to drive the clonal expansion of antigen-specific $CD8^+$ and $CD4^+$ T cells (Figure 1.2)[54]. Phenotypically, maturation is characterized by high surface MHC II expression, a loss of endocytotic activity, strong adhesion (CD54, CD58) and T cell co-stimulatory molecule expression (CD80, CD86, CD40), chemokine and cytokine production. These molecular

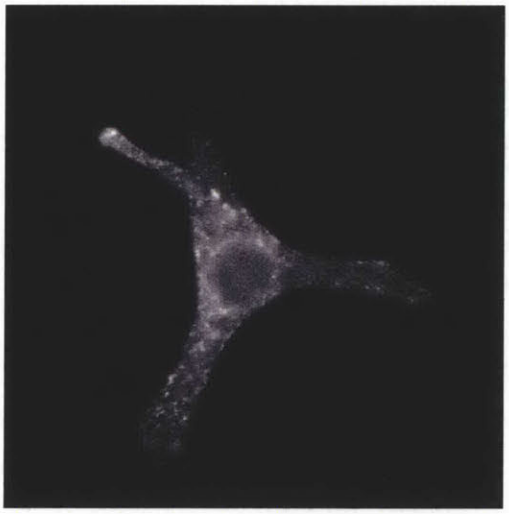

Immature DCs:
High Intracellular MHC II
Endocytosis via Fc receptors, lectins, and scavenger receptors
Low Adhesion Receptor Expression (CD54, 58)
Low T-cell co-stimulatory Molecules (CD80/86)
Low CD40 & IL-12 expression

Mature DCs:
High Surface MHC II
Low Endocytotic Activity
High CD54, CD58, CD80, CD86
High CD40 & IL-12 expression

Figure 1.2 Maturation of dendritic cells involves programmatic changes from a poor T cell stimulator with proficient antigen capture/processing capabilities to a potent T cell stimulator. Pathogen derived molecules like lipopolysaccharide (LPS), and inflammatory cytokines such as TNFα are examples of stimuli that will promote DC maturation.

changes allow DCs to attract T and B cells, form signaling complexes with the T cells and ultimately polarize the direction of the effector T cell response (i.e., T_H1 vs. T_H2)[55].

The molecular triggers for DC maturation are now understood in detail and occur as a result of signal transduction initiated by two major receptor families: the toll-like receptors (TLRs)[56,57] and the tumor necrosis factor (TNF)-receptors, particularly CD40L[43]. The TLRs are a family of germline encoded receptors that serve as sensors for molecular motifs associated with a broad spectrum of pathogens but not common to endogenous self-antigens. Detection of pathogen components by TLRs triggers a complex signaling cascade that ultimately results in activation of the NF-κB family of transcriptional control proteins (Rel A/p65, Rel B, Rel C, p50, p52), which regulate the expression of many genes encoding immune and inflammatory proteins. Thus, TLRs provide DCs (and other cell types—immune and non-immune) both a means for sensing pathogen invasion and for the direct activation of pro-inflammatory pathways required to promote the neutralization and clearance of the invading pathogen.

1.4.2 Immunogenic DCs: Turning on T cells

Maturation of DCs via TLR signaling, inflammatory cytokines such as TNFα or CD40 ligation prompts DCs to coordinate a range of protective functions via the cells of the innate and adaptive immune system. Microbial stimulation of DCs elicits production of the pro-inflammatory cytokines interleukin-12 (IL-12)[58] and interferon-α (IFN-α)[59,60]. Exposure to inflammatory cytokines at the site of infection leads to DC activation of natural killer (NK)[61,62] and natural killer T cells (NKT)[63]. Upon arrival in the draining lymph nodes, mature DCs presenting MHC class I-peptide complexes can stimulate the expansion and cytolytic activity of $CD8^+$ T cells to promote the killing of virally-infected cells and tumors[64-66]. Interactions between matured DCs and $CD4^+$ T cells can have two well-characterized outcomes. In the first case, strong IL-12 production by DCs will turn undifferentiated T_H0 helper cells into interferon-γ (IFN-γ)-producing T_H1 cells[67]. Secreted IFN-γ serves to activate the antimicrobial activities of macrophages and, together with IL-12, promotes the differentiation of T cells into killer cells. This form of T cell and macrophage activation is particularly efficient at eliminating intracellular pathogens and tumors by direct cytotoxic activity and is referred to as cell-mediated immunity. The second possible outcome of interactions between antigen-bearing mature DCs and T_H0 helper cells results when DCs produce interleukin-4 (IL-4) and thereby drive T_H0 differentiation to the interleukin-5 (IL-5), IL-4-producing T_H2 phenotype. This cytokine profile in turn activates eosinophils (IL-5) and antibody production by B cells (IL-4). The B cell promoted arm of immunity driven by this T_H2 polarization is referred to as humoral immunity.

1.4.3 Tolerogenic DCs: Keeping T Cells At Bay

Due to DCs' ability to induce strong, polarized, and lasting T cell responses *in vivo*, it was long believed that the principal function of DCs was to initiate T cell-mediated immunity. The experimental groundwork that helped to establish this paradigm largely involved *in vitro* manipulations of DCs or the introduction of some maturation factor, such as anti-CD40 antibody, that consistently induced DC maturation[55,68]. While valuable, this body of work did not address the immunological outcome of antigen capture, processing and presentation by

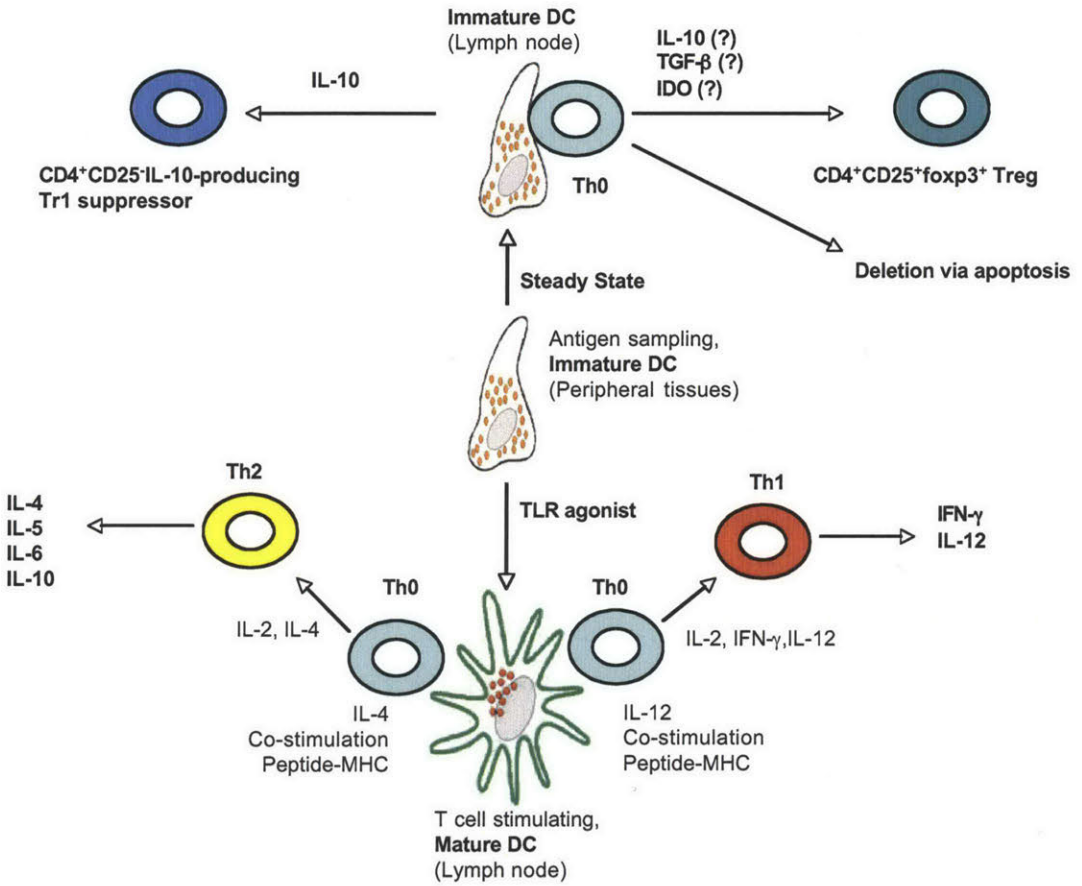

Figure 1.3 Dendritic cells reside at the center of many possible outcomes in the adaptive immune response. Steady state DCs sampling antigen are triggered by a TLR agonist (e.g., bacterial LPS), migrate to local draining lymph nodes and undergo phenotypic maturation (bottom). Depending on the nature of the agonist, DCs can polarize the T cell response along the T_H1 or T_H2 path, leading to antigen-specific cell-mediated or humoral immunity, respectively. *In vivo* evidence now suggests that if steady state accumulation of antigen is not accompanied by stimulation via TLR/TNF receptor engagement, DCs will inhibit T cell responses by prompting apoptosis in the antigen-responsive T cell; inducing formation of antigen-specific, $CD4^+CD25^+foxp3^+$ T regulatory cell, or IL-10 secreting Tr1 regulatory cells (top). These regulatory cells, in turn, are capable of mediating the active suppression of potentially deleterious T cell responses. The routine generation of these suppressor T cells by steady state DCs is thought to be instrumental in promoting peripheral tolerance to endogenous (self) antigens.

DCs in the absence of infection or pro-maturation stimuli (referred to here as 'steady state conditions'). In recent years this has changed, with a model emerging that posits steady state DCs at the center of a cellular circuit whose function is to maintain peripheral tolerance by limiting the number, character and activities of self-reactive peripheral T cells (Figure 1.3)[69-71]. These steady state DCs, with their tolerance-promoting abilities, are termed tolerogenic DCs.

The model of DC promoted peripheral T cell tolerance suggests that steady state DCs constitutively sample the tissue environments through which they traffic, picking up self-antigens (e.g., from apoptotic cells) and harmless environmental antigens (such as proteins from the food we eat). These captured antigens are subsequently processed and presented in the context of MHC class I and class II molecules to peripheral T cells in the lymph nodes. Upon encountering a self-reactive T cell capable of responding to any of these presented antigens, DCs can either induce a state of anergy (non-permanent unresponsiveness) in the responding T cell, direct the self-reactive T cell to undergo apoptosis or, in the case of $CD4^+$ T cells, promote T_H0 differentiation into immunosuppressive T regulatory cells. It should be noted that while DC promoted anergy is possible, the latter two results (apoptosis and Treg formation) appear to be more common[72,73].

1.4.3.1 Therapeutic Manipulation of Tolerogenic DCs

As the therapeutic potential of tolerogenic DCs for treatment of allergy, autoimmunity and transplantation is clear, the detailed molecular mechanisms underlying the various outcomes at the self-reactive T cell-DC interface have quickly become an active area of investigation. If the default for steady state DCs is to promote peripheral tolerance to self-antigens, a successful therapy for allergy, for example, might consist of delivering the protein allergen *in vivo* to DCs in the absence of pro-maturation stimuli. In this way, any T cells that recognize the allergen-derived peptides presented on steady state DCs would be inhibited from becoming polarized effectors by the aforementioned mechanisms. However, it will be necessary to address how one can access steady state DCs in order to pursue such therapeutics.

While a sizeable body of literature exists demonstrating the induction of peripheral tolerance to peptide antigens in mice, the quantity of peptide required to achieve tolerance is often large (routinely 300 – 800 μg/injection), and it is not certain that the ensuing state of T cell unresponsiveness is true tolerance or impermanent anergy[74-77].

An ideal therapeutic regimen would permit the administration of sub-nanogram to nanogram quantities of antigen in a fashion that selectively accessed steady state DCs. Such efficient targeting of DCs would not only allow one to utilize whole protein antigen, such that all possible antigenic peptide sequences were represented, but would have the more desirable

outcomes of promoting autoreactive T cell deletion or Treg formation. This requires the ability to target a DC-specific, endocytotically-active, receptor that can access the antigen processing and presentation machinery of DCs. (Targeting would be accomplished by way of receptor ligand-antigen conjugates). Ideally, such a receptor should be DC subset specific, so that one may access characteristics unique to that subset, have high surface expression, and should not induce DC maturation upon ligand binding. The molecular characterization of DCs in recent years has uncovered a class of surface receptors, the C-type lectins that appear to be promising candidates for the selective targeting of DCs *in vivo*[78].

1.4.3.2 C-type Lectins As Targets for *In Vivo* DC-based Therapeutics

C-type lectins represent a diverse family of calcium-dependent carbohydrate binding proteins that share primary homology in the their carbohydrate-recognition domains (CRD)[79,80]. In addition to a highly conserved disulfide-bonding pattern these CRDs are marked by 14 invariant and 18 highly conserved amino acid residues found in the 115-130 amino acid segment that constitute the CRD. In humans, more than 60 different proteins have been identified that possess a C-type lectin CRD[81]. C-type lectins can be divided between cell-associated (membrane bound) or soluble forms, and the cell-associated class can be further subdivided according to their orientation in the plasma membrane. Type I membrane lectins are oriented in the membrane such that their N termini reside in the extracellular space while type II membrane lectins are situated with their N termini in the cytoplasm of the cell. As indicated in Table 1.4, DCs express both type I and II C-type lectins.

Lectins' well-documented capacity for internalizing antigens via receptor-mediated endocytosis makes them attractive as targets for antigen delivery. Once antigen is internalized by these receptors it is delivered it to the antigen processing/presentation machinery of DCs. Examination of the cytoplasmic domains of these lectins reveals that many contain well-established internalization motifs, such as tyrosine-based coated pit localization sequences and triacidic clusters[82]. These sequences target the internalized receptor to clathrin coated pits and late endosomes, events that are important for efficient loading of antigenic peptides onto MHC molecules.

C-type lectin	Type	Amino Acids	Production	Ligand	Function
MMR (CD206)	I	1456	DCs, LCs, Mo, Mϕ, DMECs, moDC	Mannose, fucose, HIV gp120	Ag uptake
DEC-205 (CD205)	I	1722	DCs, LCs, actDCs thymic EC	?	Ag uptake
Dectin 1	II	247	DCs, LCs	β-Glucan	T-cell interaction
Dectin 2	II	209	DCs, LCs	?	Ag uptake
Langerin (CD207)	II	328	LCs	high-mannose oligosaccharides	Birbeck granule formation Ag uptake
DC-SIGN (CD209)	II	404	mucosal DCs, moDC	HIV gp120, Lewis-x, ICAM-3 high-mannose olig	T-cell interaction, pathology, migration, Ag uptake
BDCA-2	II	213	Plasmacytoid DCs	?	Ag uptake?
DCIR	II	237	DCs, Mo, Mϕ, PMN, B cells	?	?
DLEC	II	213	moDCs	?	?
ASGPR	II	291	DCs, hepatocytes	Galactose	Glycoprotein clearance Ag uptake

Abbreviations: actDCs, activated dendritic cells; DMECs, dermal microvascular endothelial cells; Mo, monocytes; Mϕ, macrophages; moDC, monocyte-derived DCs; PMN, polymorphic nuclear cells; thymic Ecs, thymic endothelial cells; LC, Langerhans cells

Table 1.4 C-type lectin expression by DCs and other cells of the immune system. Targeting these lectins with carbohydrate-antigen conjugates may offer a novel means of accessing the antigen handling and T cell modulating properties of DCs.

Two other features make DC C-type lectins attractive antigen-delivery targets. First, the expression patterns of some lectins appear to be restricted to certain DC subsets. For example, Langerin (CD207) is expressed solely in Langerhans cells (skin DCs)[83], the asialoglycoprotein receptor and DC-SIGN (CD209) are expressed in monocyte-derived DCs[84,85], and the lectin BDCA-2 in plasmacytoid DCs[86]. Targeting these lectins with ligand-antigen conjugates may allow one to modulate T cell behavior by accessing certain immunological properties unique to these subsets. Secondly, recent reports indicate that engagement of DC lectins by ligands or antibodies (employed as surrogate ligands) can promote an immunosuppressive DC phenotype. For example, cross-linking of the mannose receptor (CD206) on monocyte-derived DCs induced the production of the anti-inflammatory cytokines interleukin-10 (IL-10), and interleukin-1 receptor (IL-1R) agonist and inhibited production of pro-inflammatory IL-12[87]. Similarly, mannosylated lipoarabinomannan from *Mycobacterium tuberculosis* is capable of eliciting IL-10 production via DC-SIGN engagement on monocyte-derived DCs[88]. While these studies were all conducted *in vitro* and have yet to be verified in a more physiological setting, they highlight the

possibility that DC lectin engagement *in vivo* may be able to convert an immature, steady state DC into an actively immunosuppressive phenotype. This is of obvious interest as an immunosuppressive DC may lead to more efficient and lasting T cell tolerance.

Finally, and most convincingly, what makes DC lectins physiologically relevant targets for T cell tolerance induction is described in a series of investigations utilizing antibody-mediated targeting of the lectin DEC-205 (CD205)[72,73,89].Steinman and colleagues have demonstrated that anti-DEC-205 monoclonal antibody-antigen conjugates (peptide or whole protein) can be targeted specifically to $CD11c^+CD8\alpha^+$ DCs *in vivo*. DEC-205 mediated endocytosis of antibody-antigen conjugates delivers the antigen to late endosomal compartments where they are proteolyzed and loaded onto MHC class II molecules. In addition, DEC-205 also appears capable of accessing transporter of antigenic peptides (TAP) transporters to achieve cross-presentation of peptides to MHC class I restricted $CD8^+$ T cells[89].

As DEC-205 ligation by the monoclonal antibody does not lead to upregulation of DC co-stimulatory molecules, antigens are presented to T cells in the absence of co-stimulation. This lack of DC promoted co-stimulation has dramatic immunological consequences. First, T cells activated by antigen presented on antibody targeted cells produce only IL-2 but not IFN-γ, IL-4 or IL-10 and thus appear not to be polarized toward T_H1 or T_H2 phenotype. Second, after an initial expansion of the self-reactive T cell population, the expanded population shrinks via apoptosis and surviving members of the population are completely anergic to re-challenge with antigen. Importantly, co-injection of anti-DEC-205-antigen conjugate with anti-CD40 antibody completely blocks tolerance induction, resulting in active immunity to administered antigen. Thus, targeting DCs *in vivo* can have two potential outcomes, tolerance or immunity, depending on whether the appropriate maturation factors are delivered to DCs concomitantly with the targeted antigen.

A third study employing the same targeting strategy has revealed that at least a portion of these surviving T cells are $CD25^+$/CTLA-4^+ regulatory T cells capable of suppressing proliferation and IL-2 production by effector $CD4^+$ T cells[73]. This study also demonstrated the efficacy of the DEC-205 targeting strategy in preventing immune reactions in two animal disease models, a $CD4^+$ T cell mediated hypersensitivity reaction to ovalbumin (via adoptive transfer of DO11.10 cells to Balb/c mice) and $CD8^+$ T cell mediated allergic reactions.

1.4.3.3 Carbohydrate-Mediated Targeting of DC Lectins

The work with DEC-205 targeting clearly illustrates the role of DCs in maintaining peripheral tolerance to non-infectious self and allows the hypothesis that immunotherapies for autoimmune diseases, allergy and transplant rejection based on the tolerogenic potential of DCs will prove to be clinically relevant. Furthermore, the demonstrated therapeutic potential of targeting this single endocytically-active receptor invites investigations into the immunological outcomes of targeting other receptors on DCs. Is there something intrinsically unique to DEC-205 that enables the generation of tolerogenic DCs via its targeting or is this a strategy that can be more broadly applied to any number of DC-specific surface receptors?

Chapter 3 of this thesis seeks to address these issues in the context of a lectin targeting strategy that makes use of synthetic oligosaccharides as an alternative to the antibody conjugates utilized in the DEC-205 work. Taking advantage of the thiol-linker chemistry developed during the course of our microarray work (Chapter 2), novel oligosaccharide-antigen conjugates have been generated through simple maleimide chemistry and evaluated for their ability to access DCs *in vivo* and thereby modulate T cell behavior. In these conjugates the appended oligosaccharides serve as a means by which DC surface lectins can be engaged in order to achieve antigen internalization. While only a small series of structures were evaluated during the course of this work, the results suggest that carbohydrates should continue to be evaluated as a class of molecules that can be used to modulate the immunological properties of DCs.

1.5 References

(1) Lowe, J. B.; Marth, J. D. *Annu Rev Biochem* **2003**, *72*, 643-691.
(2) Hirschberg, C. B. *J Clin Invest* **2001**, *108*, 3-6.
(3) Shi, S.; Williams, S. A.; Seppo, A.; Kurniawan, H.; Chen, W.; Ye, Z.; Marth, J. D.; Stanley, P. *Mol Cell Biol* **2004**, *24*, 9920-9929.
(4) Ye, Z.; Marth, J. D. *Glycobiology* **2004**, *14*, 547-558.
(5) Gualtieri, R.; Andreuccetti, P. *Cell Tissue Res* **1996**, *283*, 173-181.
(6) Demetriou, M.; Granovsky, M.; Quaggin, S.; Dennis, J. W. *Nature* **2001**, *409*, 733-739.
(7) Morgan, R.; Gao, G.; Pawling, J.; Dennis, J. W.; Demetriou, M.; Li, B. *J Immunol* **2004**, *173*, 7200-7208.
(8) Xu, Z.; Weiss, A. *Nat Immunol* **2002**, *3*, 764-771.
(9) Caplen, N. J.; Mousses, S. *Ann N Y Acad Sci* **2003**, *1002*, 56-62.
(10) Chay, C. H.; Pienta, K. J. *J Cell Biochem Suppl* **2000**, *Suppl 35*, 123-129.
(11) Villalobo, A.; Gabius, H. *Acta Anat (Basel)* **1998**, *161*, 110-129.
(12) Drickamer, K.; Taylor, M. E. *Annu Rev Cell Biol* **1993**, *9*, 237-264.
(13) Drickamer, K. *Curr Opin Struct Biol* **1995**, *5*, 612-616.
(14) Varki, A.; Cummings, R. D.; Esko, J.; Freeze, H.; Hart, G.; Marth, J. *Cold Spring Harb Laboratory Press* **1999**, Chapter 22.
(15) Kornfeld, S. *Faseb J* **1987**, *1*, 462-468.
(16) Kornfeld, S. *Biochem Soc Trans* **1990**, *18*, 367-374.
(17) Lee, S. J.; Evers, S.; Roeder, D.; Parlow, A. F.; Risteli, J.; Risteli, L.; Lee, Y. C.; Feizi, T.; Langen, H.; Nussenzweig, M. C. *Science* **2002**, *295*, 1898-1901.
(18) Auge, C.; Dagron, F.; Lemoine, R.; Le Narvor, C.; Lubineau, A. *Ann Pharm Fr* **1999**, *57*, 216-222.
(19) Bruehl, R. E.; Dasgupta, F.; Katsumoto, T. R.; Tan, J. H.; Bertozzi, C. R.; Spevak, W.; Ahn, D. J.; Rosen, S. D.; Nagy, J. O. *Biochemistry* **2001**, *40*, 5964-5974.
(20) Galustian, C.; Park, C. G.; Chai, W.; Kiso, M.; Bruening, S. A.; Kang, Y. S.; Steinman, R. M.; Feizi, T. *Int Immunol* **2004**, *16*, 853-866.
(21) Houseman, B. T.; Mrksich, M. *Chem Biol* **2002**, *9*, 443-454.
(22) Wang, D.; Liu, S.; Trummer, B. J.; Deng, C.; Wang, A. *Nat Biotechnol* **2002**, *20*, 275-281.
(23) Wong, C. H.; Bryan, M. C. *Methods Enzymol* **2003**, *362*, 218-225.
(24) Adams, E. W.; Ueberfeld, J.; Ratner, D. M.; O'Keefe, B. R.; Walt, D. R.; Seeberger, P. H. *Angew Chem Int Ed Engl* **2003**, *42*, 5317-5320.
(25) Ratner, D. M.; Adams, E. W.; Disney, M. D.; Seeberger, P. H. *Chembiochem* **2004**, *5*, 1375-1383.
(26) Adams, E. W.; Ratner, D. M.; Bokesch, H. R.; McMahon, J. B.; O'Keefe, B. R.; Seeberger, P. H. *Chem Biol* **2004**, *11*, 875-881.
(27) Ratner, D. M.; Adams, E. W.; Su, J.; O'Keefe, B. R.; Mrksich, M.; Seeberger, P. H. *Chembiochem* **2004**, *5*, 379-382.
(28) Love, K. R.; Seeberger, P. H. *Angew Chem Int Ed Engl* **2002**, *41*, 3583-3586, 3513.
(29) Drickamer, K.; Mamon, J. F.; Binns, G.; Leung, J. O. *J Biol Chem* **1984**, *259*, 770-778.
(30) Haase, W. C., Seeberger, P.H. *Chemical Reviews* **2000**, *100*, 4349-4394.
(31) Plante, O. J., Palmacci, E.R., Seeberger, P.H. *Science* **2001**, *291*, 1523-1527.

(32) Kuberan, B.; Lech, M. Z.; Beeler, D. L.; Wu, Z. L.; Rosenberg, R. D. *Nat Biotechnol* **2003**, *21*, 1343-1346.
(33) Lin, C. H.; Lin, C. C. *Adv Exp Med Biol* **2001**, *491*, 215-230.
(34) Drickamer, K.; Taylor, M. E. *Genome Biol* **2002**, *3*, REVIEWS1034.
(35) Blixt, O.; Head, S.; Mondala, T.; Scanlan, C.; Huflejt, M. E.; Alvarez, R.; Bryan, M. C.; Fazio, F.; Calarese, D.; Stevens, J.; Razi, N.; Stevens, D. J.; Skehel, J. J.; van Die, I.; Burton, D. R.; Wilson, I. A.; Cummings, R.; Bovin, N.; Wong, C. H.; Paulson, J. C. *Proc Natl Acad Sci U S A* **2004**, *101*, 17033-17038.
(36) Steinman, R. M. *Annu Rev Immunol* **1991**, *9*, 271-296.
(37) Steinman, R. M.; Cohn, Z. A. *J Exp Med* **1973**, *137*, 1142-1162.
(38) Steinman, R. M.; Lustig, D. S.; Cohn, Z. A. *J Exp Med* **1974**, *139*, 1431-1445.
(39) Steinman, R. M.; Cohn, Z. A. *J Exp Med* **1974**, *139*, 380-397.
(40) Steinman, R. M., Nussenzweig, M.C. *Proc Natl Acad Sci U S A* **2002**, *99*, 351-358.
(41) Inaba, K.; Pack, M.; Inaba, M.; Sakuta, H.; Isdell, F.; Steinman, R. M. *J Exp Med* **1997**, *186*, 665-672.
(42) Caux, C.; Vanbervliet, B.; Massacrier, C.; Azuma, M.; Okumura, K.; Lanier, L. L.; Banchereau, J. *J Exp Med* **1994**, *180*, 1841-1847.
(43) Cella, M.; Scheidegger, D.; Palmer-Lehmann, K.; Lane, P.; Lanzavecchia, A.; Alber, G. *J Exp Med* **1996**, *184*, 747-752.
(44) Steinman, R. M.; Gutchinov, B.; Witmer, M. D.; Nussenzweig, M. C. *J Exp Med* **1983**, *157*, 613-627.
(45) Inaba, K.; Steinman, R. M.; Van Voorhis, W. C.; Muramatsu, S. *Proc Natl Acad Sci U S A* **1983**, *80*, 6041-6045.
(46) Randolph, G. J. *Semin Immunol* **2001**, *13*, 267-274.
(47) Itano, A. A.; McSorley, S. J.; Reinhardt, R. L.; Ehst, B. D.; Ingulli, E.; Rudensky, A. Y.; Jenkins, M. K. *Immunity* **2003**, *19*, 47-57.
(48) Sallusto, F.; Cella, M.; Danieli, C.; Lanzavecchia, A. *J Exp Med* **1995**, *182*, 389-400.
(49) Watts, C.; Powis, S. *Rev Immunogenet* **1999**, *1*, 60-74.
(50) Boes, M.; Cerny, J.; Massol, R.; Op den Brouw, M.; Kirchhausen, T.; Chen, J.; Ploegh, H. L. *Nature* **2002**, *418*, 983-988.
(51) Bryant, P. W.; Lennon-Dumenil, A. M.; Fiebiger, E.; Lagaudriere-Gesbert, C.; Ploegh, H. L. *Adv Immunol* **2002**, *80*, 71-114.
(52) Kurts, C.; Kosaka, H.; Carbone, F. R.; Miller, J. F.; Heath, W. R. *J Exp Med* **1997**, *186*, 239-245.
(53) Heath, W. R.; Belz, G. T.; Behrens, G. M.; Smith, C. M.; Forehan, S. P.; Parish, I. A.; Davey, G. M.; Wilson, N. S.; Carbone, F. R.; Villadangos, J. A. *Immunol Rev* **2004**, *199*, 9-26.
(54) Huang, Q.; Liu, D.; Majewski, P.; Schulte, L. C.; Korn, J. M.; Young, R. A.; Lander, E. S.; Hacohen, N. *Science* **2001**, *294*, 870-875.
(55) Banchereau, J.; Steinman, R. M. *Nature* **1998**, *392*, 245-252.
(56) Medzhitov, R. *Nat Rev Immunol* **2001**, *1*, 135-145.
(57) Schnare, M.; Barton, G. M.; Holt, A. C.; Takeda, K.; Akira, S.; Medzhitov, R. *Nat Immunol* **2001**, *2*, 947-950.
(58) Reis e Sousa, C.; Hieny, S.; Scharton-Kersten, T.; Jankovic, D.; Charest, H.; Germain, R. N.; Sher, A. *J Exp Med* **1997**, *186*, 1819-1829.

(59) Dalod, M.; Salazar-Mather, T. P.; Malmgaard, L.; Lewis, C.; Asselin-Paturel, C.; Briere, F.; Trinchieri, G.; Biron, C. A. *J Exp Med* **2002**, *195*, 517-528.
(60) Dalod, M.; Hamilton, T.; Salomon, R.; Salazar-Mather, T. P.; Henry, S. C.; Hamilton, J. D.; Biron, C. A. *J Exp Med* **2003**, *197*, 885-898.
(61) Fernandez, N. C.; Flament, C.; Crepineau, F.; Angevin, E.; Vivier, E.; Zitvogel, L. *Eur Cytokine Netw* **2002**, *13*, 17-27.
(62) Fernandez, N. C.; Lozier, A.; Flament, C.; Ricciardi-Castagnoli, P.; Bellet, D.; Suter, M.; Perricaudet, M.; Tursz, T.; Maraskovsky, E.; Zitvogel, L. *Nat Med* **1999**, *5*, 405-411.
(63) Fujii, S.; Shimizu, K.; Kronenberg, M.; Steinman, R. M. *Nat Immunol* **2002**, *3*, 867-874.
(64) Bender, A.; Bui, L. K.; Feldman, M. A.; Larsson, M.; Bhardwaj, N. *J Exp Med* **1995**, *182*, 1663-1671.
(65) Bhardwaj, N.; Bender, A.; Gonzalez, N.; Bui, L. K.; Garrett, M. C.; Steinman, R. M. *Adv Exp Med Biol* **1995**, *378*, 375-379.
(66) Bhardwaj, N.; Bender, A.; Gonzalez, N.; Bui, L. K.; Garrett, M. C.; Steinman, R. M. *J Clin Invest* **1994**, *94*, 797-807.
(67) Kapsenberg, M. L. *Nat Rev Immunol* **2003**, *3*, 984-993.
(68) Inaba, K.; Metlay, J. P.; Crowley, M. T.; Steinman, R. M. *J Exp Med* **1990**, *172*, 631-640.
(69) Walker, L. S.; Abbas, A. K. *Nat Rev Immunol* **2002**, *2*, 11-19.
(70) Steinman, R. M.; Nussenzweig, M. C. *Proc Natl Acad Sci U S A* **2002**, *99*, 351-358.
(71) Steinman, R. M.; Hawiger, D.; Nussenzweig, M. C. *Annu Rev Immunol* **2003**, *21*, 685-711.
(72) Hawiger, D.; Inaba, K.; Dorsett, Y.; Guo, M.; Mahnke, K.; Rivera, M.; Ravetch, J. V.; Steinman, R. M.; Nussenzweig, M. C. *J Exp Med* **2001**, *194*, 769-779.
(73) Mahnke, K., Qian, Y., Knop, J., Enk, A. *Blood* **2003**, *101*, 4862-4869.
(74) Aichele, P.; Brduscha-Riem, K.; Oehen, S.; Odermatt, B.; Zinkernagel, R. M.; Hengartner, H.; Pircher, H. *Immunity* **1997**, *6*, 519-529.
(75) Aichele, P.; Brduscha-Riem, K.; Zinkernagel, R. M.; Hengartner, H.; Pircher, H. *J Exp Med* **1995**, *182*, 261-266.
(76) Aichele, P.; Kyburz, D.; Ohashi, P. S.; Odermatt, B.; Zinkernagel, R. M.; Hengartner, H.; Pircher, H. *Proc Natl Acad Sci U S A* **1994**, *91*, 444-448.
(77) Kyburz, D.; Aichele, P.; Speiser, D. E.; Hengartner, H.; Zinkernagel, R. M.; Pircher, H. *Eur J Immunol* **1993**, *23*, 1956-1962.
(78) Figdor, C. G.; van Kooyk, Y.; Adema, G. J. *Nat Rev Immunol* **2002**, *2*, 77-84.
(79) Drickamer, K. *Curr Opin Struct Biol* **1999**, *9*, 585-590.
(80) Drickamer, K. *Biochem Soc Trans* **1996**, *24*, 146-150.
(81) Drickamer, K.; Fadden, A. J. *Biochem Soc Symp* **2002**, 59-72.
(82) Mahnke, K.; Guo, M.; Lee, S.; Sepulveda, H.; Swain, S. L.; Nussenzweig, M.; Steinman, R. M. *J Cell Biol* **2000**, *151*, 673-684.
(83) Takahara, K.; Omatsu, Y.; Yashima, Y.; Maeda, Y.; Tanaka, S.; Iyoda, T.; Clausen, B. E.; Matsubara, K.; Letterio, J.; Steinman, R. M.; Matsuda, Y.; Inaba, K. *Int Immunol* **2002**, *14*, 433-444.
(84) Valladeau, J.; Duvert-Frances, V.; Pin, J. J.; Kleijmeer, M. J.; Ait-Yahia, S.; Ravel, O.; Vincent, C.; Vega, F., Jr.; Helms, A.; Gorman, D.; Zurawski, S. M.; Zurawski, G.; Ford, J.; Saeland, S. *J Immunol* **2001**, *167*, 5767-5774.
(85) Geijtenbeek, T. B.; Torensma, R.; van Vliet, S. J.; van Duijnhoven, G. C.; Adema, G. J.; van Kooyk, Y.; Figdor, C. G. *Cell* **2000**, *100*, 575-585.

(86) Dzionek, A., Sohman, Y., Nagafune, J., Cella, M., Colonna, M. et al. *J Exp Med* **2001**, *194*, F59-63.
(87) Chieppa, M.; Bianchi, G.; Doni, A.; Del Prete, A.; Sironi, M.; Laskarin, G.; Monti, P.; Piemonti, L.; Biondi, A.; Mantovani, A.; Introna, M.; Allavena, P. *J Immunol* **2003**, *171*, 4552-4560.
(88) Geijtenbeek, T. B.; Van Vliet, S. J.; Koppel, E. A.; Sanchez-Hernandez, M.; Vandenbroucke-Grauls, C. M.; Appelmelk, B.; Van Kooyk, Y. *J Exp Med* **2003**, *197*, 7-17.
(89) Bonifaz, L.; Bonnyay, D.; Mahnke, K.; Rivera, M.; Nussenzweig, M. C.; Steinman, R. M. *J Exp Med* **2002**, *196*, 1627-1638.

Chapter 2

The Development of Carbohydrate Microarrays

Note: The work described in this chapter was completed in close collaboration with Dr. Daniel Ratner. Dan furnished the carbohydrate structures discussed below while I designed and executed the protein-binding studies. A detailed discussion of the preparation/characterization of the oligosaccharides utilized can be found in Dan's thesis, "Solution-Phase and Automated Solid-Phase Synthesis of High-Mannose Oligosaccharides: Application to Carbohydrate Microarrays and Biological Studies," MIT, 2004. I would also like to acknowledge Mr. Sean Milton of MIT's Biomicroarray Center for his invaluable assistance with array fabrication and for technical assistance with the Digital Genome software employed in the studies described below.

2.1 Introduction: Carbohydrate-Binding Proteins in Biology

Long considered little more than 'plant insecticides'[1] or useful tools for the efficient isolation of glycoproteins, it is of no surprise that it has taken so long for interest to develop in the possible roles played by lectins in mammalian biology. Recent years, however, have revealed that lectins—a genetically and biochemically diverse family of carbohydrate-binding proteins—are involved in diverse biological processes such as the intracellular routing of glycoproteins, mediation of cell-cell interactions, pathogen recognition and receptor-mediated endocytosis[2]. Since the discovery of the asiaologlycoprotein receptor by Ashwell, the first mammalian lectin to be identified, the primary sequences of well over 100 mammalian lectins have been determined[3]. These lectins are found in serum, in the extracellular matrix, as membrane-bound cell-surface proteins and intracellularly. It is of particular interest that so many of the total mammalian lectins found to date are expressed on cells of the immune system, as discussed in Chapter 1 with regard to dendritic cells in particular[4].

It has been suggested that the existence of so many carbohydrate-binding proteins in mammalian systems indicates that the carbohydrates appended to glycoconjugates—protein and lipid—present biologically important information and that one of main functions of lectins is to decode that information[2]. This act of decoding is presumed to occur by way of lectins' specificity for certain carbohydrate structures as well as the geometries imposed by glycosidic linkages, ultimately leading to downstream physiological processes, such as leukocyte rolling

or—though the case has not been made very convincingly as of this writing—signal transduction.

One factor that has confounded efforts to elucidate the many potential roles for lectins in cellular physiology is the difficulty in determining the nature of the specific carbohydrate ligands for these proteins. This difficulty arises from the fact that glycans recognized by lectins cannot be routinely attained in quantities appropriate for detailed biochemical analysis. In addition, the substitution of native glycoproteins to study lectin-carbohydrate interactions is often frustrated by oligosaccharide 'microheterogeneity,' wherein the protein bears markedly different glycan structures at its various glycosylation sites, a phenomenon that introduces uncertainty into one's binding measurements[5].

In an effort to overcome these limitations and enable the facile determination of lectin carbohydrate specificity, we undertook the development of high-density carbohydrate microarrays bearing structurally defined oligosaccharides obtained via chemical synthesis. Our rationale for choosing the microarray format as a platform for identifying protein-carbohydrate interactions was three-fold: 1.) this format enables one to produce hundreds of individual arrays with minimal material (i.e., picomoles) being required, thus making prudent use of carbohydrate derived from laborious chemical synthesis; 2.) arrays bearing a high density of structurally diverse oligosaccharides would allow one to screen several thousand potential binding events on a single array; and finally, 3.) the choice of the proper array format would allow one to use conventional screening technologies (such as fluorescence detection) for detection of protein-carbohydrate interactions. It should also be noted here that we chose to employ carbohydrate structures drawn from chemical synthesis (as opposed to isolating them from natural sources) due to the aforementioned concerns with oligosaccharide isolation in addition to the fact that chemical synthesis can give one routine access to structural derivatives not commonly found in nature (see Figure 2.2). As detailed in this chapter, the use of these structural derivatives can offer powerful insight into the precise structural moieties required for carbohydrate recognition.

This chapter details the development of two distinct array platforms for studying carbohydrate-binding events with fluorophore-labeled proteins. The first system described consists of an array of bar-coded carbohydrate-modified microspheres that utilizes fiber-optic technology to detect the specific fluorescence (i.e., binding events) associated with each microsphere in the array. The second system, and the system we chose for all of our subsequent

studies, consists of chemically-modified glass slides that are derivatized with functionalized saccharides to achieve covalent immobilization. These arrays are printed with precision DNA array robotics to achieve high densities of immobilized carbohydrate and are analyzed for binding events with DNA array scanners.

The arrays described below were utilized to study the binding profiles of various proteins for carbohydrates representing the major structural determinants of the high-mannose oligosaccharide $(Man)_9(GlcNAc)_2$[6]. Our initial experimental emphasis was placed on proof-of-concept experiments with the human immunodeficiency virus (HIV)-entry inhibitor cyanovirin-*N*, a novel protein isolated from cyanobacteria[7]. Later experiments emphasized the use of these arrays to extract detailed information regarding the structural motifs required for protein-carbohydrate interactions and the potential role of these interactions in HIV infection of T cells.

2.2 Randomly-Ordered Microsphere Arrays for the Detection of Protein-Carbohydrate Interactions

The first array system we explored for studying protein-carbohydrate interactions was developed in collaboration with Professor David R. Walt of Tufts University and Dr. Joern Uberfeld, a post-doctorate in the Walt laboratory. The Walt laboratory has had long-standing interest in utilizing fiber optic technology for highly sensitive detection of specific DNA hybridization events[8,9]. The platform that we adapted for use with synthetic carbohydrates is referred to as a randomly-ordered microsphere array (Figure 2.1).

In this system, an etched fiber optic bundle (containing approximately 24,000 individual assay wells) is dipped into a dilute solution of carbohydrate-modified 4.5 μm microspheres. The microspheres are distributed among the wells via Brownian motion, generating a randomly-ordered array. In our application, the particle dispersion consists of many different microspheres, each of which contains a unique carbohydrate structure covalently attached to its surface as well as an internally encoded spectral signature, or barcode (an entrapped fluorescent dye with an emission maximum at 690 nm). The internal dye serves two purposes: it identifies the carbohydrate present on the surface of the bead and aids in determining the position of each type of microsphere in the array. To detect specific binding events, the fiber optic bundle is incubated in a solution of fluorophore-labeled protein, washed and interrogated at two separate

wavelengths: the first wavelength excites the internally-entrapped dye, thereby allowing one to ascertain the position of the bead and the carbohydrate linked to it; the second wavelength excites any bound fluorophore-labeled protein. By overlaying the barcode fluorescence with that of the protein in question, one can readily determine which beads (and therefore which carbohydrates) were bound in the array.

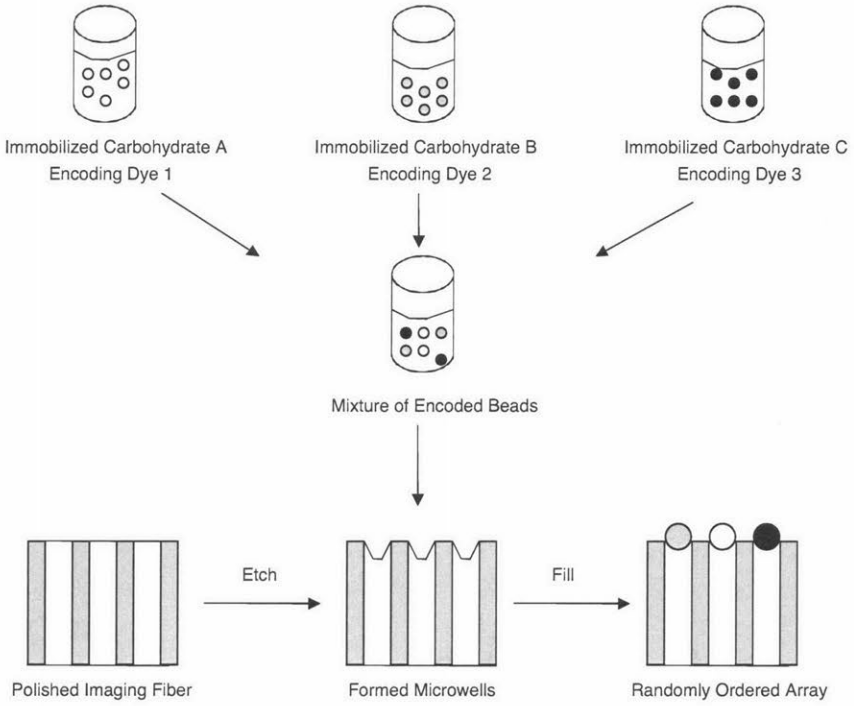

Figure 2.1 Schematic of randomly-ordered microsphere arrays. Populations of internally-encoded microspheres bearing immobilized carbohydrates are mixed and applied to the end of an etched fiber optic bundle. The beads are dispersed among the various assay wells by Brownian motion to generate a 'random' array. The fiber optic cables are used to channel excitation wavelengths for both the internal 'barcode' dye and the protein-bound fluorophore as well as to collect the light emitted from both fluorophores.

2.2.1 Choice of Oligosaccharides for Proof-of-Concept Experiments

For the purposes of our initial proof-of-concept experiments with the microsphere array we chose to concentrate on synthetic derivatives of the *N*-linked high-mannose oligosaccharide $(Man)_9(GlcNAc)_2$ (Figure 2.2). This choice was guided by an active collaboration with Dr. Barry O'Keefe of the Molecular Targets Discovery Program at the National Cancer Institute that sought to determine the structural features in high-mannose oligosaccharides required for recognition by plant and bacterial proteins with demonstrated anti-HIV activity. As many of

these proteins display carbohydrate-binding activity it is of interest to determine the structural facets of that binding activity.

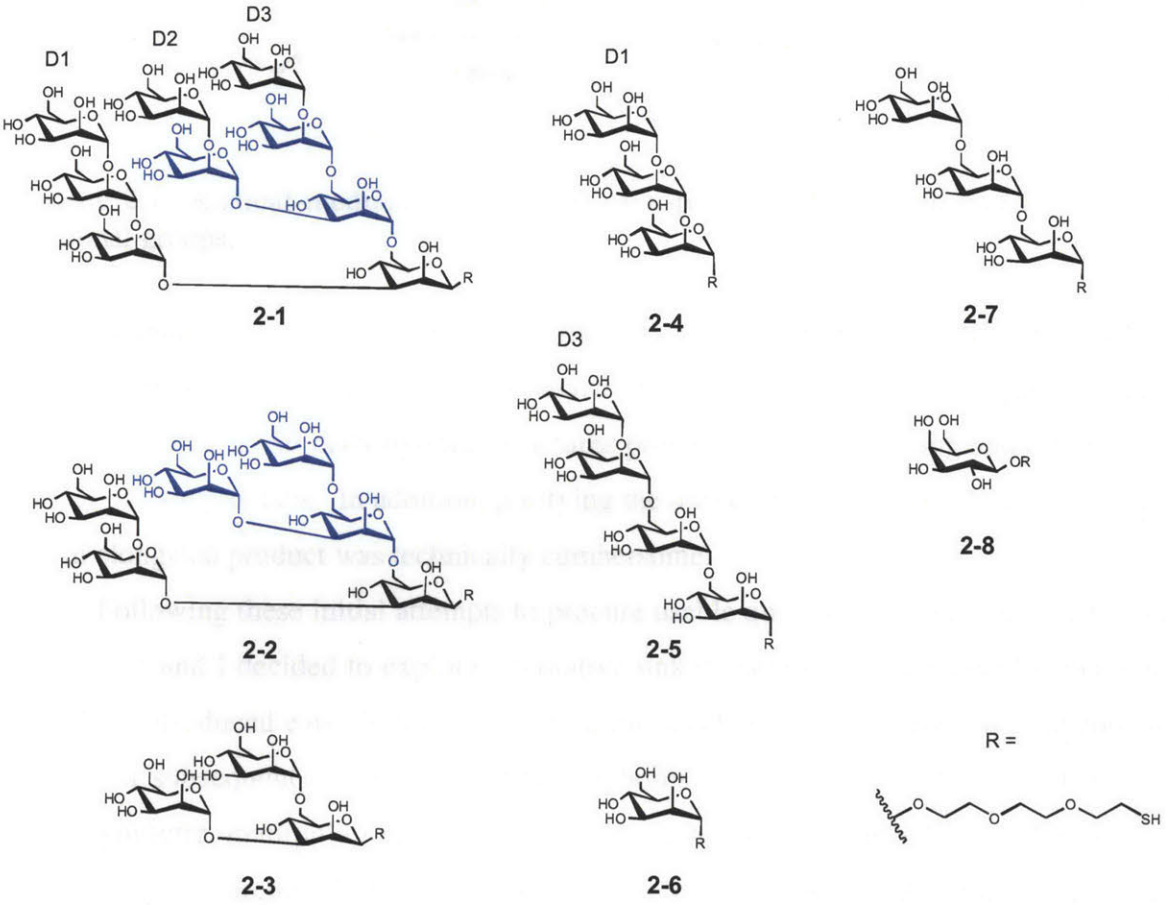

Figure 2.2 High mannose nonamannoside **2-1** and structural derivatives thereof employed in the carbohydrate microarray studies described in Chapter 2. Note that the thiol-terminated tri(ethylene oxide) linker has been substituted for the $(GlcNAc)_2$ disaccharide found in naturally occurring $(Man)_9(GlcNAc)_2$. The D1, D2, and D3 designations corresponding to each of the three arms in **2-1** and **2-2** are used for clarification in the following discussion. The outer branched trimannoside discussed in Section 2.4.6.6 is highlighted here in blue. Also included here is the non-mannosyl pyranoside galactose, **2-8**.

2.2.2 Installation of the 2-(2-(2-mercaptoethoxy)ethoxy)ethyl Linker

In order to proceed with the fabrication of the microsphere arrays we first needed to determine the best way to functionalize the pentenyl functional group present in all of the high-mannose oligosaccharides Dan Ratner had prepared during the course of his thesis work. This

chemistry offered an attractive route to creating a panel of functionalized saccharides, as one could theoretically attain carboxylates, masked thiols, primary amines and hydroxyl groups by

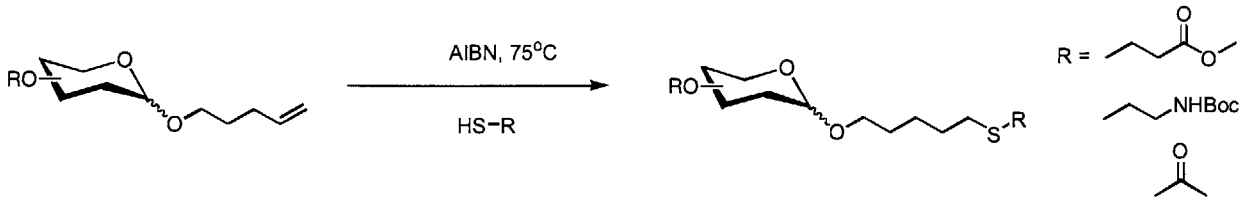

Scheme 2.1 Radical-mediated elongation of n-pentenyl mannosides to introduce useful functional groups.

simply changing the nature of the thiol in the radical mediated reaction (Scheme 2.1)[10]. While model reactions on monosaccharides, protected and unprotected, worked in high yield, extending this chemistry to larger carbohydrate structures proved to be low yielding and often generated a number of side products. In addition, purifying the unreacted pentenyl starting material from the radical elongated product was technically cumbersome.

Following these initial attempts to procure usable quantities of functionalized saccharide, Dan Ratner and I decided to explore alternative linker chemistries. We decided that our linker should be introduced early in the synthesis of the saccharide, should have the functional group needed for subsequent conjugation (to fluorophores or proteins) already present to avoid late stage synthetic manipulations, and should be reasonably hydrophilic. Based on these considerations I prepared an ethylene-dioxy linker with a benzyl thioether protecting group (Scheme 2.2)[11]. This linker has three features that have proven very useful in all of our subsequent manipulations: 1.) The unprotected hydroxyl group allows for direct incorporation of the linker into appropriately activated monosaccharide donors or epoxidized glycals; 2.) The benzyl thioether protecting group is stable throughout subsequent synthetic manipulations; and 3.) deprotection *via* Birch reduction yields a free thiol that can be subsequently reacted, in high yield, with maleimide-functionalized moieties.

Model glycosylations utilizing a differentially protected mannopyranosyl trichloroacetimidate and **2-9** followed by deprotection and conjugation to maleimide-activated bovine serum albumin (BSA) and ovalbumin (see Chapter 3) proved successful; therefore the high-mannose series plus the $\alpha 1 \rightarrow 2$ linear trimannoside **2-4** were produced with the 2-(2-(2-

mercaptoethoxy)ethoxy)ethyl linker installed at the reducing end, deprotected and used for the generation of the BSA neoglycoconjugates (Figure 2.2).

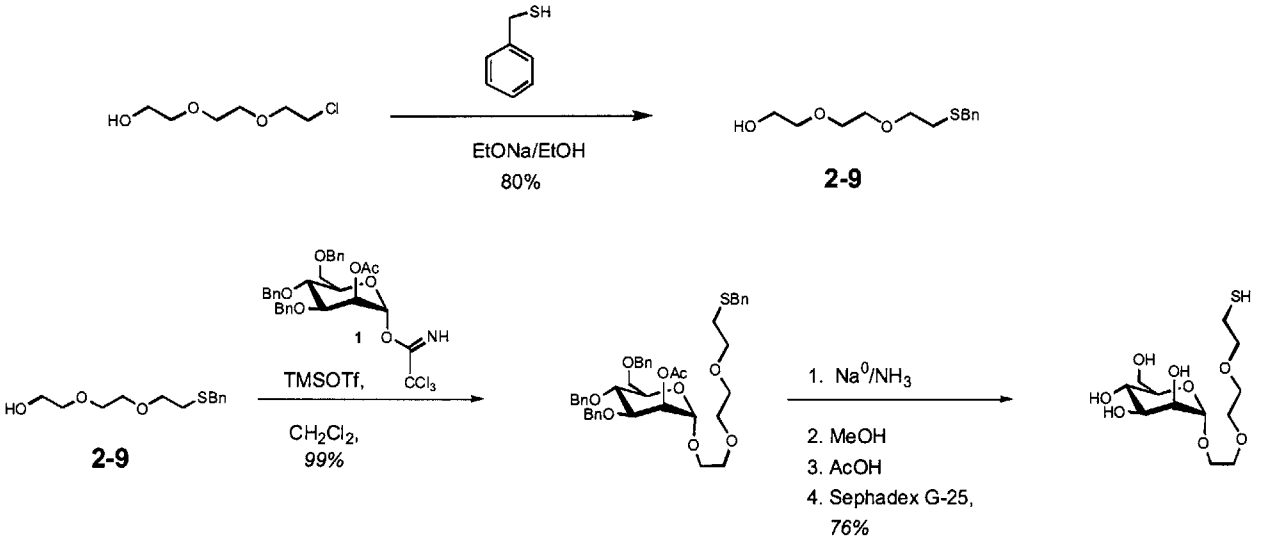

Scheme 2.2 2-(2-(2-mercaptoethoxy)ethoxy)ethyl linker and model glycosylation with differentially protected monosaccharide. Installation of this linker introduces a terminal thiol moiety into synthetic mannans for use in future derivatizations.

2.2.3 Carbohydrate Modification of Microspheres for the Randomly-Ordered Array

To generate a series of carbohydrate-modified microspheres I chose a conjugation strategy that involved first coupling each respective saccharide to maleimide-activated BSA and thereafter coupling these neoglycoproteins to the microsphere surface via water-soluble carbodiimide chemistry. This strategy was chosen for two principal reasons: first, given the small size of the ethylene-dioxy linker, it was important to find a way to achieve adequate spacing between the underlying polymer support and the attached carbohydrate in order to avoid any steric issues that may impede binding by solution-phase proteins; secondly, BSA, which has no endogenous carbohydrate, is a highly efficacious agent for passivating surfaces to minimize non-specific interactions[12]. Thus, by attaching our carbohydrates directly to BSA we could minimize steric hindrance at the lectin-microsphere interface and reduce the non-specific binding that would otherwise lead to high background levels.

It should be noted here that the microspheres chosen for our experiments were intensity-encoded—that is, all beads contained the same entrapped fluorophore, but each of the five distinct groups utilized in our studies contained a different concentration of that fluorophore.

The specific details of the neoglycoprotein preparation and microsphere conjugation are as follows:

Neoglycoprotein preparation: Maleimide-activated BSA and Tris(2-carboxyethyl)phosphine hydrochloride (TCEP) were purchased from Pierce Chemical. Compound **2-1** (50 μg, 152 nmol) was incubated with 1 equiv TCEP in 10 mm HEPES buffer (pH 7.5) at room temperature for 1 h with constant mixing to reduce any disulfide bonds that formed via oxidation during storage. This solution was added to 100 μg maleimide-modified BSA in 100 μL of the same buffer. The solution was incubated overnight at room temperature with constant mixing. Without further purification the encoded microspheres were added to this neoglycoprotein solution. This coupling chemistry was used for all structures (**2-1** thru **2-4, 2-6** and **2-8**) in this study. It should be noted that the same molar quantity of each saccharide was used for each conjugation reaction.

Microsphere preparation: Internally-encoded QuantumPlex microspheres (4.4 μm) were purchased from Bangs Laboratories. The Quantum Plex kit utilized for this study consists of five separate microsphere dispersions that are dyed internally with increasing quantities of Starfire Red fluorophore (ex. 640 nm, em. 690 nm). Stock beads (100 μL) were washed by centrifugation/re-dispersion (3x with 10 mm HEPES buffer, pH 7.5) and conjugated to neoglycoproteins with 100 μg of the water-soluble crosslinker 1-ethyl-3-(3-dimethylaminopropyl)-carbodiimide, (EDC) for 4 hours at room temperature with constant mixing. Beads were purified from excess neoglycoprotein by centrifugation/redispersion (3x in HEPES buffer). Microspheres were stored in 10 mm HEPES buffer with 0.1% Tween 20 at 4° C until use.

2.2.4 Array Fabrication

To form a randomly-ordered array of carbohydrate-modified, internally-encoded microspheres, equal amounts (10 μL) of the above bead suspensions were mixed and 1 μL of the mixture was added to the etched end of an imaging fiber (about 2.4 x 10^4 microwells, well

diameter 5 μm, Illumina, San Diego, USA). The mixture was left to dry before the excess beads were rinsed away with deionized water. About 30 beads of each type were present on the array.

2.2.5 Detection of Protein-Carbohydrate Interactions

Images of the fiber optic carbohydrate array were acquired with a custom-built epifluorescence microscope equipped with a xenon arc lamp and a CCD camera (Hamamatsu C4742-95-12-ER, Optical Analysis Corp., Nashua, NH). The system was controlled with IPLab software (Scananalytics, Fairfax, VA) that was also used for image processing. The positions of the microspheres were registered by exciting their internal encoding dye StarfireRed at 640 nm (emission maximum at 690 nm). The decoding of the different carbohydrate structures was achieved by analyzing the emission intensities at 690 nm. The array was incubated with the fluorescently labeled lectin at various concentrations for 5 min (V=200 μL). Then the lectin solutions were replaced with buffer and an image of the array was taken at the emission wavelength of the label (520 nm, exposure time 1 s). Reported background-subtracted fluorescence intensities represented mean intensities of approximately 30 of each type of bead present in a given array.

2.2.6 Detecting Protein-Carbohydrate Interactions with Randomly-Ordered Microsphere Arrays

To demonstrate the utility of these arrays for identifying and characterizing protein-carbohydrate interactions, we examined two systems: the mannose-binding lectin concanavalin A (ConA), and cyanovirin N (CVN), a novel HIV-inactivating 11-kDa protein derived from the cyanobacterium Nostoc ellipsosporum with known specificity for oligosaccharides with high-mannose content[13]. Our goal was first to establish if this system would enable the detection of simple monosaccharide-protein interactions and then extend the analysis to more complex oligosaccharides.

2.2.6.1 Specific Recognition of Monosaccharide Mannose by Concanavalin A

In our first proof-of-concept experiment, arrays were formed of microspheres bearing the monosaccharide mannose **2-6** and microspheres bearing the monosaccharide galactose **2-8**, chosen to represent a non-mannosyl pyranoside. ConA binding was detected by incubating the fiber optic array in a solution of ConA labeled with Alexa488 at 50 μg mL^{-1} for five minutes. Then, the lectin solution was removed, replaced with a fresh buffer solution and the fluorescence signal at the Alexa488 wavelength (520 nm) was measured. Only those beads bearing **2-6** were bound by labeled ConA (Figure 2.3). The intrinsic non-specific-binding levels of fiber optic arrays in this assay were very low and the specificity of carbohydrate–protein interactions was clearly observed as no ConA was detected in the empty wells or associated with beads functionalized with **2-8**. To determine the concentrations of labeled ConA required to observe signals easily discriminated over background, the fiber optic arrays were incubated with a dilution series of labeled ConA ranging from 0 to 400 μg mL^{-1}. ConA concentrations as low as 25 μg mL^{-1} yielded fluorescence signals easily discernible over background (Figure 2.4). Even at very high lectin concentrations, no increase in fluorescence was observed associated with the beads presenting **2-8**, again indicating both the specificity of the detected interactions between **2-6** and ConA as well as the resistance of the fiber optic arrays to fouling. Thus, we conclude from these experiments that randomly-ordered arrays supported on an etched fiber optic bundle can be used for the detection of specific protein-carbohydrate recognition events.

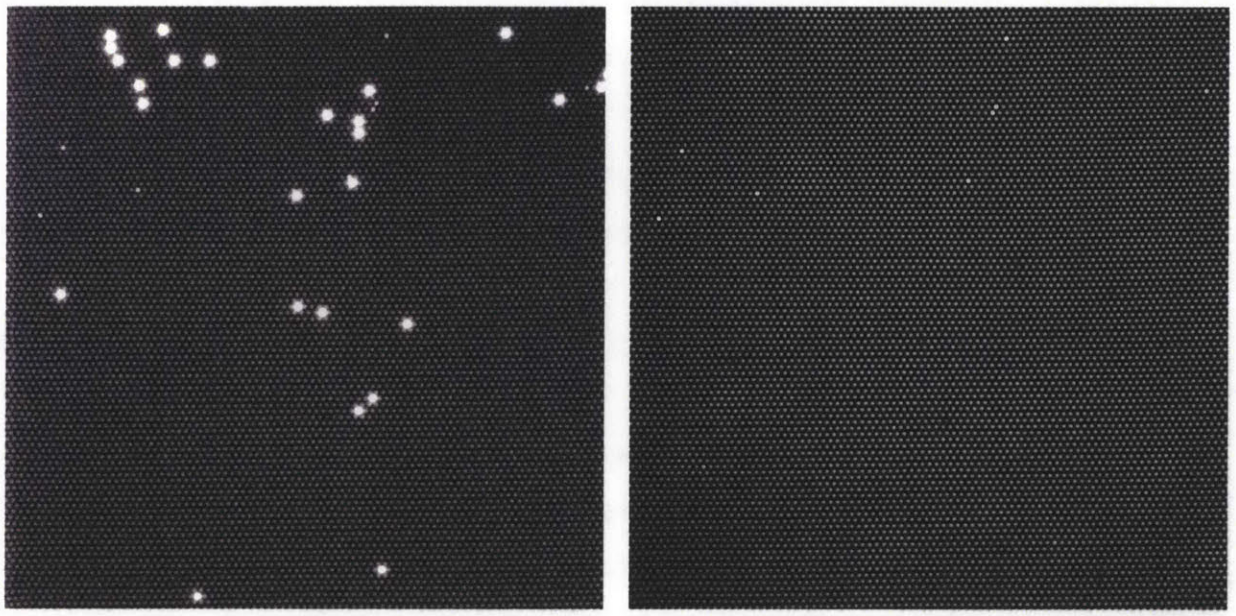

Figure 2.3 Internally-encoded microsphere array bearing immobilized **2-6** and **2-8**, post-incubation with Alexa488-ConA. *Left*, fluorescence at 690 nm prior to Alexa488-ConA incubation; *Right*, fluorescence at 530 nm after incubation with Alexa488-ConA. Only those beads bearing **2-6** and bound by ConA are visible at the 530 nm wavelength.

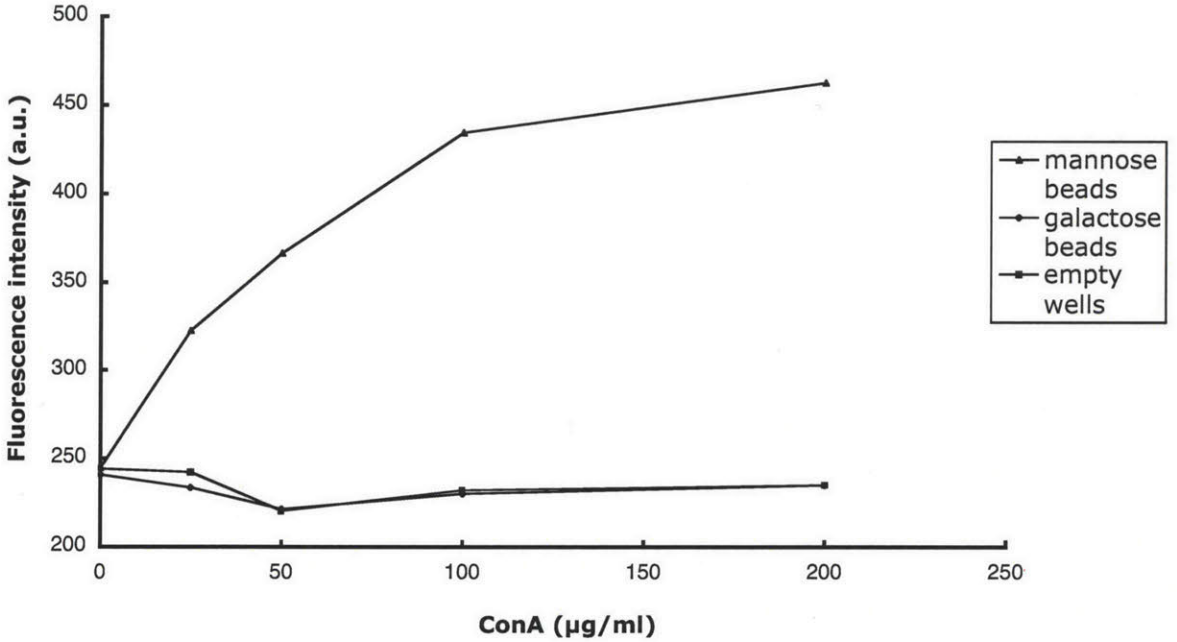

Figure 2.4 Dilution series of Alexa488-ConA to determine the amount of protein required for detection on the microsphere array. A microsphere array presenting **2-6** and **2-8** was incubated with increasing concentrations of Alexa488-ConA and bound fluorescence was collected at 530 nm. The plotted fluorescence intensities are normalized to background fluorescence.

2.2.6.2 Cyanovirin-N (CVN) Recognition of High-Mannose Oligosaccharide

Having demonstrated the detection of specific protein-carbohydrate interactions with a simple lectin-monosaccharide system, we wished to extend our application of this system to more complex oligosaccharides. Synthetic structures **2-1** thru **2-4** and **2-6** were immobilized on microspheres as described above; small aliquots of these bead preparations were mixed and used to prepare a fiber optic microsphere array.

CVN–oligosaccharide binding was assayed by incubating the array in a solution of BODIPY-labeled CVN (BODIPY-CVN) at 50 μg mL^{-1} for five minutes before the CVN solution was removed and replaced with fresh buffer. Light at the BODIPYexcitation wavelength (488 nm) was passed through the optical fiber bundle and the BODIPY emission was collected with a CCD camera. Three of the five structures (**2-1**,**2-2**,**2-4**) present were bound by CVN (Figure 2.5) in accordance with isothermal microcalorimetry studies. Beads that were not bound by CVN did not show any fluorescence signals over background levels.

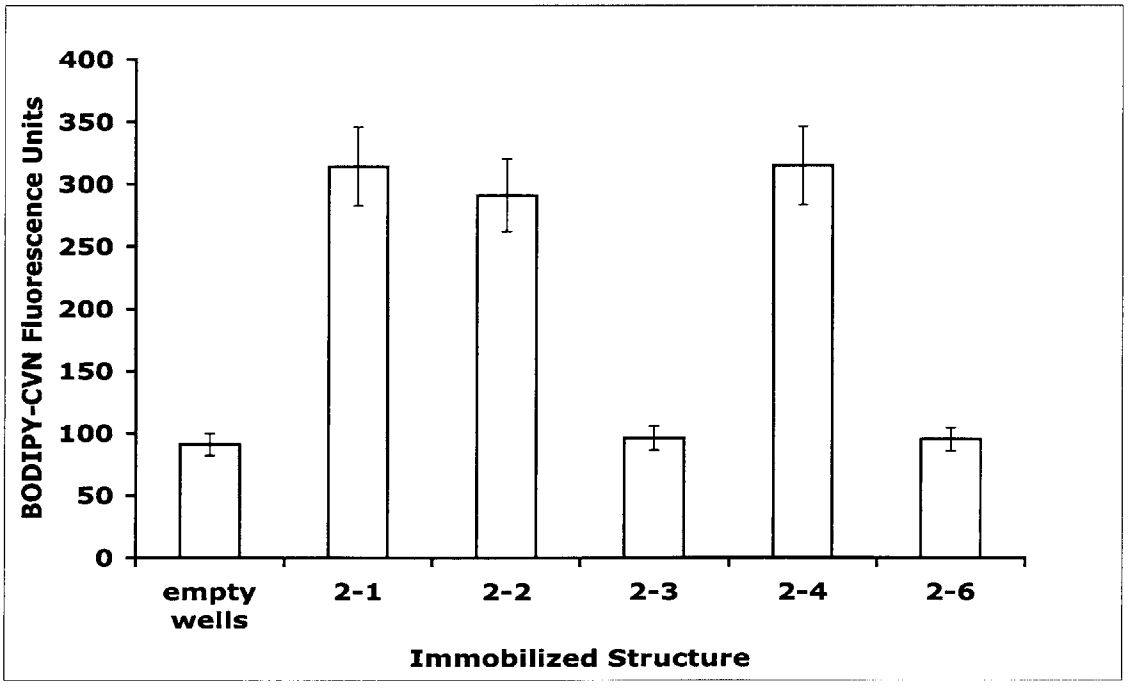

Figure 2.5 CVN recognition of Manα(1→2)Man linkages. BODIPY-CVN was incubated (50 μg mL^{-1}) with a microsphere array presenting the above structures. BOPIDY fluorescence was collected at 530 nm and normalized to background fluorescence.

In summary, these simple experiments demonstrated that optically bar-coded microspheres arrayed among the wells of a fiber optic bundle could be optically interrogated to ascertain bead position, carbohydrate identity, and binding interactions with fluorophore-labeled proteins. Using this system we were able to evaluate five distinct structures against a carbohydrate-binding protein simultaneously and with unambiguous results.

2.2.6.3 Evaluation of Microsphere Array

Our experience with the described array system led us to conclude that it had a number of limitations that would ultimately render it ill suited as a dedicated research tool for elucidating protein-carbohydrate interactions. The first and foremost limitation, from our viewpoint, was the requirement for highly sophisticated optics and deconvolution software for image acquisition and data analysis. Second, the requirement for fluorophore-labeled beads and fluorophore-labeled proteins imposed serious technical restraints on the number of distinct carbohydrates represented in any given array and the number of potential binding interactions one could screen; this is due to the fact that each distinct group of beads requires its own spectral signature and each spectral signature cannot—in order to avoid high background and/or false positives—have an emission spectrum that overlaps with that of other beads or with that of the fluorophore-protein conjugate. A third and final concern was that the system was technically cumbersome and expensive: once a fiber optic bundle was used it could not be regenerated, which made the idea of routine screening a rather expensive prospect.

Given these reservations we undertook the development of our own in-house screening platform. Inspired by the high-density of immobilized molecules achievable on conventional DNA microarrays, the availability of precision robotics for microarray manufacture and the ease of use of array scanners and software, we decided to focus on developing chip-based, high-density carbohydrate arrays. This work is described in the following sections.

2.3 First Generation Carbohydrate Microarrays

The microarrays described in the following sections explore two different 25 x 75 mm glass surfaces that are chemically-modified to render them reactive to the thiols present in our 2-

(2-(2-mercaptoethoxy)ethoxy)ethyl linker-modified saccharides. This first system begins with aldehyde-functionalized glass slides.

2.3.1 Modification of Aldehyde-Functionalized Slides

In order to generate a thiol-reactive surface starting from aldehyde-functionalized slides, we adapted a strategy detailed by MacBeath and Schreiber[14]. This strategy involves first incubating the aldehyde slides in a solution of BSA to generate Schiff-base anchored BSA via the primary amines present on BSA (Figure 2.6). Thereafter the remaining unreacted primary amines are modified with the heterobifunctional crosslinker succinimidyl-4-(N-maleimidomethyl) cyclohexane-1-carboxylate. This crosslinker incorporates amine reactivity (an *N*-hydroxysuccinmidyl ester) and thiol reactivity (a maleimide group); use of this crosslinker converts any available amines on BSA to sites of thiol reactivity, thus providing a chemical means of covalently immobilizing our thiol-functionalized saccharides.

In addition to gaining sites of thiol reactivity via modification of BSA's primary amines, the use of BSA as a scaffold for small molecules on similar arrays had been shown to enhance the ability of the immobilized small molecules to interact with their target proteins.

The general slide functionalization protocol we employed was as follows: SuperAldehyde slides (TeleChem International) were immersed in phosphate buffered saline (1X PBS, 50 mL) containing 1% BSA (w/v) and incubated overnight at room temperature. The slides were rinsed twice with distilled water (100 mL) and twice with 95% ethanol (50 mL), then dried under a stream of dry argon. Subsequently, the slides were immersed in anhydrous DMF (45 mL; Aldrich) containing succinimidyl-4-(N-maleimidomethyl)cyclohexane-1-carboxylate (65 mg; Pierce Chemical) and N,N-diisopropylethylamine (100 mM; Aldrich). The slides were incubated in this solution for 24 h at room temperature, washed four times with 95% ethanol (50 mL), and stored in a vacuum dessicator until use

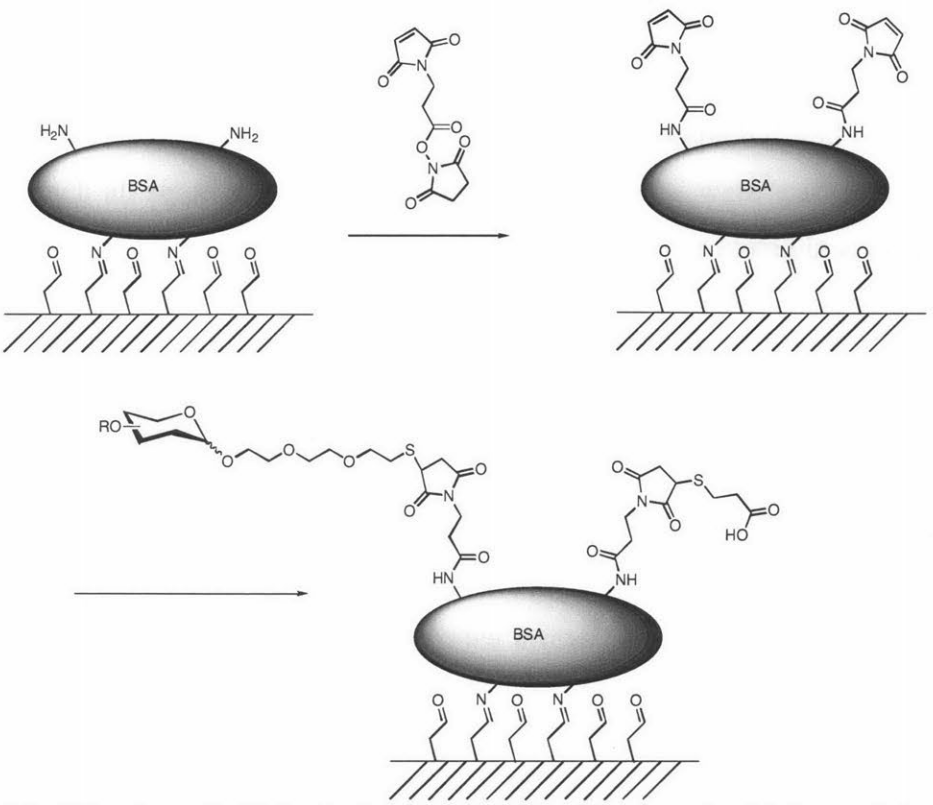

Figure 2.6 Modification of aldehyde functionalized slides to gain thiol reactivity. Slides are first coated with an inert, non-glycosylated protein (here, BSA); primary amines of the protein are then reacted with the heterobifunctional crosslinker SMCC to introduce thiol-reactive maleimide groups. Finally, thiol-functionalized saccharides are printed on the slides and any unreacted maleimide groups are quenched with 3-mercaptopropionic acid.

2.3.2 Microarray Layout and Printing Conditions

A standard DNA microarray printer robot equipped with either a 16- or 32-pin print head was employed to spot maleimide-presenting slides with thiol-functionalized carbohydrates. A 32-pin print head was employed most frequently in order to array 8 distinct synthetic structures at 4 different concentrations (typically in a range of 2 – 0.2 mM). Each structure was printed 100 times in redundant grids (10 x 10 grids for the 32-pin print) for ease of software-based statistical analysis of fluorescence units.

The specific details of microarray fabrication are as follows: Thiol-functionalized carbohydrates were incubated for 1 h at room temperature with one equivalent of tris(carboxyethyl)phosphine hydrochloride (TCEP) in 1X PBS, and printed on the maleimide-derivatized glass slides by using a MicroGrid TAS array printer. Prints were performed at 30%

humidity by using either a 16- or 32-pin format, with a spot size of 120 μm and 300 μm spacing. Thereafter the slides were stored in a humid chamber at room temperature for 12 h, washed twice with distilled water, and then incubated for 1 h in 3-mercaptopropionic acid in 1X PBS (1 mM, 50 mL) to quench all remaining maleimide groups. The slides were washed three times with distilled water (50 mL), twice with 95% ethanol (50 mL), and then stored in a vacuum dessicator until use.

2.3.3 Detection of Protein-Carbohydrate Interactions

To determine if the thiol-modified saccharides immobilized according to the above chemistry could be recognized by carbohydrate-binding proteins, we again employed the two tier approach outlined in Section 2.2: first we printed arrays containing mannose **2-6** and the non-mannosyl pyranoside galactose **2-8** and tested for the ability of ConA to recognize immobilized **2-6**. Thereafter, we wished to extend this platform to include more complex oligosaccharides, thus structures **2-1** thru **2-4** and **2-6** were printed and probed with BODIPY-labeled CVN.

The general protocol for detecting protein-carbohydrate interactions was as follows: FITC-labeled ConA (25 μg mL^{-1}; Sigma), was used in HEPES-BSA buffer (10 mM; pH 7.5; 1mM CaCl2, 1mM MnCl2, 100 mM NaCl, 1% BSA (w/v)) and BODIPY-labeled CVN (25 μg mL^{-1}) was used in PBS (10mM) containing BSA (1 %, w/v). For all incubations, 20 μL of protein solution was applied between the microarray slide and a plain glass slide. Following a 0.5 - 1 h incubation at room temperature, the slides were washed three times with incubation buffer (50 mL), twice with distilled water (50 mL), and then centrifuged at 200g for 5 min to ensure complete dryness. The slides were scanned using an ArrayWoRx fluorescence slide scanner (Applied Precision) to visualize fluorescence.

2.3.3.1 Detection of Concanavalin A-Monosaccharide Interactions

Microarrays printed with mannose **2-6** and galactose **2-8** covering a concentration range of 10 mM to 0.05 mM were probed with fluorescein isothiocyanate (FITC)-labeled ConA for 30 minutes, rinsed to remove unbound lectin and read with a fluorescence slide scanner. As shown in Figure 2.7, ConA binding was observed only at regions on the array that corresponded to

immobilized mannose **2-6** while no fluorescence was associated with galactose **2-8**. In addition, the intensity of bound FITC-ConA appears to correlate with the amount of immobilized **2-6**, as the fluorescence associated with second column of **2-6** (corresponding to printing concentrations of 0.6 – 0.07 mM, two-fold dilutions) decreases as a function of printing concentration. It is also noteworthy that we observe very low background signal with these arrays (high signal-to-noise ratios), which may be due to efficient passivation of the glass surface by associated BSA as observed previously by MacBeath[14].

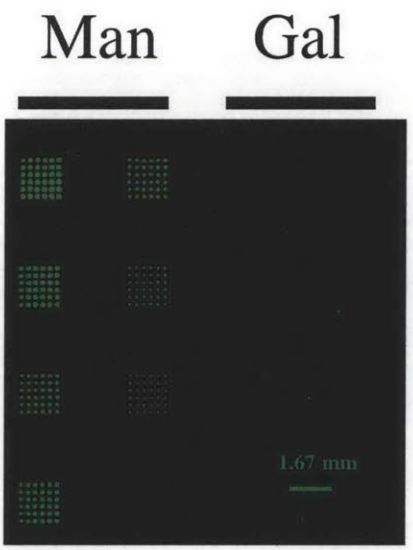

Figure 2.7 Specific detection of ConA-mannose interactions on carbohydrate microarrays. Microarrays were printed with thiol-functionalized mannose **2-6** and galactose **2-8** and probed with FITC-ConA. Arrays were washed and scanned on an ArrayWoRx scanner. No fluorescence is observed at spots corresponding to galactose **2-8**. Scale bar included to indicate feature size of printed grids.

2.3.3.2 Detection of Cyanovirin-N-Oligosaccharide Interactions

To examine the utility of our microarrays for identifying protein interactions with more complex carbohydrates, we prepared arrays bearing thiol-terminated saccharides **2-1** thru **2-6** by the chemistry described above (section 2.3.1) and probed these arrays with fluorophore-labeled CVN. Using these arrays we found that we were able to fully recapitulate the most salient features known about CVN's recognition of high-mannose oligosaccharides: analysis of binding by BODIPY-CVN revealed that only the high-mannose nonasaccharide **2-6**, hexasaccharide **2-5**

and linear trisaccharide **2-3** were bound by CVN (Figure 2.8). This binding profile is in accordance with the previous observation that CVN's affinity for high-mannose oligosaccharides derives from its structural specificity for Manα(1→2)Man glycosidic linkages which are found only in structures **2-3**, **2-5**, and **2-6**[15].

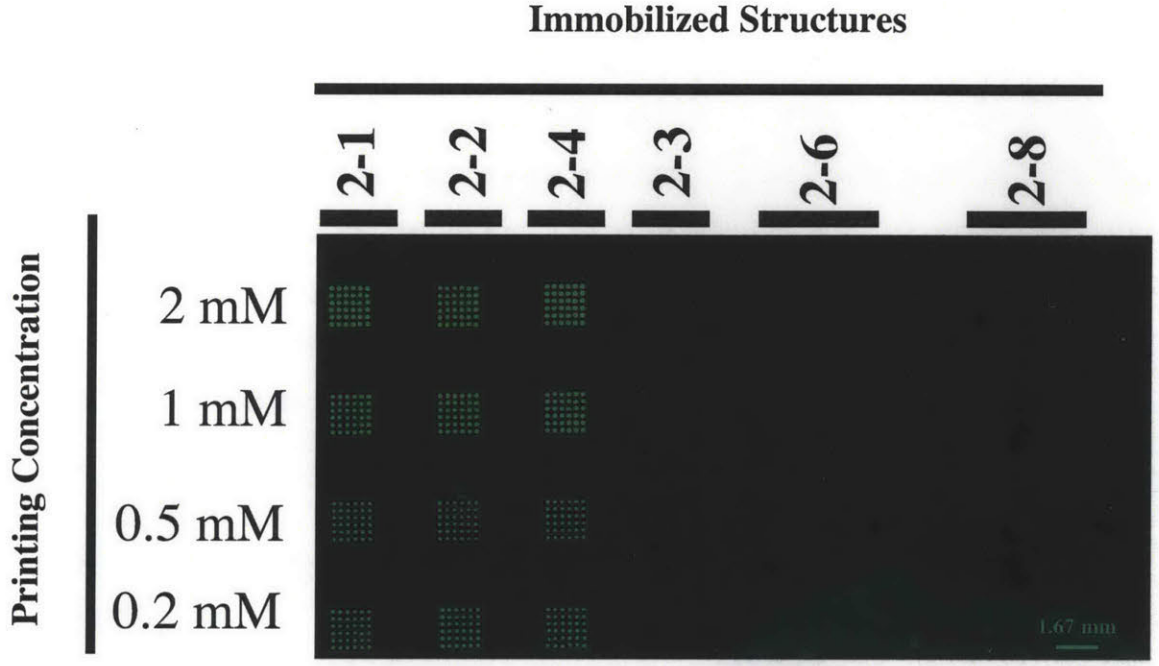

Figure 2.8 High-mannose oligosaccharide array reveals that CVN binds Manα(1→2)Man linkages exclusively. Oligosaccharide microarray bearing nonamannoside **2-1** and derivatives thereof were printed and probed with BODIPY-CVN, washed and scanned for BODIPY fluorescence.

2.3.3.3 Conclusions of First Generation Microarray Study

While the above binding experiments did not establish anything new with regard to these particular protein-carbohydrate interactions, this exercise did allow us to establish the utility of carbohydrate microarrays for studying such interactions. In particular, this early work drew our attention to the fact that the use of microarrays as an assay platform would dramatically minimize the quantity of reagent required to conduct such analyses. By using robotics employed for DNA array fabrication, as little as 20 nanomoles of synthetic saccharide (a 10μL, 2 mM solution) can give rise to hundreds of individual array slides. To put this in perspective with regard to the study just described, 20 nanomoles of nonasaccharide **2-1** corresponds to just 32

μgrams; thus, even a synthetic procedure that generated < 1 milligram of pure, thiol-functionalized carbohydrate could be used to fabricate thousands of arrays bearing that carbohydrate.

Another feature of these arrays that deserves mention is the density of information presented on a single array. Taking advantage of robotic printing to achieve high densities of immobilized molecules, we were able to represent the high-mannose nonasaccharide **2-1** and important structural derivatives thereof on a single glass slide. Incubation with fluorophore-labeled CVN revealed, in a single binding experiment, the structural basis for CVN recognition of high-mannose oligosaccharides. Analogous to cDNA microarrays that present many thousands of potential hybridization partners on a single array, future carbohydrate arrays will display hundreds of defined oligosaccharides and structural derivatives that will enable the facile determination of a given protein's carbohydrate specificity, both in terms of the ligand bound (e.g., mannose vs. galactose) as well as the underlying geometries imposed by specific glycosidic linkages.

2.4 Second-Generation Microarrays & Their Application to Glycobiology

Having established that high-density microarrays could serve as a platform for the analysis of protein-carbohydrate interactions, we wished to apply this tool to a relevant problem in glycobiology with the hopes of gleaning new structure-function information that may not be easily obtainable with another tool/set of techniques. Before setting out to do this, however, we undertook a modification of our slide surface chemistry in order to render it more chemically homogeneous and amenable to modification with thiol-modified saccharides or proteins, glycosylated and non-glycosylated. To achieve these ends we switched from aldehyde-functionalized slides to the commercially available GAPS II slides used so often in the fabrication of DNA microarrays. In contrast to the aldehyde-functionalized slides that require an initial modification with an inert protein (BSA) to obtain primary amines for further derivitization, GAPS II slides are modified to present primary amines. From this substrate one can readily obtain thiol-reactive surfaces by a one-step modification with the heterobifunctional crosslinker SMCC or amine-reactive surfaces by a similar one-step modification with the homobifunctional crosslinker ethylene-glycol-bis(succinimidylsuccinate, EGS) (Figure 2.9).

It should be noted that the switch to this new surface functionalization strategy with its concomitant removal of BSA as a chemical scaffold required a new means of surface passivation after immobilization of printed carbohydrates. To this end, SMCC-modified slides that were printed with thiol-functionalized saccharides were incubated in a solution of 2-(2-(2-mercaptoethoxy)ethoxy)ethanol to quench any unreacted maleimides on the slide surface. In

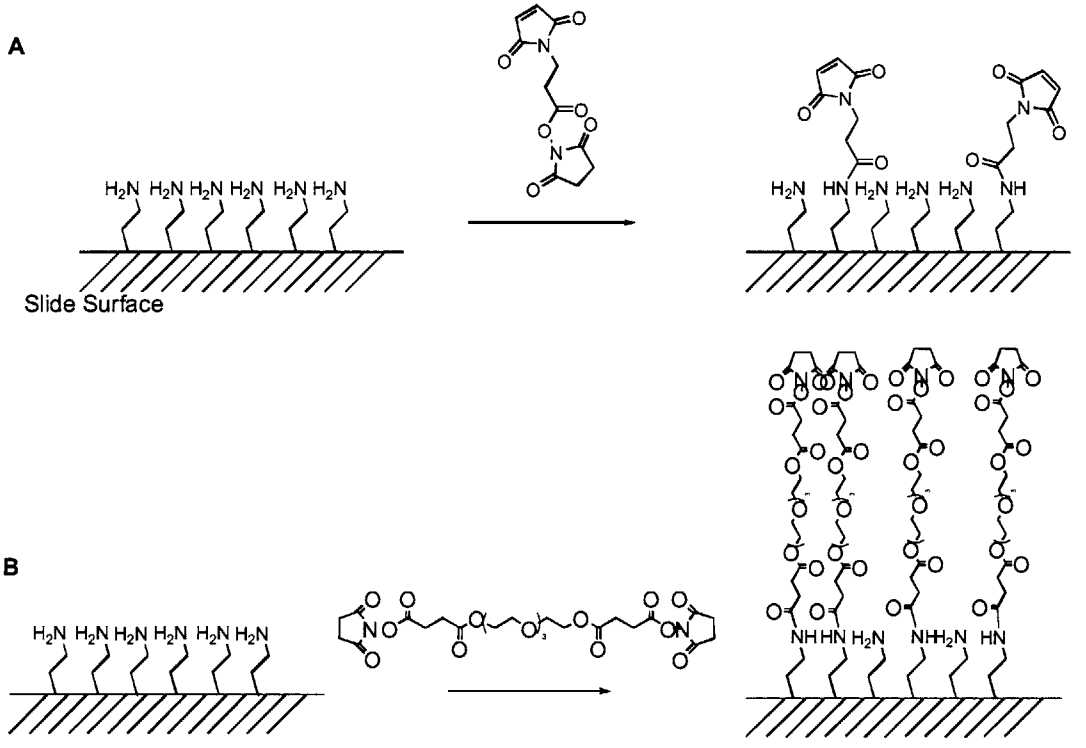

Figure 2.9 Two surface chemistries employed in the modification of amine-bearing GAPS II slides. (A). To generate maleimide-modified surfaces for the immobilization of thiol functionalized saccharides, slides were incubated in a solution of the heterobifunctional crosslinker SMCC. After carbohydrate printing, remaining maleimide groups were quenched with 2-(2-(2-mercaptoethoxy)ethoxy)ethanol. (B). For protein immobilization, *N*-hydroxysuccinimidyl-modified surfaces were generated by incubating slides in a solution of EGS. After protein immobilization, remaining succinimidyl groups were quenched by incubation with excess BSA.

addition to quenching remaining maleimide groups, the hydrophilic nature of the tri(ethylene oxide) linker renders the glass surface resistant to non-specific adsorption of proteins from solution. For slides modified with EGS, surface passivation after protein immobilization was achieved by incubating the slides in a buffered solution of BSA.

A comparison of the aldehyde-BSA slides versus GAPS II slides revealed that both slides gave very similar results (D.M. Ratner, Ph.D. Thesis, Chapter 4). Given the ease of

immobilization of carbohydrates and proteins obtainable with GAPS II slides, their availability and compatibility with DNA printing robotics, we employed these slides for all future microarray experiments.

2.4.1 Microarray Surface Functionalization

Microarrays were functionalized to present maleimide groups (thiol-reactive surface) or succcinimidyl groups (amine-reactive surface) by the following methods: Sulfhydryl-reactive slides were prepared in batches of two. GAPS slides (Corning) were incubated overnight at room temperature in 45 ml anhydrous *N,N*-dimethylformamide (DMF, Aldrich), 10 mg succinimidyl-4-(*N*-maleimidomethyl)cyclohexane-1-carboxylate (SMCC, Pierce Endogen) and 880 μL *N,N*-diisopropylethylamine (Aldrich). Slides were washed with 3 volumes methyl alcohol, dried under a stream of nitrogen, and stored in a dessicator prior to printing. To generate amine-reactive slides, the same procedures was followed as above with the exception that SMCC was replaced by 10 mg ethylene-glycol-bis(succinimidylsuccinate) (EGS). All other treatments were kept the same.

2.4.2 Microarray Printing

The conditions employed for microarray printing on GAPS II slides, including carbohydrate preparation (i.e., TCEP reduction) were the same as described in section 2.3.2).

2.4.3 Microarray Application to HIV Glycobiology

With a surface chemistry established that enabled the efficient immobilization of carbohydrates and proteins alike, we wished to devise a microarray study that would merge the distinct advantages of microarray-based assays with the diversity of structures obtainable via organic synthesis. The timely discovery of the dendritic cell lectin DC-SIGN's oligosaccharide-mediated interaction with HIV's envelope protein gp120, an event that appears to enhance viral transmission to $CD4^+$ T cells[16,17], propelled us to study the glycan-dependent gp120-protein

interactions of various proteins of immunological importance involved—either directly or as potential entry inhibitors—in the HIV infection process.

2.4.4 Glycosylation and HIV

Of the many mechanisms evolved by HIV, the etiologic agent of acquired immunodeficiency syndrome (AIDS), to evade the body's numerous immunological checkpoints, glycosylation of viral proteins has emerged as a particularly efficacious roadblock to neutralizing humoral immunity[18]. The external leaflet of each HIV particle is decorated with non-covalently associated trimers of the glycoprotein gp120 in association with an integral membrane glycoprotein, gp41. Each gp120 monomer is highly glycosylated, possessing 24 conserved sites for *N*-linked glycosylation. Indeed, a fully glycosylated gp120 monomer is 50% carbohydrate by mass. A thorough analytical characterization of the glycans on HIV has revealed that of the 24 potential sites of *N*-linked glycosylation, 11 of these bear high-mannose oligosaccharides, with 50% of these high-mannose structures being $(Man)_9(GlcNAc)_2$ or $(Man)_8(GlcNAc)_2$[19]. Not only does the presence of these glycans aid in proper folding of the nascent gp120 (and gp41) polypeptide chain, it also appears to confer a distinct insulating effect to each viral particle, shielding the virus from recognition by host antibody molecules long enough for productive T cell infection to occur.

Glycan-promoted evasion of humoral immune responses is thought to occur by three main mechanisms. The first mechanism employs steric occlusion of the underlying polypeptide chain by the appended glycans: with a highly glycosylated protein, such as gp120, the glycans occupy so much space that host antibodies may not be able to physically access potential protein epitopes[20]. Second, as viruses co-opt the host's glycosylation enzymes and pool of activated carbohydrate monomers, viruses emerge from the host cell bearing host glycans; as a result, the immune system is largely unresponsive to these glycoforms, and may even actively suppress whatever immune responses are mounted. The final and most recent mechanism to emerge postulates the existence of an evolving 'glycan shield' wherein viral evolution during successive genome replications shifts the *N*-linked glycosylation sites from one region of the gp120 primary amino acid sequence to another, previously non-glycosylated, region[21]. This shifting of glycan location results in masking of previously exposed (or potentially exposed) protein epitopes by

the appended carbohydrates. Antibodies that once recognized these exposed protein epitopes are no longer efficacious as their epitope has been structurally distorted by carbohydrate. This mechanism has been invoked to explain how HIV can escape antibody neutralization even in the presence of a rigorous and prolonged humoral response.

2.4.5 Microarray Analysis of HIV-Binding Proteins

Given the significance of HIV's high-mannose glycans in aiding viral evasion of antibody neutralization and the glycans' role in other facets of the infection process, we designed a microarray study to evaluate the structural basis for various glycan-dependent protein-gp120 interactions. To give breadth to this investigation, we chose three proteins of immunological significance, the dendritic cell lectin DC-SIGN[17], the glycan-specific HIV-neutralizing antibody 2G12[22], and the T cell receptor protein CD4[23], in addition to two experimental HIV entry inhibitors, cyanovirin-N[7] and scytovirin[24]. The central aims of this study were to determine exactly which structural moieties present in high-mannose glycans were required for each protein-carbohydrate interaction investigated and to determine if CD4-gp120 interactions (glycan independent) could be inhibited by these glycan-binding proteins.

Using microarrays of immobilized mannans representing structural derivatives of $(Man)_9(GlcNAc)_2$ in addition to protein microarrays, we were able to unambiguously determine the structural basis for the protein-carbohydrate interactions studied, recognized a mechanism by which CVN may exert its HIV-inhibitory properties and identified a potential strategy for the design of an HIV vaccine aimed at eliciting a strong anti-glycan neutralizing antibody response.

2.4.6 Microarray Results and Discussion

Our first objective was to establish if the high-mannose-binding activity displayed by the proteins listed above was at all dependent on the protein context in which these glycans were presented. To this end, microarrays of natural and modified glycoproteins, as well as neoglycoproteins (where carbohydrates were chemically coupled to the protein) were printed and each slide was probed with one fluorophore-labeled protein. Among the proteins represented

were gp120, deglycosylated gp120 (p120), gp41, ovalbumin, nonamannoside-modified OVA (OVA-**2-1**), and mannosylated BSA.

2.4.6.1 Protein Microarray Analysis

As depicted in Figure 2.10a, each of the proteins with known gp120 binding activity was observed to bind the regions of the array corresponding to immobilized gp120. Of those proteins known to interact with gp120 via its high-mannose oligosaccharides (i.e., all but CD4), binding to gp120 was inhibited when incubations were performed in the presence of soluble $(Man)_9(GlcNAc)_2$ (*not shown*). Each of the five proteins was also observed to interact with gp41 and, as in the case of gp120, this activity could be blocked by soluble carbohydrate except in the case of CD4. Previous studies on CVN[25] and scytovirin[24] had demonstrated gp41-binding activity while this was the first demonstration of gp41 binding by DC-SIGN and 2G12. Whether these observed interactions have any physiological relevance remains to be seen.

2.4.6.2 Inhibition of CD4-gp120 Interactions by CVN

Taking advantage of the four-color capability of the ArrayWoRx scanner, we next conducted a series of sequential incubations to determine if any of the above glycan-binding proteins could inhibit CD4-gp120 interactions on the microarray. Two separate orders of incubation were employed for these experiments. In the first instance the protein microarrays were incubated with fluorophore-labeled inhibitor, washed extensively and then incubated with soluble CD4. Bound CD4 was then detected with a fluorophore-labeled anti-CD4 monoclonal antibody. In the second instance the order of incubations was reversed, with CD4 being applied to the microarrays first, followed by potential inhibitor. With the first incubation conditions described we found that CD4 was able to bind gp120 in all pretreated samples, suggesting that gp120 binding by these agents does not induce significant conformational changes in the CD4-binding face of gp120. Interestingly, however, we observed that when gp120 was pretreated with soluble CD4 and then incubated with CVN, CD4 was completely displaced (Figure 2.10b). In accordance with the glycan-dependent nature of CVN's binding activity, CD4 bound to nonglycosylated gp120 (p120) was not displaced by CVN. Previous mechanistic explanations

for CVN's potent inhibitory properties postulated that CVN may form aggregates on the virion surface that prevent membrane-bound receptors from interacting with their respective gp120 binding domains[26]. Our findings suggest a new mechanism in which treatment of cell-associated

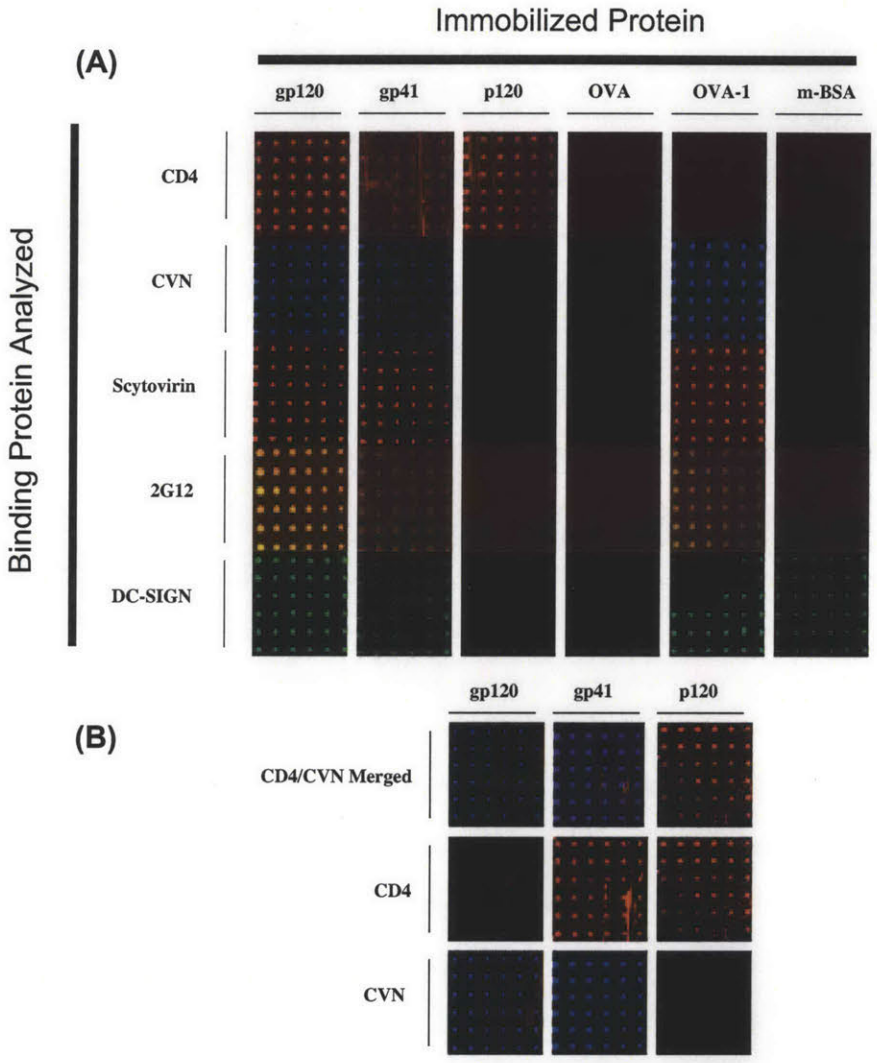

Figure 2.10 Protein microarrays reveal OVA-**2-1** binding by high-mannose specific binding proteins 2G12, CVN, scytovirin and DC-SIGN (A) and displacement of CD4 from gp120 by CVN (B). (A). Individual protein microarrays were incubated with one fluorophore-labeled protein (25 μg mL^{-1}) and scanned. Column headings designate which proteins were immobilized and row headings designate which binding protein was incubated with that array. (B). Sequential incubations with CD4 and CVN demonstrate displacement of CD4 from its complex with gp120.

(i.e., CD4-bound) gp120 with CVN induces conformational changes in gp120 that disrupt existing gp120-CD4 interactions. As our experiments were conducted with soluble CD4 and

immobilized gp120, additional inhibition experiments with cell-associated CD4 and whole virion are needed to support this mechanism.

2.4.6.3 Insights From Neoglycoproteins

The immobilization of neoglycoproteins on our microarrays made it possible to determine the influence of the peptide context in protein-carbohydrate interactions. While ovalbumin, a glycoprotein with both hybrid and complex-type oligosaccharides[5], was not bound by any of the proteins under study, ovalbumin that was chemically modified with high-mannose nonasaccharide **2-1** (OVA-**2-1**) was bound by DC-SIGN, CVN, scytovirin and the antibody 2G12. This observed binding suggests that the underlying polypeptide scaffold does not significantly influence glycan recognition by these proteins, lending support to the hypothesis that the density of carbohydrate is a greater factor in determining the affinity of protein-carbohydrate interactions.

2.4.6.4 Carbohydrate Recognition by 2G12

The human monoclonal antibody 2G12 is an interesting exception to the immunological tolerance typically displayed by the human immune system for 'self' glycans. This antibody was first isolated from a HIV-infected, long-term non-progressor and has been shown to be a potent neutralizing antibody capable of neutralizing a wide-array of primary isolates[27]. Investigations have revealed that the epitope for 2G12 is a cluster of high-mannose oligosaccharides present on the 'silent face' of gp120 which 2G12 binds with nanomolar affinity; furthermore, biochemical analysis has further revealed that Manα(1→2)Man linkages are required for 2G12 recognition of this oligosaccharide cluster[20,28]. Our observation that 2G12 bound OVA-**2-1** prompted us to ask if 2G12 would bind clusters of oligosaccharide in the absence of a polypeptide backbone. Our reasoning was that if 2G12 could bind immobilized mannans alone, a synthetic vaccine composed of high-mannose clusters may aid in generating a glycan-restricted, 2G12-like response to HIV gp120 glycans.

To address this question, microarrays were printed with structure **2-1** and five other substructures related to **2-1** (Figure 2.2). These arrays were incubated with Cy3-labeled 2G12

and the integrated fluorescence intensity of each 10 x 10 grid corresponding to a unique carbohydrate structure was measured and graphed (Figure 2.11a). Here we observed 2G12 binding at spots corresponding to structures **2-1**, **2-2**, **2-4**, **2-5**, but not to the branched

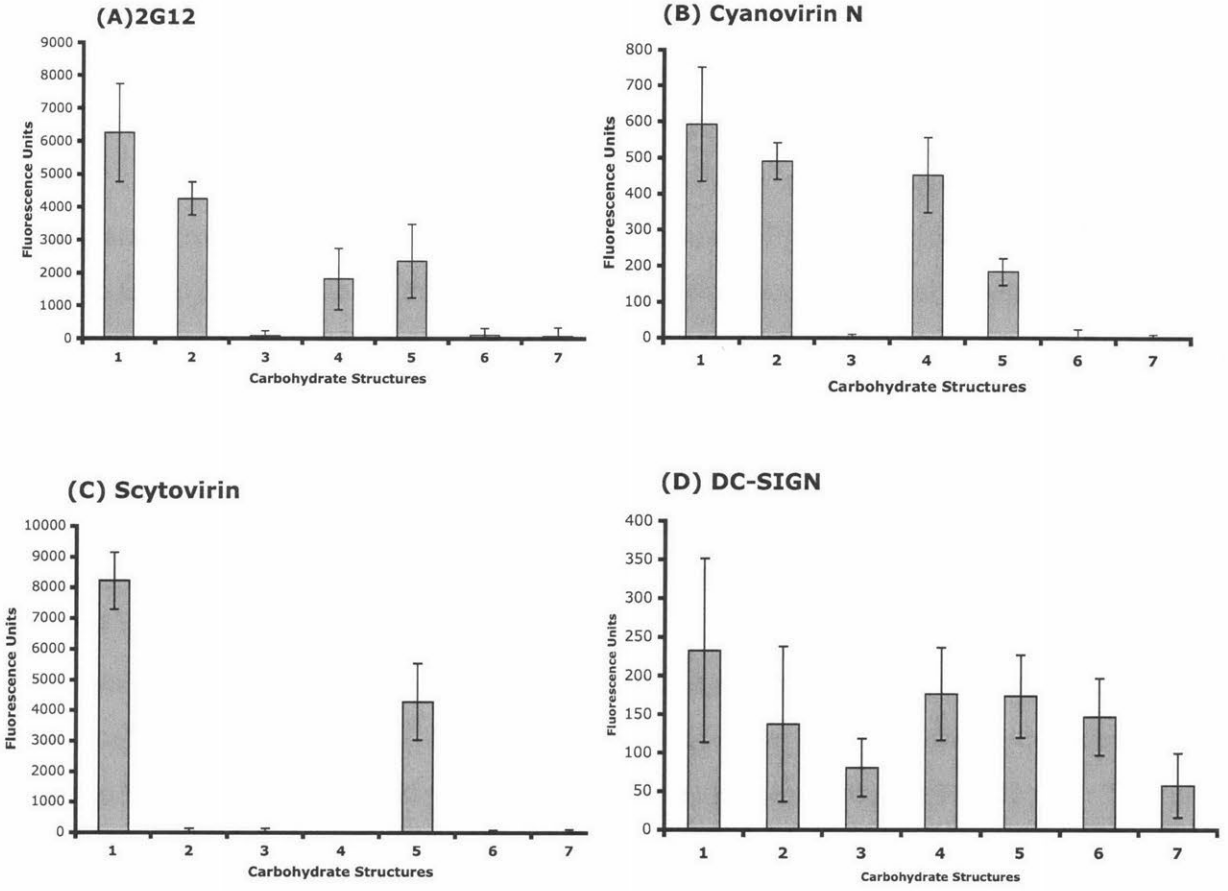

Figure 2.11 Carbohydrate microarray analysis reveals precise structural basis for high-mannose recognition by 2G12 (A), CVN (B), and scytovirin (C) and demonstrates DC-SIGN (D) recognition of clusters of linear saccharides. Microarrays were prepared with structures **2-1** thru **2-7** and analyzed for binding by the above proteins. Integrated fluorescence units for each 10 x 10 grid of immobilized structure were taken and normalized to background.

trimannoside **2-3** nor the monosaccharide mannose **2-6.** As the only common structural motif shared between saccharides **2-4** and **2-5** is the Manα(1$\rightarrow$2)Man glycosidic linkage, this result suggests that this linkage is necessary and sufficient for recognition by 2G12. Further support for this claim comes from enzymatic digest experiments wherein treatment of gp120 with an α(1$\rightarrow$2) mannosidase led to significantly diminished 2G12 binding[20]. Thus, we have rapidly confirmed, in a single microarray experiment, the importance of a particular glycosidic linkage

in carbohydrate recognition by 2G12. In addition, we were able to directly test and verify that 2G12 is capable of binding clusters of oligosaccharide in the absence of a protein scaffold.

2.4.6.5 Carbohydrate Recognition by Scytovirin

The search for inhibitors of virus-host cell fusion events has become a very active area of investigation and has lead to the identification of agents that may serve as useful prophylaxes to inhibit T cell infection by HIV. Given their accessibility and the conservation of *N*-linked glycosylation over all HIV clades, the high-mannose oligosaccharides of gp120 offer an attractive target for entry inhibitors. High-throughput screens of natural products derived from plants and from *Cyanobacteria* have discovered a variety of novel, low-molecular weight carbohydrate-binding proteins with demonstrated ability to prevent infection of HIV-susceptible T lymphocyte cell lines. More recently, the protein CVN has been shown to prevent SIV transmission in macaques when applied as a topical gel[29]. Spurred on by these results, we undertook the study of another cyanobacterial protein, scytovirin in order to establish the structural basis for its high-mannose specificity[24].

Isolated from cultures of the cyanobacterium *Scytonema varium*, scytovirin is a 9.7 kDa protein capable of protecting T-lymphoblastoid cells from HIV-1-induced cell death when applied to laboratory adapted and primary viral isolates in the range of 0.3 to 22 nM. The initial characterization of scytovirin revealed that it bound gp160, gp120 and gp41 in a manner that could be blocked by co-incubation with soluble $(Man)_9(GlcNAc)_2$, and $(Man)_8(GlcNAc)_2$, but not $(Man)_7(GlcNAc)_2$[24]. What the structural differences were between $(Man)_8(GlcNAc)_2$ and $(Man)_7(GlcNAc)_2$ that could account for the inability of $(Man)_7(GlcNAc)_2$ to inhibit scytovirin's binding were not determined.

Microarrays bearing structures **2-1** thru **2-6** were probed with Cy5-labeled scytovirin and analyzed to reveal that scytovirin, in stark contrast to CVN, the first cyanobacterial protein with demonstrated gp120-binding activity, bound only structures **2-1** and **2-5** (Figure 2.11b and c). Examination of the structural features of these two oligosaccharides strongly suggests that scytovirin recognizes the $\alpha(1\rightarrow6)$ trimannoside moiety unique to the D3 arm but that this recognition can only be achieved when the D3 arm is terminated with the natural $\alpha(1\rightarrow2)$ mannose linkage. If Man$\alpha(1\rightarrow6)$Man linkages were sufficient for scytovirin binding, protein

binding should have been observed for oligosaccharides **2-2** and **2-3** as well. Furthermore, if Manα(1→2)Man linkages were sufficient, structures **2-2** and **2-4** would have been by scytovirin. These structural subtleties point to a unique mode of carbohydrate recognition by scytovirin not shared by the high-mannose binding proteins CVN and 2G12. As shown in Figures 2.11a and 2.11b, both 2G12 and CVN recognize terminal Manα(1→2)Man irrespective of the underlying glycosidic linkages present in the D1, D2 and D3 arms of high-mannose glycans.

To provide absolute verification of the necessity of having a terminal α(1→2) mannose linkage for recognition of the D3 arm, a synthetic derivative of the D3 arm lacking this terminal linkage was prepared and screened against scytovirin, 2G12 and CVN. None of the proteins bound the truncated D3 **2-7** (Figures 2.15a, b, and c), providing direct verification of the terminal α(1→2) mannose requirement in D3 recognition by scytovirin as well as confirming the specificity of 2G12 and CVN for Manα(1→2)Man linked saccharides. To our knowledge, this mechanism of high-mannose recognition by scytovirin has not been demonstrated for any other high-mannose binding protein. It will be very interesting to learn from ongoing crystallographic and NMR studies how scytovirin's tertiary structure dictates these specific interactions with the D3 arm.

2.4.6.6 Microarray Analysis of DC-SIGN

Due to its recent identification as a glycan-dependent, high-affinity receptor for HIV on DCs, we completed our microarray study with an analysis of the DC lectin DC-SIGN[17]. DC-SIGN is a 44kDa C-type lectin expressed by dermal DCs as well as in the mucosal tissues by interstitial DCs of the lung, intestine, rectum, cervix, and placenta[30]. DC-SIGN expression is also found on DCs in the lymph nodes. While initially cloned from a human placenta cDNA library and shown to be a CD4-independent receptor for gp120, it was not until the recent identification of this lectin on DCs that its role in HIV pathology became clear[16,31]. Investigations have revealed that DC-SIGN binds gp120 in a carbohydrate dependent manner via the high-mannose oligosaccharides present on gp120[32,33]. This interaction leads to internalization of some of the captured virus by the DC to a low pH, but non-lysosomal compartment, where HIV appears to be protected from degradation and remains infection-competent for long periods

of time. Upon DC-T cell interactions, the captured virus is efficiently transferred to CD4+ T cells leading to productive infection of the recipient lymphocyte[16,34].

Overall, these events, coupled with the *in vivo* tissue expression pattern of DC-SIGN, have led to a model of sexual transmission of HIV via DC-promoted viral infection of T cells. In this model, virus present in the mucosal tissues is engaged and internalized by DC-SIGN expressing DCs; these same DCs migrate to local lymph nodes where they interact with naïve T cells and transfer captured virus particles[34,35]. This model has prompted several studies of DC-SIGN's carbohydrate binding profile, including a recent crystal structure of DC-SIGN bound to a complex oligosaccharide[32]. While this work suggested that DC-SIGN specifically recognized the branched outer trimannoside motif common to high-mannose oligosaccharides (Figure 2.2, highlighted region), other studies have shown that this same lectin is capable of high affinity interactions with branched fucosylated structures, such as the Lewis blood group determinants[36].

We used our arrays to further analyze DC-SIGN-carbohydrate interactions and determine the importance of branched glycosidic linkages for carbohydrate recognition. Incubation of the labeled-extracellular domain of DC-SIGN with carbohydrate arrays bearing structures **2-1** thru **2-7** revealed that all structures were bound by DC-SIGN (Figure 2.11d). The integrated fluorescence signals from each structure suggests that DC-SIGN binds these carbohydrates in the following order: **2-1>2-2≥2-5>2-4>2-7>2-3>2-6**. The observation that **2-3** is bound with less affinity than any of the other oligosaccharides is likely due to the stereochemistry at the reducing end. As noted in the crystal structure of DC-SIGN, a β-linkage at the anomeric carbon of the central mannose residue would cause substituents at this center to clash with Phe[32532]. This structural constraint is relieved in **2-1** and **2-2** where the core mannose of the branched outer trimannoside moiety (Figure 2.2) (Manα1-6[Manα1-3]Man) is in the α-anomeric conformation.

DC-SIGN's binding of unbranched oligosaccharides must be explained by additional protein-carbohydrate interactions. All C-type lectins studied to date bind carbohydrates through contacts promoted via calcium chelation by the 3' and 4' hydroxyl groups of the non-reducing terminal carbohydrate residue. If the unbranched oligosaccharides **2-4**, **2-5**, and **2-7** were bound by DC-SIGN in this manner, it would be expected that these structures plus monosaccharide **2-6** would be bound with similar affinities. However, the observed fluorescence intensities (Figure 2.11d) indicate that other contacts between DC-SIGN's carbohydrate recognition domain and oligosaccharides **2-4**, **2-5**, and **2-7** must occur and account for the higher affinities observed here.

2.4.7 Conclusion of Carbohydrate Microarray Study

In an effort to go beyond the simple proof-of-concept array experiments described in sections 2.2 and 2.3, we have demonstrated the utility of carbohydrate microarrays for elucidating the carbohydrate affinity and structural requirements for four glycan-depenendent gp120 binding proteins. By employing arrays bearing several unique structural constituents of high-mannose oligosaccharides it was possible to rapidly ascertain which glycosidic linkages dictated carbohydrate recognition by CVN, 2G12, and scytovirin. Analysis of the latter protein revealed a new mechanism of high-mannose recognition while our analysis of 2G12 revealed that 2G12 binds clusters of immobilized mannans in the absence of a polypeptide scaffold. We feel that this result, in combination with the synthetic derivatives of $(Man)_9(GlcNAc)_2$ used in this study, will prove to be important in aiding the design of glycan-based vaccines against HIV and other heavily glycosylated viruses. In addition to carbohydrate microarrays, the use of microarrays bearing neoglycoproteins, glycosylated and non-glycosylated proteins allowed us to investigate the influence of the peptide context in which glycans are presented. The use of these same arrays also allowed us to uncover a mechanism that may account for CVN's effectiveness as a HIV entry inhibitor.

2.4.8 Chapter Summary and Conclusions

This chapter described the development of two separate microarray systems and their use in binding studies involving carbohydrates derived from organic synthesis and various glycan-binding proteins. First, a bar-coded microsphere-based assay system that employed a fiber optic bundle detection system was described. Many significant drawbacks with this system were discovered during exploratory proof-of-concept experiments that led us to develop our own in-house assay platform to facilitate lectin screens. The platform we focused on consisted of glass slides modified to have thiol reactivity. These slides served as a substrate for printing thiol-functionalized carbohydrates with DNA array robotics. The formed arrays were probed with fluorophore-labeled proteins and analyzed with a conventional DNA array scanner. After performing routine binding studies to ensure that the specificity of carbohydrate-protein

interactions were maintained on this assay platform and that signal-to-noise ratios were high, we employed these microarrays to study various HIV gp120-binding proteins.

While the studies discussed here were rather limited in terms of the number of saccharides immobilized per array, this work nonetheless conveys the kind of structural data obtainable with carbohydrate arrays. To fully realize the potential of such arrays, improved linking chemistries that enable the facile immobilization of glycans from natural isolates will need to be developed (see D.M. Ratner Ph.D. Thesis, Chapter 4) in order to rapidly expand the diversity of oligosaccharides represented per array. As the library of structures available for microarray fabrication increases, we anticipate that these arrays will become invaluable tools for a range of applications such as epitope mapping of glycan-specific antibodies and ligand identification for cell-surface receptors.

2.5 References Cited

(1) Sharon, N.; Goldstein, I. J. *Science* **1998**, *282*, 1049.
(2) Drickamer, K.; Taylor, M. E. *Annu Rev Cell Biol* **1993**, *9*, 237-264.
(3) Drickamer, K.; Fadden, A. J. *Biochem Soc Symp* **2002**, 59-72.
(4) Figdor, C. G.; van Kooyk, Y.; Adema, G. J. *Nat Rev Immunol* **2002**, *2*, 77-84.
(5) Huang, C. C.; Montgomery, R. *Carbohydr Res* **1972**, *22*, 83-89.
(6) Ratner, D. M., Plante, O.J., Seeberger, P.H. *Eur J Org Chem* **2002**, 826-833.
(7) Boyd, M. R.; Gustafson, K. R.; McMahon, J. B.; Shoemaker, R. H.; O'Keefe, B. R.; Mori, T.; Gulakowski, R. J.; Wu, L.; Rivera, M. I.; Laurencot, C. M.; Currens, M. J.; Cardellina, J. H., 2nd; Buckheit, R. W., Jr.; Nara, P. L.; Pannell, L. K.; Sowder, R. C., 2nd; Henderson, L. E. *Antimicrob Agents Chemother* **1997**, *41*, 1521-1530.
(8) Ferguson, J. A.; Boles, T. C.; Adams, C. P.; Walt, D. R. *Nat Biotechnol* **1996**, *14*, 1681-1684.
(9) Michael, K. L.; Taylor, L. C.; Schultz, S. L.; Walt, D. R. *Anal Chem* **1998**, *70*, 1242-1248.
(10) Buskas, T.; Soderberg, E.; Konradsson, P.; Fraser-Reid, B. *J Org Chem* **2000**, *65*, 958-963.
(11) Boden, N.; Bushby, R. J.; Clarkson, S.; Evans, S. D.; Knowles, P. F.; Marsh, A. *Tetrahedron* **1997**, *53*, 10939-10952.
(12) Graves, H. C. *J Immunol Methods* **1988**, *111*, 167-178.
(13) Bolmstedt, A. J.; O'Keefe, B. R.; Shenoy, S. R.; McMahon, J. B.; Boyd, M. R. *Mol Pharmacol* **2001**, *59*, 949-954.
(14) MacBeath, G.; Schreiber, S. L. *Science* **2000**, *289*, 1760-1763.
(15) Shenoy, S. R.; Barrientos, L. G.; Ratner, D. M.; O'Keefe, B. R.; Seeberger, P. H.; Gronenborn, A. M.; Boyd, M. R. *Chem Biol* **2002**, *9*, 1109-1118.
(16) Geijtenbeek, T. B.; Kwon, D. S.; Torensma, R.; van Vliet, S. J.; van Duijnhoven, G. C.; Middel, J.; Cornelissen, I. L.; Nottet, H. S.; KewalRamani, V. N.; Littman, D. R.; Figdor, C. G.; van Kooyk, Y. *Cell* **2000**, *100*, 587-597.
(17) Geijtenbeek, T. B.; Torensma, R.; van Vliet, S. J.; van Duijnhoven, G. C.; Adema, G. van Kooyk, Y.; Figdor, C. G. *Cell* **2000**, *100*, 575-585.
(18) Poignard, P.; Saphire, E. O.; Parren, P. W.; Burton, D. R. *Annu Rev Immunol* **2001**, *19*, 253-274.
(19) Mizuochi, T.; Spellman, M. W.; Larkin, M.; Solomon, J.; Basa, L. J.; Feizi, T. *Biomed Chromatogr* **1988**, *2*, 260-270.
(20) Scanlan, C. N.; Pantophlet, R.; Wormald, M. R.; Ollmann Saphire, E.; Stanfield, R.; Wilson, I. A.; Katinger, H.; Dwek, R. A.; Rudd, P. M.; Burton, D. R. *J Virol* **2002**, *76*, 7306-7321.
(21) Wei, X.; Decker, J. M.; Wang, S.; Hui, H.; Kappes, J. C.; Wu, X.; Salazar-Gonzalez, J. F.; Salazar, M. G.; Kilby, J. M.; Saag, M. S.; Komarova, N. L.; Nowak, M. A.; Hahn, B. H.; Kwong, P. D.; Shaw, G. M. *Nature* **2003**, *422*, 307-312.
(22) Armbruster, C.; Stiegler, G. M.; Vcelar, B. A.; Jager, W.; Michael, N. L.; Vetter, N.; Katinger, H. W. *Aids* **2002**, *16*, 227-233.

(23) McDougal, J. S.; Maddon, P. J.; Dalgleish, A. G.; Clapham, P. R.; Littman, D. R.; Godfrey, M.; Maddon, D. E.; Chess, L.; Weiss, R. A.; Axel, R. *Cold Spring Harb Symp Quant Biol* **1986**, *51 Pt 2*, 703-711.
(24) Bokesch, H. R.; O'Keefe, B. R.; McKee, T. C.; Pannell, L. K.; Patterson, G. M.; Gardella, R. S.; Sowder, R. C., 2nd; Turpin, J.; Watson, K.; Buckheit, R. W., Jr.; Boyd, M. R. *Biochemistry* **2003**, *42*, 2578-2584.
(25) O'Keefe, B. R.; Shenoy, S. R.; Xie, D.; Zhang, W.; Muschik, J. M.; Currens, M. J.; Chaiken, I.; Boyd, M. R. *Mol Pharmacol* **2000**, *58*, 982-992.
(26) Esser, M. T.; Mori, T.; Mondor, I.; Sattentau, Q. J.; Dey, B.; Berger, E. A.; Boyd, M. R.; Lifson, J. D. *J Virol* **1999**, *73*, 4360-4371.
(27) Trkola, A.; Purtscher, M.; Muster, T.; Ballaun, C.; Buchacher, A.; Sullivan, N.; Srinivasan, K.; Sodroski, J.; Moore, J. P.; Katinger, H. *J Virol* **1996**, *70*, 1100-1108.
(28) Calarese, D. A.; Scanlan, C. N.; Zwick, M. B.; Deechongkit, S.; Mimura, Y.; Kunert, R.; Zhu, P.; Wormald, M. R.; Stanfield, R. L.; Roux, K. H.; Kelly, J. W.; Rudd, P. M.; Dwek, R. A.; Katinger, H.; Burton, D. R.; Wilson, I. A. *Science* **2003**, *300*, 2065-2071.
(29) Tsai, C. C.; Emau, P.; Jiang, Y.; Tian, B.; Morton, W. R.; Gustafson, K. R.; Boyd, M. R. *AIDS Res Hum Retroviruses* **2003**, *19*, 535-541.
(30) Soilleux, E. J.; Barten, R.; Trowsdale, J. *J Immunol* **2000**, *165*, 2937-2942.
(31) Curtis, B. M.; Scharnowske, S.; Watson, A. J. *Proc Natl Acad Sci U S A* **1992**, *89*, 8356-8360.
(32) Feinberg, H.; Mitchell, D. A.; Drickamer, K.; Weis, W. I. *Science* **2001**, *294*, 2163-2166.
(33) Mitchell, D. A.; Fadden, A. J.; Drickamer, K. *J Biol Chem* **2001**, *276*, 28939-28945.
(34) Borleffs, J. C.; Boucher, C. A. *Ned Tijdschr Geneeskd* **2000**, *144*, 786-788.
(35) Steinman, R. M. *Cell* **2000**, *100*, 491-494.
(36) Appelmelk, B. J.; van Die, I.; van Vliet, S. J.; Vandenbroucke-Grauls, C. M.; Geijtenbeek, T. B.; van Kooyk, Y. *J Immunol* **2003**, *170*, 1635-1639.

Chapter 3

Oligosaccharide-Mediated Targeting of Dendritic Cells

3.1 Abstract

Harnessing the unique immunological properties of dendritic cells (DCs) for the treatment of allergy, autoimmunity and transplant rejection is predicated upon our ability to selectively deliver antigens, drugs and nucleic acids (e.g., antisense or short-interfering RNA sequences) to DCs *in vivo*. This chapter describes a method for delivering whole protein antigens to DCs based on carbohydrate-mediated targeting of DC lectins. A series of synthetic carbohydrates were chemically-coupled to a model antigen, ovalbumin (OVA), and evaluated for their ability to increase the efficiency of antigen presentation by DCs to OVA-specific T cells ($CD4^+$ and $CD8^+$). *In vitro* data is presented demonstrating that carbohydrate modification of OVA leads to a 50-fold enhancement of presentation of antigenic peptide to $CD4^+$ T cells. A 10-fold enhancement is observed for $CD8^+$ T cells, indicating that the targeted lectin(s) can achieve cross-presentation of peptides to MHC class I restricted cells. Importantly, our data indicate that the observed enhancements are unique to the complex oligosaccharides utilized here, as monosaccharide-modified OVA did not lead to significant presentation enhancement. *In vivo* targeting of DCs with one carbohydrate, a synthetic derivative of the high-mannose nonasaccharide $(Man)_9(GlcNAc)_2$, resulted in OVA-specific T cell expansion with sub-microgram quantities of antigen. After this initial expansion, however, the T cells become unresponsive to rechallenge of antigen in highly stimulatory adjuvant. We conclude that targeting of DC lectins in the steady state via conjugates of the type described here leads to a state of antigen-specific T cell tolerance.

3.2 Introduction

In recent years the dual immunological function of DCs has become increasingly appreciated (Chapter 1, section 1.4.3)[1]. On the one hand, DCs are the most potent of the professional antigen-presenting cells (APCs) in initiating immune responses to pathogens; in the absence of infection, however, DCs play a second, crucial role of maintaining peripheral tolerance by regulating the numbers and states of self-reactive T cells. Given the importance of DCs in orchestrating the human immune system along these two paths, strategies that can selectively access these different functions will greatly advance immunotherapy and facilitate the

design of more rational, mechanistic vaccines. The selective modulation of DC function in the steady state, however, will depend upon our ability to specifically target DCs/DC subsets.

One approach to accessing DCs *in vivo* consists of targeting DC-specific surface receptors with ligand-antigen or ligand mimetic-antigen conjugates that deliver targeted antigens to the antigen processing/presentation machinery of DCs via receptor-mediated endocytosis. One such manifestation of this strategy involves chemically coupling an antibody against a defined DC surface receptor to an antigen of interest. Antibody targeting of the DC integrin CD11c, for example, has been reported to dramatically improve the kinetics and quality of antibody responses against a model antigen in mice[2]. At the other end of the immunological spectrum of responses, Steinman and colleagues targeted the C-type lectin DEC-205 with anti-DEC-205-antigen conjugates and demonstrated the DC-mediated induction of T cell tolerance (see Chapter 1, section 1.4.3.2)[3-5]. These studies demonstrate that targeting DCs *in vivo* can lead to defined immunological outcomes, and serve to underscore the fact that targeting different receptors on the same cell type can produce dramatically different results. This latter facet is probably due in large part to the differential activation of signal transduction pathways downstream of receptor ligation.

While antibodies can offer unparalleled specificity for their cognate antigens, as a therapeutic agent they have the distinct disadvantages of being very expensive to produce and immunogenic in many patients. In addition to these issues, there may be circumstances in which more versatile chemistries are required for the formation of an antigen conjugate than those offered by the antibody's protein sequence. Thus, a need exists for developing robust, therapeutically useful methods of accessing DCs *in vivo*.

Here we explore the use of synthetic carbohydrate structures as an alternative to antibody-based targeting of DCs. As discussed in Chapter 1 (section 1.4.3.2 & Figure 1.4), DCs express a number of cell surface lectins of the C-type class that recognize carbohydrate ligands appended to glycoproteins and, in some cases, mediate adsorptive uptake of bound ligand. With carbohydrate chemistry at a stage where biologically useful quantities of complex oligosaccharide can be routinely prepared[6] and with glycan microarrays that can aid in the determination of highly specific lectin-ligand interactions[7], the requisite tools are in place to pursue a DC targeting strategy founded upon lectin-carbohydrate interactions.

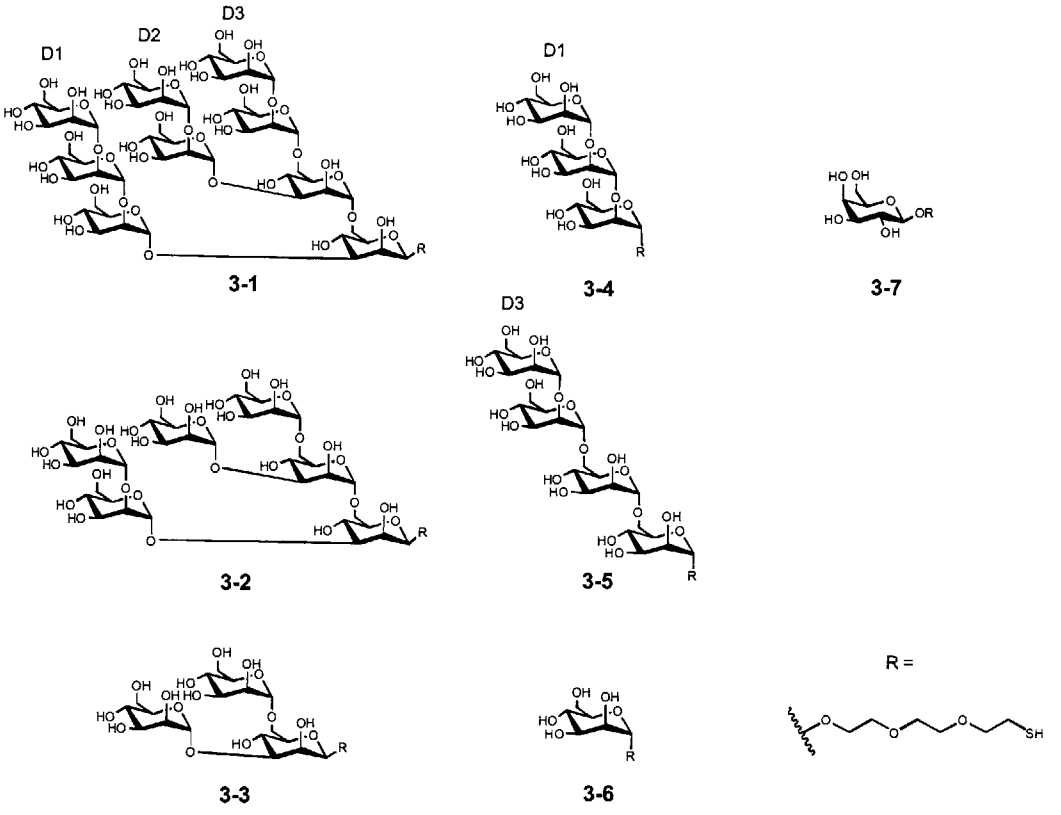

Figure 3.1 Synthetic analogs of the high-mannose oligosaccharide $(Man)_9(GlcNAc)_2$ used in the preparation of ovalbumin conjugates for dendritic cell targeting. These structures were chosen for DC targeting on the basis of their recognition by the DC lectin, DC-SIGN. The panel of structures consists of three branched oligosaccharides (**3-1** thru **3-3**), two linear trisaccharides (**3-4** and **3-5**) derived from the D1 and D3 arms of the high-mannose nonasaccharide and two monosaccharides, mannose **3-6** and galactose **3-7**. Conjugation of each structure was made possible by the incorporation of a thiol-bearing linker (shown as 'R' here).

3.3 Results

Inspired by our microarray study of the DC lectin DC-SIGN, wherein we observed lectin recognition of proteins chemically modified with structure **3-1** (Figure 3.1 and Chapter 2, Figure 2.10), we proposed to use high-mannose oligosaccharides to target DCs. For this work we decided to work with mouse DCs and T cells (see Materials and Methods for details) as this would give us the opportunity to track the T cell responses to DC-presented antigen in a physiological *in vivo* setting. The following sections detail the *in vitro* evaluation of these conjugates' ability to enhance presentation of antigenic peptides to T cells and the application of these conjugates in an *in vivo* setting.

3.3.1 Carbohydrate Modification of a Model Antigen Leads to Enhanced Presentation

To examine the ability of high-mannose oligosaccharide-antigen conjugates to engage DC surface receptors such as lectins and lead to presentation through the MHC class I and class II pathways, we prepared a series of ovalbumin (OVA) conjugates bearing structures **3-1** thru **3-7**. OVA is a useful model antigen to work with as it is known to be presented on H-2K^b MHC class I molecules to CD8$^+$ T cells and I-A^b MHC class II molecules to CD4$^+$ T cells[4]; transgenic mice bearing only these T cell receptor specificities have been generated and were employed here to monitor the T cell responses to DC-presented peptides.

OVA was modified with the heterobifunctional crosslinker SMCC to introduce maleimide functional groups; incubation with thiol-bearing saccharides **3-1** thru **3-7** lead to the formation of carbohydrate-OVA conjugates with an average coupling efficiency of 40% (Figure 3.2 A). An average of 3 saccharides were added per molecule of OVA, leading to a change in OVA molecular weight from 45 kDa to 48-50 kDa, depending on the appended structure.

We assessed the ability of these conjugates to enhance antigen uptake by DCs in comparison to unmodified OVA by incubating graded doses of conjugate and OVA with unfractionated splenocytes (containing T cells, B cells, DCs, macrophages) isolated from OTII (CD4$^+$) transgenic mice. The ability of DCs to present antigenic peptides derived from targeted proteins was measured as a function of T cell proliferation in response to those presented peptides. T cell proliferation is quantified by [^{3}H]thymidine incorporation during cellular division. All conjugates tested resulted a reproducible enhancement of antigen uptake and presentation to T cells when compared to unmodified OVA over the same dosage range (Figure 3.2 B). Among the structures tested, the nonasaccharide **3-1** led to the greatest enhancement of T cell proliferation compared to OVA. To verify that this enhancement was due to the carbohydrate moiety attached to OVA, we incubated splenocytes with conjugate (OVA)-**3-1** in the presence and absence of an unrelated protein, bovine serum albumin (BSA) that was also modified with **3-1**. As peptides derived from BSA cannot be recognized by the transgenic OTII cells, competitive inhibition of OVA-**3-1** uptake by (BSA)-**3-1** leads to a corresponding diminution of OTII proliferation (Figure 3.2 C), indicating that uptake of (OVA)-**3-1** is due to the appended oligosaccharide. Co-incubation of unmodified BSA did not affect (OVA)-**3-1**

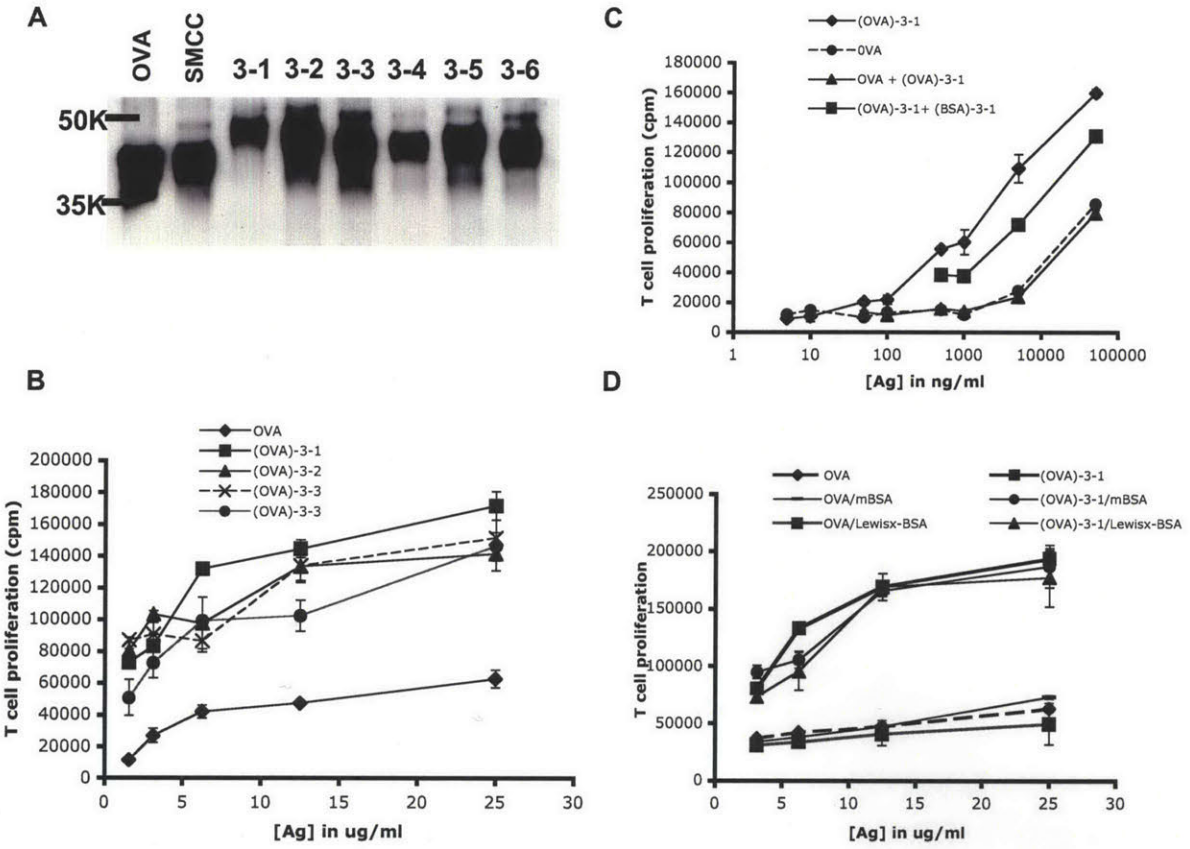

Figure 3.2 Carbohydrate modification of OVA leads to enhanced presentation to antigen specific T cells. (A) OVA, SMCC-activated OVA and carbohydrate modified OVA were resolved by SDS-PAGE electrophoresis and immunoblotted with anti-OVA polyclonal antibody to reveal changes in molecular weight as a function of carbohydrate addition. (B) Oligosaccharide modification of OVA elicits stronger presentation to OTII T cells than unmodified OVA. Unfractionated OTII splenocytes (3 x 10^5/well) were incubated with graded doses of OVA or oligosaccharide-modified OVA for 84 hours with [^{3}H]thymidine (1μCi) added for the last 12 hours. Thereafter [^{3}H]thymidine incorporation levels were measured and plotted. (C) Observed enhancements in antigen presentation of (OVA)-**3-1** to T cells is carbohydrate dependent. Splenocytes were incubated with antigen as in (B) ± (BSA)-**3-1** (10 μg mL^{-1}). In cases where (OVA)-**3-1** was added to OVA wells to assess the possibility of direct activation of T cells (see text), (OVA)-**3-1** was present at 50 ng mL^{-1}; incubations were performed for 72 hours with [^{3}H]thymidine (1μCi) added for the last 12 hours. (D) The receptor mediating uptake of (OVA)-**3-1** has a different binding profile than that observed for DC-SIGN. Unfractionated splenocytes were incubated with OVA or (OVA)-**3-1** ± mBSA or Lewis^x-BSA (each at 100 μg mL^{-1}). Incubations were performed for 72 hours with [^{3}H]thymidine (1μCi) added for the last 12 hours. All values reported are the mean of triplicate measurements.

promoted enhancements (not shown). To ensure that our (OVA)-**3-1** conjugate was not directly activating T cells and inducing their proliferation, we added a small amount (0.05 μg mL^{-1}) to the

graded doses of unmodified OVA. If (OVA)-**3-1** directly activated T cells we would detect an enhanced level of T cell proliferation across the graded does of OVA compared to just OVA alone. Our results indicate that this does not occur (Figure 3.2 C) as the T cell response curves for OVA vs. OVA + (OVA)-**3-1** are identical. Furthermore, the addition of (OVA)-**3-1** to purified T cells in the absence of APCs does not lead to T cell proliferation nor does it enhance the mixed leukocyte reaction between DCs and allogeneic T cells (not shown), evidence that these conjugates do not directly activate T cells or DCs.

Our previous microarray analysis of glycan binding by DC-SIGN revealed that DC-SIGN can recognize both complex branched mannans like **3-1** and **3-2** as well as dense arrays of linear oligosaccharides and simple monosaccharides (Chapter 2, Figure 2.11). In addition, carbohydrate profiling by another group has revealed that DC-SIGN can recognize non-sialylated Lewis blood group antigens (e.g. Lewis^x)[8]. As five murine homologs of DC-SIGN have been described[9], with one homolog, CIRE, being expressed exclusively in CD8α^-CD4$^+$ and CD8α^-CD4$^-$ DCs[10], we wished to address the possibility that a lectin with a DC-SIGN-like binding profile may be mediating the recognition and uptake of (OVA)-**3-1**. To this end, we incubated splenocytes with (OVA)-**3-1** in the presence or absence of mannose-derivatized BSA (mBSA) or Lewis^x-modified BSA (Lewis^x-BSA) and measured the ability of these conjugates to inhibit uptake of (OVA)-**3-1** (Figure 3.2 D). Neither mBSA nor Lewis^x-BSA appeared to significantly impair endocytosis and presentation of (OVA)-**3-1** to OTII T cells, suggesting that neither of these conjugates serve as a ligand for the receptor mediating uptake of (OVA)-**3-1**.

Accessing the transporter of antigenic peptides (TAP) and thereby achieving cross-presentation of antigen by DCs to MHC class I restricted CD8$^+$ T cells leads to efficient stimulation of these T cells and, in the steady state, their apoptotic deletion from the T cell repertoire[4]. To determine if the receptor promoting (OVA)-**3-1** uptake can process proteins through the MHC class I pathway, we incubated (OVA)-**3-1** and OVA with unfractionated splenocytes isolated from OTI (CD8$^+$) mice. The T cells from transgenic OTI mice recognize an eight amino acid residue sequence (SIINFEKL) derived from OVA and can therefore be utilized to gauge the efficiency of DC presentation of MHC class I antigenic peptides. We observed a moderate (10-fold) increase in the efficiency of MHC class I presentation with (OVA)-**3-1** compared to OVA alone (Figure 3.3 A). Inhibition of this enhancement is again achieved by co-

incubation with (BSA)-**3-1** and, as shown for OTII T cells, (OVA)-**3-1** does not appear to achieve this enhancement via direct activation of T cells. As all of our ensuing work focused on

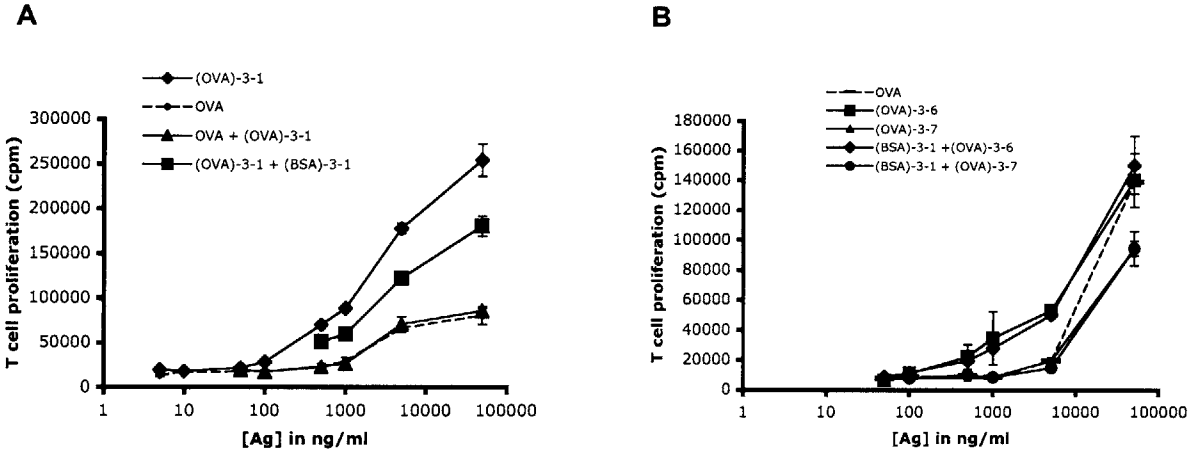

Figure 3.3 Nonasaccharide **3-1**-promoted presentation via MHC class I pathway for presentation to $CD8^+$ T cells. (A) (OVA)-**3-1** enhances presentation of antigenic peptides to $CD8^+$ T cells in a dose- and carbohydrate-dependent fashion. Unfractionated OTI splenocytes (3 x 10^5/well) were incubated with graded doses of OVA ± (OVA)-**3-1** (50 ng mL^{-1}) or (OVA)-**3-1** ± (BSA)-**3-1** (10 μg mL^{-1}). Incubations were performed for 72 with [^{3}H]thymidine (1μCi) added for the last 12 hours. (B) The monosaccharide mannose **3-6** targets a different receptor than **3-1**. OTII splenocytes were incubated with graded doses of monosaccharide-modified OVA ± (BSA)-**3-1** and T cell proliferation was measured as in (A). Values present the mean of triplicate measurements.

the $CD4^+$ responses to DC-presented antigen, we have not been able to establish if the 10-fold enhancement observed here at lower antigen concentrations will translate to an *in vivo* enhancement compared to similar amounts of OVA.

In an effort to determine if the increased efficiencies of antigen presentation obtained via (OVA)-**3-1** could be attained via simple monosaccharide-antigen conjugates, we repeated our splenocyte incubations with (OVA)-**3-6** and (OVA)-**3-7** (Figure 3.3 B). We found that the monosaccharide mannose **3-6** only weakly enhanced presentation to $CD4^+$ T cells while galactose **3-7** did not aid promote increased presentation at all compared to unmodified OVA. Interestingly, co-incubation of (OVA)-**3-6** with (BSA)-**3-1** did not inhibit the uptake of (OVA)-**3-6**, indicating that the monosaccharide **3-6** and the more complex **3-1** are likely to interact with different DC receptors.

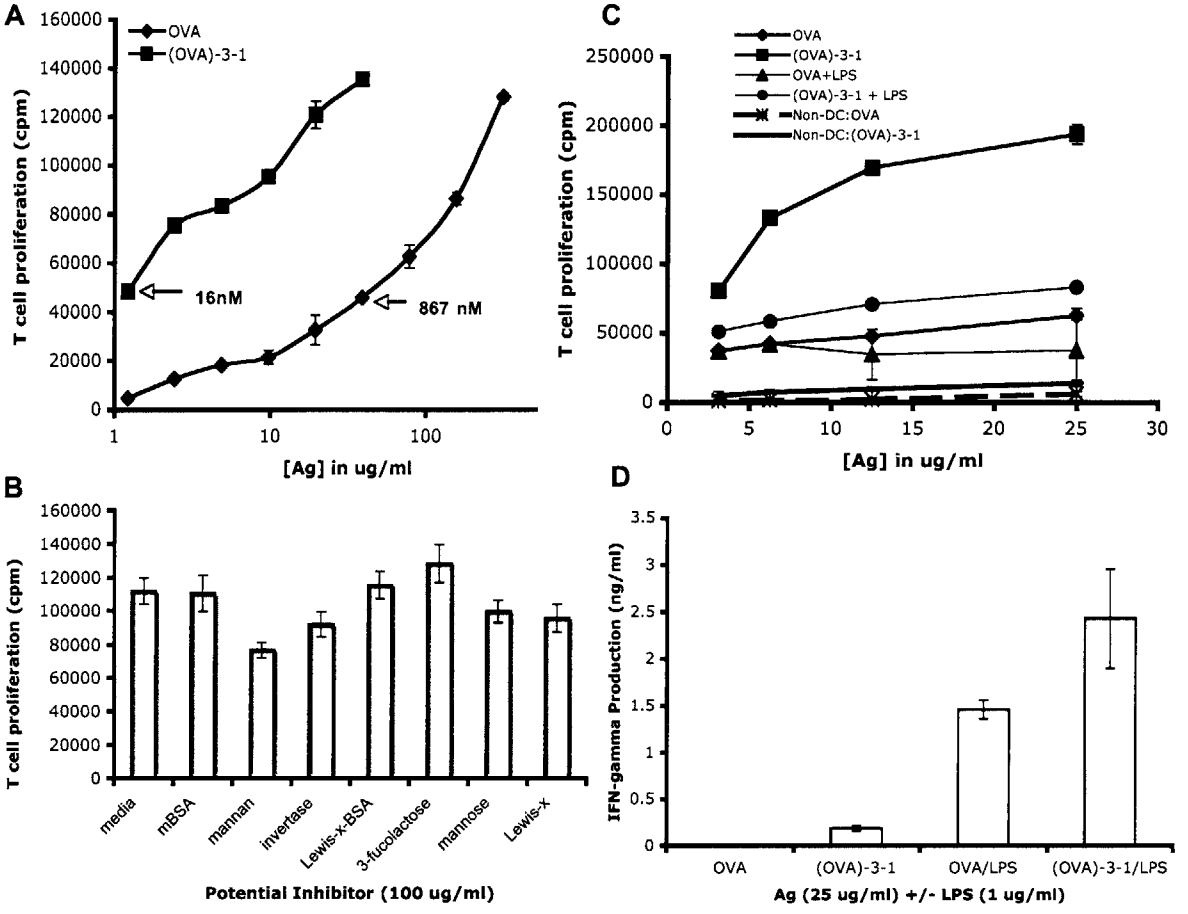

Figure 3.4 CD11c$^+$ DCs are the main APC presenting **3-1**-targeted antigen. (A) Purified CD11c$^+$ DCs efficiently present (OVA)-**3-1** to purified CD4$^+$ T cells. 1.5 x 10^4 Splenic CD11c$^+$ DCs purified from C57BL/6 mice and 3.0 x 10^4 purified OTII T cells were incubated with OVA (starting concentration 300 μg mL^{-1}) or (OVA)-**3-1** (starting concentration 25 μg mL^{-1}) in graded doses for 84 hours with [^{3}H]thymidine (1μCi) added for the last 12 hours. (B) The receptor mediating uptake of (OVA)-**3-1** preferentially binds complex mannans. Purified CD11c$^+$ DCs and OTII T cells were incubated with (OVA)-**3-1** (25 μg mL^{-1}) ± each potential inhibitor (100 μg mL^{-1}). T cell proliferation was determined as in (A). (C) Toll-like receptor induced DC maturation significantly decreases uptake and presentation of (OVA)-**3-1** to T cells. CD11c$^+$ DCs and OTII T cells were incubated with OVA or (OVA)-**3-1** ± lipopolysaccharide (1 μg mL^{-1}). Also included are all 'non-DCs' (macrophages and B cells) obtained during the purification of the DCs . T cell proliferation was determined as in (A). (D) Targeting (OVA)-**3-1** to DCs leads to a more vigorous T cell response in a highly pro-inflammatory situation. Supernatants from (C) were collected at 48 and 72 hrs and measured for IFN-γ by ELISA; the values presented are from the 72 hour time point. All measurements here were performed in triplicate.

3.3.2 Enhanced T Cell Proliferation is Due to Uptake Exclusively by CD11c$^+$ DCs

To confirm that the increased T cell proliferation observed with (OVA)-**3-1** was due to the selective uptake of this conjugate by DCs and not B cells or macrophages, we prepared purified CD11c$^+$ DCs from wild-type C57BL/6 mice and the OVA-specific T cells from transgenic OTII mice (see Materials & Methods) and repeated the *in vitro* antigen presentation assays as described above. A parallel titration series of (OVA)-**3-1** and unmodified OVA revealed that CD11c$^+$ DCs are highly efficient at capturing and presenting (OVA)-**3-1** compared to soluble OVA, even at concentrations as low as 16 nM (Figure 3.4 A). By comparison, it required > 50-fold more unmodified OVA to obtain similar levels of T cell proliferation. When B cells and macrophages were used as APCs in place of purified DCs, the resulting T cell responses were negligible (Figure 3.4 C), providing strong confirmation that CD11c$^+$ DCs are the main APC mediating uptake and presentation of (OVA)-**3-1** to OTII T cells. This latter result is also very strong confirmation that (OVA)-**3-1** does not directly activate T cells; if direct activation of T cells by (OVA)-**3-1** was operative, the levels of T cell proliferation observed here should have equaled the levels observed when DCs are used as the APC.

In our previous attempts to inhibit (OVA)-**3-1** internalization with mBSA and Lewis^x-BSA (Figure 3.2 D) we may have missed the inhibitory effect of these molecules due to their potential effects on other non-DC cell types present in the splenocyte population. To address this possibility and to try other potential inhibitors of (OVA)-**3-1** internalization, we repeated the inhibition experiment with purified DCs and T cells (Figure 3.4 B). As in our previous experiments, neither mBSA nor Lewis^x-BSA were inhibitory; even when utilized at a > 300-fold excess over (OVA)-**3-1**, soluble Lewis^x had marginal effects on (OVA)-**3-1** presentation by DCs. Likewise, a 1000-fold excess of soluble mannose only reduced conjugate presentation by 10%. More inhibitory were the complex mannan derived from *Saccharomyces cerevisiae* (31%) and the high-mannose-bearing glycoprotein invertase (18%). The inhibition of (OVA)-**3-1** presentation with an invertase concentration of 0.5μM compared to the 0.55 mM mannose concentration required to achieve similar levels of inhibition further underscores the specificity exhibited by the high-mannose oligosaccharide receptor on DCs. Incubation with the common milk oligosaccharide, 3-fucosyllactose (3-FL) had no inhibitory action; in fact, we observed a slight increase in T cell proliferation with 3-FL (14%). It is premature to speculate on the

relevance of this enhancement, as more experiments are required to determine if this is due to an effect of 3-FL at the DC or T cell level.

As some DC lectins are known to be strongly down-regulated upon toll-like receptor (TLR) engagement with bacterial agonists[10,11], we wished to determine if the receptor mediating (OVA)-**3-1** uptake was similarly down-regulated upon TLR engagement or if DC maturation induced by TLR agonists would further augment the presentation of (OVA)-**3-1** to OTII T cells. An *in vitro* presentation assay was performed in which lipopolysaccharide (LPS), a potent agonist of the toll-like receptor 4 signaling pathway[12], was added to graded doses of OVA or (OVA)-**3-1** (Figure 3.4 C). In agreement with what has been reported for the macrophage mannose receptor[11] and the DC-SIGN murine homolog CIRE, wherein TLR agonists led to dramatically decreased mRNA production for each lectin, we observed a significant decrease (60%) in presentation of (OVA)-**3-1** to T cells as a result of TLR-mediated DC maturation. In the case of unmodified OVA, TLR activation led to a 30% decrease in antigen presentation to OTII T cells. This is likely due to a decrease in macropinocytosis by DCs on the path to terminal differentiation.

It is interesting to note that despite the significant diminution of (OVA)-**3-1** presentation by DCs upon TLR-4 stimulation, targeting with nonasaccharide **3-1** was still better than unmodified OVA. This implies that antigen capture of (OVA)-**3-1** by DCs prior to full maturation is considerably more efficient than unmodified OVA; this fact is further strengthened by analysis of pro-inflammatory IFN-γ production by responding OTII T cells (Figure 3.4 D) where we observe an average of 40% less IFN-γ produced by T cells responding to OVA vs. (OVA)-**3-1**.

3.3.3 Both CD8α$^+$ and CD8α$^-$ DC Subsets Can Present Carbohydrate-Modified Antigen

Having established that DCs are the main APC capable of capture, processing, and presentation of (OVA)-**3-1**, our next objective was to establish if any particular subset of DCs was responsible for this activity. In the mouse, there are three subsets of DCs defined by their expression of the cellular antigens CD8 and CD4, namely CD8α$^+$CD4$^-$, CD8α$^-$CD4$^+$, and CD8α$^-$ CD4$^-$[13,14]. Many functional differences among these subsets have been described and it has been argued that the CD8α$^+$ subset may be solely responsible for maintaining peripheral tolerance

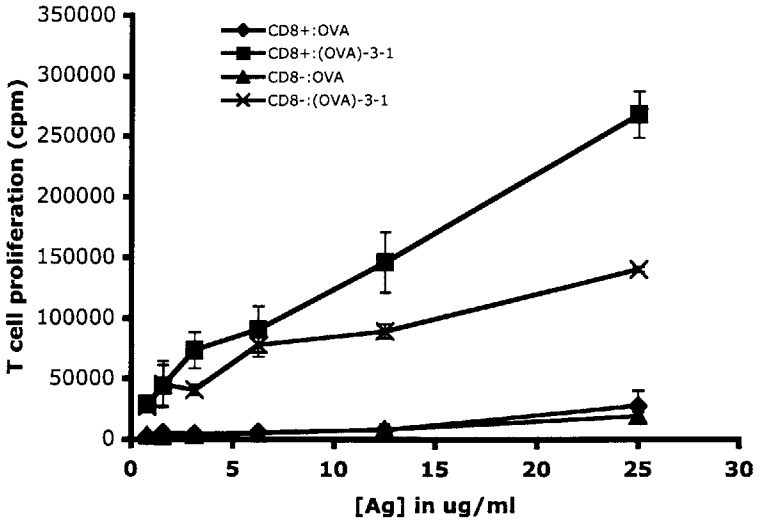

Figure 3.5 Both DC subsets can present (OVA)-**3-1**. CD11c$^+$ DCs were stained with antibody against CD8α and I-A^b MHC class II molecules and sorted into their respective CD8α$^+$ and CD8α$^-$ populations. 2 x 10^4 cells of each subtype were incubated with 1 x 10^5 purified OTII T cells with graded doses of OVA or (OVA)-**3-1** for 84 hours with [^{3}H]thymidine (1μCi) added for the last 12 hours. All data points were performed in triplicate.

while the CD8α$^-$ subset induces immunity to captured antigen[15] To determine if the high-mannose receptor was restricted to a particular subset, we used a fluorescence cell sorter to separate DCs into their respective CD8α$^+$ and CD8α$^-$ subsets and tested each subset for its ability to present OVA and (OVA)-**3-1** to OTII T cells (Figure 3.5). We were surprised to learn that while OVA is only weakly presented to T cells by the individual subsets, (OVA)-**3-1** is presented by each subset, with the CD8α$^+$ subset being approximately 2-fold more efficient than the CD8α$^-$ subset. Thus, we conclude that both DC subsets express a receptor capable of binding nonasaccharide **3-1** and mediating uptake of antigens modified with this oligosaccharide.

3.3.4 *In Vivo* Targeting of DCs Leads to Efficient Antigen-Specific T Cell Activation

In order to determine what the immunological implications of (OVA)-**3-1** internalization and presentation by DCs may be *in vivo*, we employed the technique of adoptive transfer (Figure 3.6 A) to track the T cell responses to DC presented antigen[16]. In this technique, ovalbumin-specific transgenic CD4$^+$ T cells expressing a specific isoform of the surface antigen CD45 (designated CD45.2) are injected intravenously into a strain of mice that is genetically identical

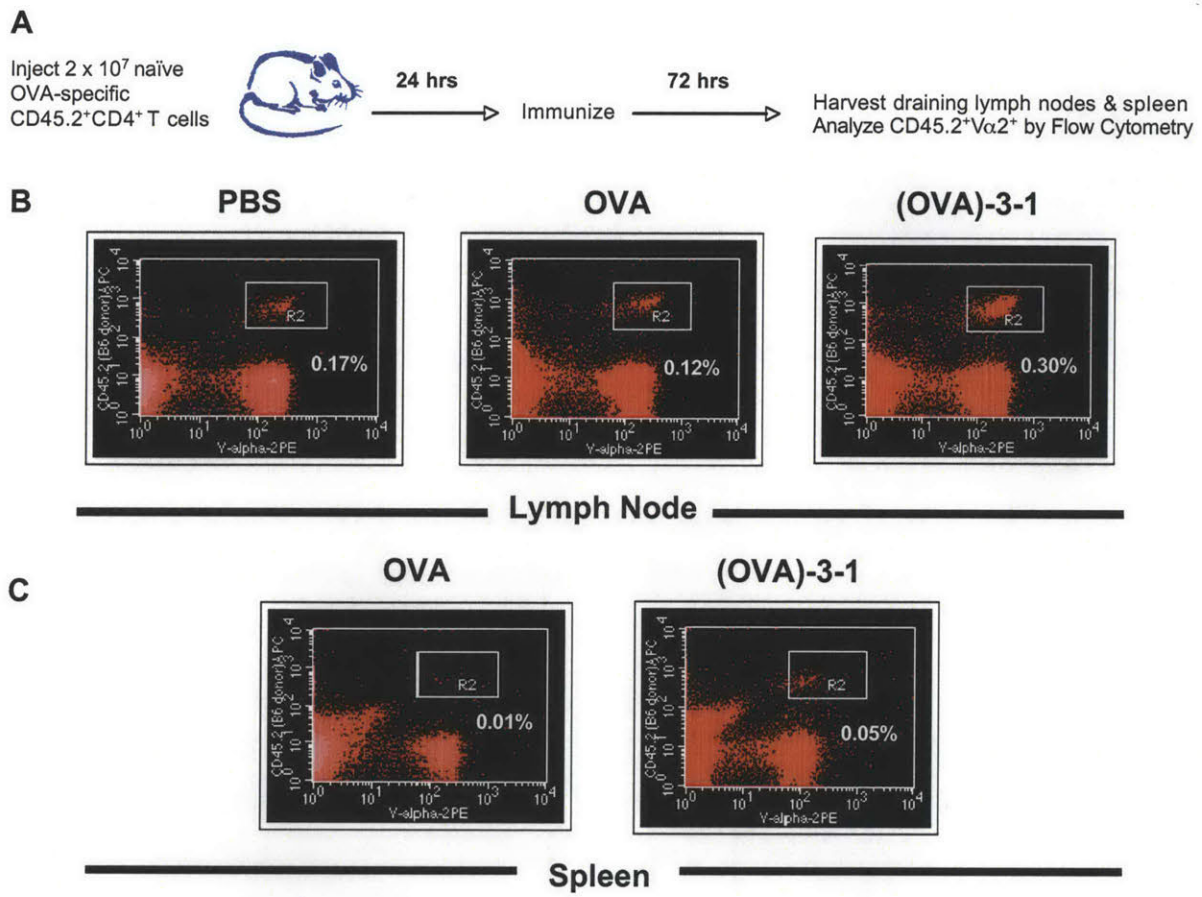

Figure 3.6 Targeting of DCs *in vivo* with (OVA)-**3-1** leads to antigen-specific T cell activation. (A) Schematic of the adoptive transfer technique: $CD4^+CD45.2^+$ ovalbumin-specific T cells are adoptively transferred to congenic $CD45.1^+$ recipients. After immunization the draining lymph nodes and other lymph organs (e.g., the spleen) are isolated. Cells from these tissues are stained with antibody against the CD45.2 isoform and the OTII T cell receptor to identify the original donor cells. (B) Immunization with (OVA)-**3-1** promotes expansion of OVA-specific T cells. B6.Ly5.2/Cr mice were injected intravenously with 2×10^7 OTII splenocytes. 24 hours later the mice were injected subcutaneously with PBS, OVA (200 ng), or (OVA)-**3-1** (200 ng). 3 days after immunization, draining inguinal lymph nodes and spleen (C) were isolated and the expansion of $CD45.2^+V\alpha2$ cells was evaluated by flow cytometry. Each panel represents two or more experiments.

except at the CD45 locus. Using antibodies against the CD45.2 isoform expressed by the donor T cells, one can easily distinguish these cells from recipient cells during the course of an experiment.

$CD45.2^+$ OVA-specific T cells were transferred to B6.Ly5.2/Cr ($CD45.1^+$) recipients and, after a 24-hour rest period, the mice were immunized subcutaneously with PBS, OVA or (OVA)-**3-1**. After 72 hours, cells were isolated from the draining inguinal lymph nodes and counted by

FACS to determine the extent of OTII cell division induced by the immunization regimen (Figure 3.6 B). Immunization with the (OVA)-**3-1** conjugate led to proliferation of OTII specific T cells in the draining lymph node, with a doubling of total OTII cell number compared to soluble OVA. In addition, we observe an appreciable increase in the total OTII cell number in the spleen of (OVA)-**3-1** immunized mice, implying that the injected conjugate is capable accessing DCs at sites distal from the site of immunization. Thus, we conclude that (OVA)-**3-1** can target DCs *in vivo* and that targeting leads to improved antigen-specific T cell activation relative to soluble antigen.

3.3.5 Co-injection of a TLR Agonist Does Not Significantly Increase the Efficiency of (OVA)-3-1 Targeting Relative to Soluble OVA

A number of studies have indicated that DC presentation of poorly immunogenic soluble proteins can be significantly augmented by the concomitant administration of an adjuvant or agent that can promote the release of pro-inflammatory cytokines such as TNF-α or IL-1β[17,18]. These cytokines aid in the recruitment and activation of monocytes and DCs at the site of administration, thereby promoting a heightened immune response. As our *in vitro* data indicated that TLR-4 signaling significantly attenuated (OVA)-**3-1** processing and presentation by DCs, we wished to extend this experiment to an *in vivo* setting to more accurately assess the physiological outcome. To do this, we employed the adoptive transfer system described above but prior to transferring the CD45.2 OTII T cells to the B6.Ly5.2/Cr recipients the cells were stained with 5-(6)-carboxyfluorescein diacetate succinimidyl ester (CFSE). This is a cell-permeable dye that freely crosses the cell membrane; once inside the cell, however, cellular esterases hydrolyze the dye's ester functional groups to generate a negatively charged molecule that cannot cross back across the cell membrane. This dye is used to monitor cell division by flow cytometry as each successive cell division leads to a dilution of CFSE among the daughter cells.

To administer pro-inflammatory stimuli at the same time as soluble antigen, OVA and (OVA)-**3-1** were emulsified in Complete Freund's Adjuvant (CFA) prior to immunization. CFA is an oil-based mixture of mycobacterial cell wall components that is known to induce strong T_H1 T cell responses[3]. 72 hours after immunization, cells from the draining lymph nodes were

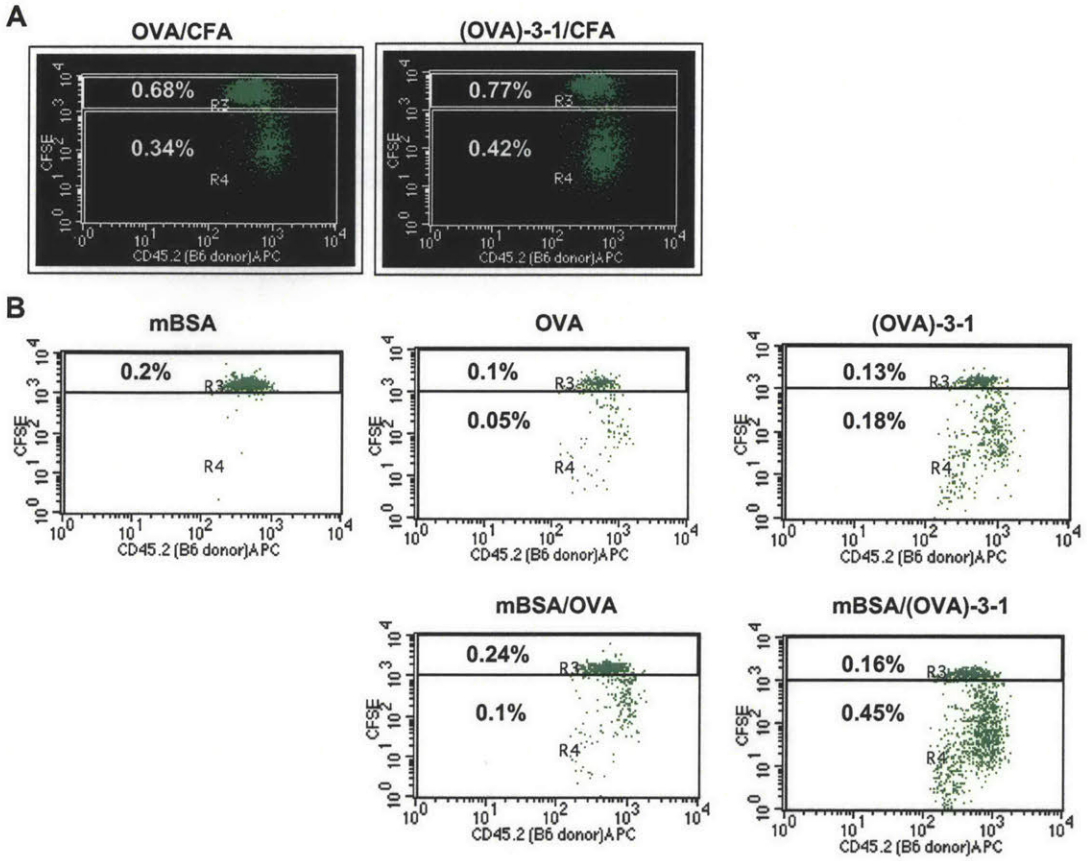

Figure 3.7 Inflammatory stimuli dampen the effects of DC targeting by (OVA)-**3-1** (A) 2 x 10^7 CFSE-labeled OTII splenocytes were adoptively transferred to B6.Ly5.2/Cr recipients and the mice were immunized subcutaneously with OVA (200 ng) or (OVA)-**3-1** (200 ng) emulsified in Complete Freund's Adjuvant. At 72 hours post immunization the draining inguinal lymph nodes were isolated and the expansion of $CD45.2^+V\alpha2^+$ was evaluated for CFSE dilution by flow cytometry. 4 x 10^5 total counts were collected. The plots display the CFSE intensity associated with the gated population of $V\alpha2^+CD45.2^+$ donor cells. The numbers indicate the percentage of CFSE high (undivided; R3 gate) and CFSE low (divided; R4 gate) OTII T cells (B) Enhancements in T cell proliferation promoted by neoglycoprotein mBSA. CFSE-labeled OTII splenocytes were adoptively transferred as in (A) and mice were immunized subcutaneously with mBSA (50 μg); OVA (50 ng); (OVA)-**3-1** (50 ng); OVA (50 ng) + mBSA (50 μg) or (OVA)-**3-1** (50 ng) + mBSA (50 μg). At 3 days the mice were sacrificed and isolated cells were analyzed as described in (A). Both (A) and (B) are results from one of two separate experiments.

isolated and analyzed by flow cytometry for cell number and divisions (Figure 3.7 A). While the total OTII cell number increased for (OVA)-**3-1** administered with CFA relative to (OVA)-**3-1** in PBS (Figures 3.6 B and 3.7 B), it did not lead to a corresponding increase in number relative to OVA/CFA. In fact, the enhancement previously observed relative to soluble OVA (Figure 3.6 B) was largely diminished. However, tracking CFSE dilution due to cell division indicates that

more OTII cells are actively dividing in mice that received (OVA)-**3-1**/CFA than those that received OVA/CFA, suggesting that DCs targeted by (OVA)-**3-1** are slightly more efficient at promoting antigen-specific T cell proliferation under these pro-inflammatory conditions. One potential reason for this could be that DCs targeted with (OVA)-**3-1** produce more peptide-MHC class II complexes than those targeted by OVA as receptor-mediated endocytosis delivers more antigen to the cell before full maturation is reached[11].

As the strong enhancements we observed with (OVA)-**3-1** *in vitro* (Figure 3.4 A) appeared to be substantially reduced *in vivo*, we speculated that other cells expressing a lectin capable of engaging high-mannose oligosaccharides could be competing with DCs for (OVA)-**3-1**. Of the mammalian lectins known to bind high-mannose oligosaccharides, langerin (CD207)[19] and the mannose receptor (CD206)[20] are appropriately anatomically positioned to bind and internalize injected (OVA)-**3-1**. Langerin is expressed in the Langerhans cells of the skin and has been demonstrated to mediate uptake of high-mannose bearing glycoproteins by these cells and cells transfected with cDNA encoding this receptor[21,22]. The mannose receptor is expressed in many different tissues and cell types, but most importantly for our application, its expression has been confirmed on the endothelial venules leading to draining lymph nodes and on endothelial cells of the skin[20].

To address the possibility that (OVA)-**3-1** was competitively endocytosed by langerin and/or the mannose receptor, antigen immunizations were performed with a large excess of soluble mannose in an attempt to competitively inhibit this activity. This treatment did not lead to an improvement of (OVA)-**3-1**-mediated targeting as judged by the level of T cell proliferation as described above (*not shown*). Since most lectins have weak affinities for monosaccharides, we repeated these experiments with BSA that had been modified with approximately 25 mannose residues per protein molecule (mBSA). Mannose-derivatized BSA was selected as it is a nanomolar ligand for the mannose receptor[23,24] and has also been shown to be bound by langerin in solid-phase binding studies[22]. Mice that had received CFSE-labeled OTII T cells were immunized with mBSA, OVA, (OVA)-**3-1**, OVA plus mBSA, and (OVA)-**3-1** plus mBSA and their T cell responses were analyzed at 72 hours (Figure 3.7 B). Consistent with our previous experiments, (OVA)-**3-1** led to a 2-fold increase in OTII T cell number compared to OVA. In addition, of these T cells, 58% had undergone cell division whereas only 33% of the T cells in OVA immunized mice had divided. As anticipated, T cells from mice that had been

immunized with mBSA did not proliferate as the appropriate antigenic peptides for OTII cells cannot be derived from BSA. Surprisingly, when OVA and (OVA)-**3-1** were injected along with mBSA, we observed an increase in OTII T cell numbers for both antigens. The T cell number increased 1.7-fold in mice receiving soluble OVA plus mBSA (mBSA/OVA, Figure 3.7 B, bottom row) over the cell number observed for OVA alone. Likewise, the number of OTII T cells increased 2-fold for mBSA/(OVA)-**3-1** injections compared to (OVA)-**3-1** alone. In addition to having an increased OTII cell numbers, both OVA and (OVA)-**3-1** had increased percentages of cells undergoing cell division: T cells from the OVA group increased from 33% to 42% while T cells from the (OVA)-**3-1** group increased from 55% to 74%.

It is not yet clear how the co-injection of mannose-derivatized BSA led to the enhancements of T cell proliferation observed for both administered antigens. One explanation could be the presence of bacterial endotoxin in the mBSA preparation that could serve to activate DCs at the site of injection and thereby increase antigen presentation as we observed with CFA (Figure 3.7 A). We tested each mBSA preparation used throughout these studies, however, and found them to have negligible quantities of endotoxin. Another possible explanation is that the injected mBSA blocked lectins that would normally bind OVA (which bears one *N*-linked glycan at Asn-392) in addition to (OVA)-**3-1**. This would enable both antigens to reach the draining lymph nodes where they would be endocytosed by DCs and presented to T cells. Since the addition of mBSA to *in vitro* antigen presentation assays did not significantly effect presentation of (OVA)-**3-1** or OVA to T cells (Figures 3.2 D and 3.4 B), with unfractionated OTII splenocytes or purified DCs and T cells, mBSA does not appear to directly activate DCs or T cells. Thus, it remains to be determined how mBSA contributes to enhanced presentation of OVA and (OVA)-**3-1** to T cells.

3.3.6 Oligosaccharide-Mediated Targeting of Steady State DCs Leads to a State of T Cell Unresponsiveness

At three days post-immunization, antibody-based targeting of the DEC-205 receptor lead to a 6.5-fold enhancement of T cell activation relative to non-targeted antigen[3]. After seven days, however, the activated T cell population diminished in number by 88% and the remaining T cells were unresponsive to systemic challenge of antigen in the highly stimulatory adjuvant

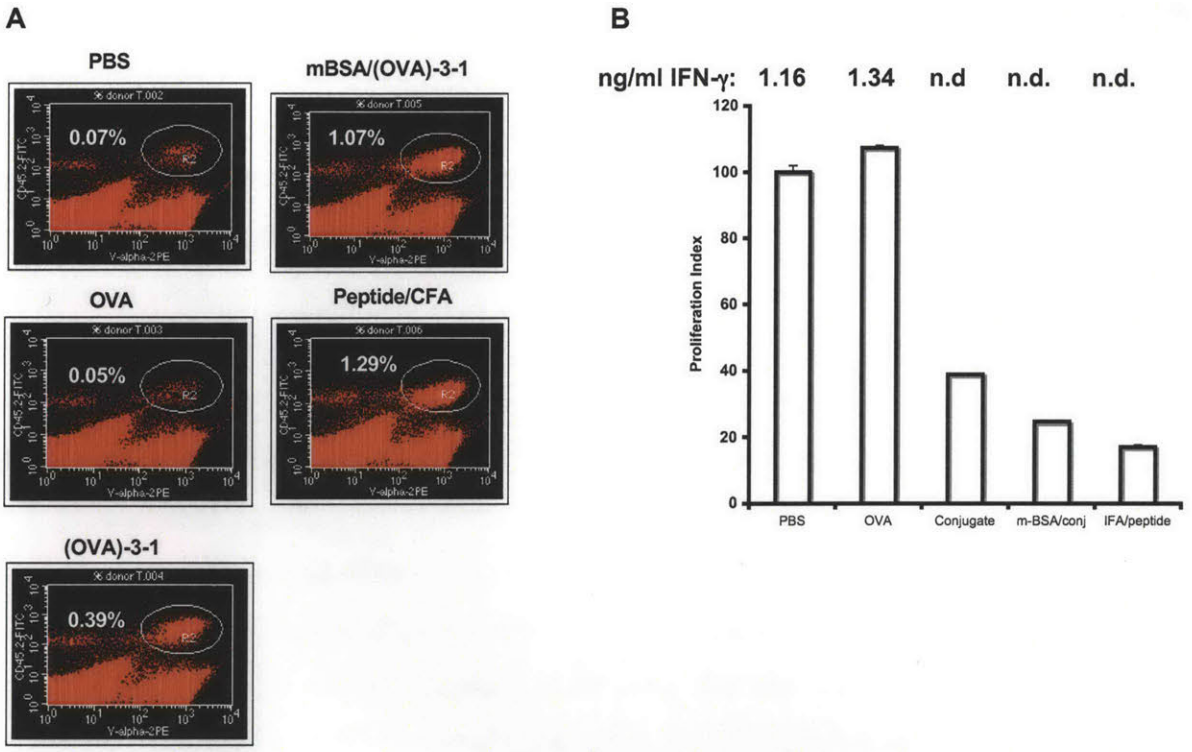

Figure 3.8 Oligosaccharide-mediated targeting of steady state DCs leads to T cell tolerance. (A) At day 10 (OVA)-**3-1** immunized mice have a much greater number of OTII T cells than OVA immunized mice. 2 x 10^7 OTII splenocytes were adoptively transferred into B6.Ly5.2/Cr recipients and then immunized by subcutaneous injection with PBS, OVA (200 ng), (OVA)-**3-1** (200 ng), (OVA)-**3-1** (200 ng) + mBSA (50 μg) or OVA peptide (100 μg) in Incomplete Freund's Adjuvant. At 8 days after these initial immunizations, mice received an antigenic rechallenge of OVA peptide (100 μg) in Complete Freund's Adjuvant. On day 10 mice were sacrificed and cells were isolated from the draining lymph node, total T cells were purified by negative selection and the number of OTII T cells were counted by FACS as in Figure 3.6. (B) Isolated T cells from (OVA)-**3-1** immunized mice are refractory to antigenic stimulation *in vitro*. Purified T cells from each experimental group were seeded at 3 x 10^5 cells/well with purified CD11c$^+$ DCs (9 x 10^4/well) and were incubated for 24 hours ± OVA peptide (100 μg mL^{-1}) with [^{3}H]thymidine (1μCi) added for the last 10 hours. Prior to [^{3}H]thymidine addition, an aliquot of supernatant was removed for IFN-γ determination by ELISA.

CFA. We observe a reproducible 2-fold enhancement of T cell activation with (OVA)-**3-1** immunization in saline and a 4-fold enhancement with mBSA/(OVA)-**3-1** immunization relative to OVA in saline. To more fully understand the immunological consequences of these enhancements, we administered OVA peptide (100 μg) in CFA at eight days post-antigen immunization and then T tested for the T cells' ability to respond to DC-presented peptide *in vitro* two days later (Figure 3.8)[3]. Among our immunization conditions we included a positive control for T cell tolerance, consisting of a high dose administration of OVA peptide (100 μg) in

Incomplete Freund's Adjuvant. This regimen has been shown in a number of different studies to lead to a state of T cell unresponsiveness upon antigen rechallenge[25,26].

At 2 days post-antigen rechallenge in CFA we observed a significant difference in the number of OTII cells in (OVA)-**3-1** relative to unmodified OVA (7.8-fold) and the saline control group (6-fold). Co-injection of mBSA with (OVA)-**3-1** (mBSA/(OVA)-**3-1**) lead to a 21-fold increase in OTII number compared to soluble OVA while the OTII number in the peptide/IFA control group was 26-fold greater than OVA.

When the T cells from each group were tested for their ability to respond to DC-presented peptide *in vitro*, we observed that OTII cells from the (OVA)-**3-1** and mBSA/(OVA)-**3-1** groups were significantly less responsive to antigen than cells from the PBS and OVA groups, as was the peptide/IFA control group (Figure 3.8 B). This was very surprising as the OVA-specific T cell numbers for the (OVA)-**3-1** and mBSA/(OVA)-**3-1** groups were so much higher than the OVA and PBS groups, indicating that the latter two groups were strongly activated by the peptide/CFA rechallenge while the (OVA)-**3-1** and mBSA/(OVA)-**3-1** (in addition to the peptide/IFA control) were refractory to antigenic stimulation. This lack of antigen responsiveness is further mirrored in the levels of IFN-γ produced by these cells during the 24 hours of peptide stimulation *in vitro* (Figure 3.8 B). While T cells from the PBS and OVA groups produced IFN-γ (and no IL-4) in response to peptide, indicating their T_H1 status, there was no detectable IFN-γ produced by the (OVA)-**3-1**, mBSA/(OVA)-**3-1**, or, as previously documented, the peptide/IFA groups. IL-4 was also not detected in these groups, indicating a lack of T cell polarization. Thus, from these data we can conclude that nonasaccharide **3-1**-mediated antigen delivery to DCs in the steady state leads to peripheral T cell unresponsiveness to subsequent antigenic rechallenge.

3.4 Discussion

The aims of the present study were to determine if low-molecular weight synthetic oligosaccharides conjugated to a whole protein antigen could be used to selectively enhance the presentation of that antigen by DCs to T cells; to determine if these oligosaccharide conjugates could access DCs *in vivo*; and to elucidate the immunological outcome of that targeting. Based on our glycan microarray analysis of the DC lectin DC-SIGN (Chapter 2, section 2.4.6.6), we

chose a panel of synthetic analogs of the high-mannose oligosaccharide $(Man)_9(GlcNAc)_2$ with which to prepare carbohydrate-OVA conjugates for targeting murine DCs. Here we have shown that these synthetic oligosaccharides can target $CD11c^+CD8\alpha^+$ and $CD11c^+CD8\alpha^-$ DCs, deliver their appended antigen to the requisite antigen processing pathways for presentation on MHC class I and class II molecules, and lead to enhanced activation of OVA-specific T cells. *In vivo*, a conjugate comprising (OVA)-**3-1** targets DCs and increases the efficiency of presentation by 2-fold compared to unmodified OVA. The simultaneous co-injection of a highly mannosylated neoglycoprotein, mBSA, further enhances DC targeting by (OVA)-**3-1**, leading to a 4-fold enhancement of T cell proliferation relative to OVA. Finally, we have shown that the immunological outcome of oligosaccharide-mediated targeting of antigen to DCs in the steady state promotes antigen-specific T cell tolerance, or unresponsiveness, demonstrated by the fact that T cells obtained from (OVA)-**3-1** immunized mice are refractory to restimulation with peptide *in vitro* and do not appear to produce T_H1 or T_H2 cytokines.

In order to elucidate the mechanistic basis for the induction of T cell tolerance via nonasaccharide **3-1**-mediated targeting, future work in this area should aim to characterize the T cell phenotype resulting from this targeting approach. As we do not see appreciable T cell deletion induced by (OVA)-**3-1** targeting of DCs *in vivo* (Figure 3.8 A), the expanded T cell population may represent T regulatory cells induced by steady state DCs. To address this possibility, OTII T cells should be isolated from (OVA)-**3-1** immunized mice (in parallel with PBS, OVA and peptide/IFA immunizations) and assayed for foxp3 expression by intracellular staining or PCR. (Foxp3 is an inhibitor of transcription that serves as a specific molecular signature of T regulatory cells)[27]. In addition, T cells should be tested at the functional level for their ability to suppress the proliferation of naive $CD4^+$ T cells incubated with OVA-presenting DCs. While analyzing these cells for their status as canonical $CD4^+CD25^+foxp3^+$ Tregs, their capacity to produce IL-10 and TGF-β should also be assessed, as these are functional markers for another class of suppressive T cells referred to as T_R1 cells[28]. Finally, this targeting method and the antibody-based DEC-205 targeting method should be directly compared to determine how well the nonasaccharide **3-1** compares to anti-DEC-205 antibody and to determine if both methods elicit the same T cell phenotype.

Throughout the course of this work many attempts were made to identify the receptor mediating uptake of the oligosaccharides employed here. The murine DC-SIGN homolog

CIRE[10] was analyzed as a potential receptor; a cell line stably expressing this lectin was used to assay for binding and internalization of fluorophore-labeled **3-1** and fluorophore-labeled (OVA)-**3-1**. These experiments did not reveal any interactions between the high-mannose oligosaccharide and CIRE. Subsequent flow cytometry analysis of splenic DCs with anti-CIRE antibody revealed that CIRE expression was extremely low on $CD11c^+$ DCs, making this an unlikely candidate. Attempts to identify the receptor biochemically by cross-linking it to bound (OVA)-**3-1** and immunoprecipitating the complex with polyclonal sera raised against ovalbumin have also proved unsuccessful.

If follow-up experiments to this work reveal that the observed T cell tolerance is due to Treg formation, a dedicated effort should be made to determine the nature of the receptor on DCs that is targeted by the high-mannose structures used here. Identification of the receptor would enable the determination of its human homolog. Knowing this, one could study the receptor's expression in human DCs and tissues and assess the possibility of targeting the receptor with carbohydrate-modified antigens, such as allergens, in an effort to promote T cell tolerance.

While the notion of targeting carbohydrate modified antigens to cells of the immune system via their cell surface lectins is not new, all prior work in this area was restricted to the *in vitro* evaluation of one receptor, the macrophage mannose receptor, expressed on human monocyte-derived DCs and macrophages. In addition to being restricted to non-physiological *in vitro* measurements, these studies all employed simple monosaccharide-antigen conjugates. Here we have revisited the idea of carbohydrate-mediated targeting of antigens with the aims of employing more complex oligosaccharide structures and extending this targeting approach to an *in vivo* setting. In doing so, we have uncovered a receptor on DCs that preferentially engages complex, branched oligosaccharides over simple monosaccharides and that can be targeted *in vivo* to effect T cell function. Accordingly, the carbohydrate-based targeting approach described here seems to hold promise as an alternative to antibody-based targeting of lectins or other surface receptors.

We feel that this work has laid the foundation for a more in-depth investigation of lectin-based targeting of DCs with the goal of providing a means to rationally modulate immune cell behavior. Improving targeting to these receptors will require a detailed understanding of their ligand binding requirements as well as new tools, such as the carbohydrate microarrays described here (Chapter 2), to evaluate the specificity and affinity of interactions between C-type lectins

and synthetic ligands. Thus, the exploration of cell-surface lectins of the immune system presents an exciting opportunity for synthetic carbohydrate chemists and immunologists to work together in the design, synthesis, and evaluation of unique glycoconjugates as potential therapeutics.

3.5 Materials and Methods

3.5.1 Mice

6-12 week old females were used in all experiments and were maintained under specific pathogen free conditions. C57BL/6 were purchased from Taconic and B6.Ly5.2/Cr were purchased from NCI-Frederick. OTI and OTII mice were bred in an in-house facility; OTI mice were genotyped by analyzing expression of $V\alpha_2V\beta_{5.1/5.2}$ by FACS.

3.5.2 Antibodies

Antibodies to CD45.2 (104) and all other surface markers (Vα2/B20.1, CD8α/53-6.7, I-A^b/AF6-120.1) were purchased from BD Biosciences, as was streptavidin-APC. Rabbit anti-ovalbumin was purchased from Research Diagnostics.

3.5.3 Reagents

Mannose, invertase, mannan, and mannose-BSA, BSA, and ovalbumin were all purchased from Sigma Chemical. 3-fucosyllactose, Lewis-^{x} and Lewis-^{x}-BSA were purchased from Dextra Laboratories.

3.5.4 Carbohydrate Modification of Ovalbumin

1.9 mg sulfosuccinimidyl 4-[maleimidomethyl]-cyclohexane-1-carboxylate (Sulfo-SMCC, Pierce Endogen) was dissolved in 88 μL dimethylformamide (DMF) and added to 5 mg ovalbumin (OVA) in 315 μL PBS. The reaction solution was mixed for 1 hr at room temperature. Maleimide-activated OVA was purified from nonreacted Sulfo-SMCC by gel

filtration on a NAP-25 desalting column (Amersham) preequilibrated in PBS. The OVA fractions were collected and mixed with thiol-containing oligosaccharides (0.6 μmoles/per structure) that had been previously reduced with 1 equivalent tris-(carboxyethyl)phosphine hydrochloride (TCEP). This reaction proceeded for 12 hr at room temperature with constant mixing. Modified OVA was purified from excess oligosaccharide by multiple rounds of centrifugal ultrafiltration with Vivaspin 10,000 MW cut-off cartridges (Vivascience). Purified protein was lyophilized and stored at -20^0 until use.

3.5.5 Cell Culture and Proliferation Assays

Pooled inguinal lymph nodes were dissociated in 10% Fetal Bovine Serum RPMI (supplemented with 2 mM L-glutamine) and either mechanically dissociated between two glass slides or, to improve the overall cell yield, incubated in the presence of collagenase (Boehringer) and EDTA for 25 min at 37°C/5% CO_2 to dissociate DC-T cell clusters. For antigen presentation assays with whole splenocytes, isolated spleens were injected with collagenase/EDTA, gently teased apart and incubated as described above. Splenocytes were cultured in 96-well round-bottom plates at a density of 3 x 10^5 cells/0.2 mL. In antigen presentation assays utilizing purified DCs and T cells, DCs were isolated from the spleens of C57BL/6 mice following collagenase/EDTA treatment by labeling the DCs with Miltenyi anti-CD11c$^+$ microbeads (according to the Miltenyi Biotec protocol) and separating labeled DCs from non-DCs by application of a magnetic field. Similarly, purified CD4$^+$ T cells were obtained from spleens of OTII transgenic mice using Dynal anti-CD4 magnetic beads. Purified DCs and T cells were seeded onto 96-well plates round-bottom plates at a 1:2 DC:T cell ratio unless stated otherwise in the Figures.

For T cell proliferation assays in adoptive transfer experiments, inguinal lymph nodes from each experimental group (3 mice/group) were pooled and dissociated with collagenase/EDTA as described above. In order to ensure that the CD4$^+$ T cells were not activated during the isolation procedure, we purified the cells by negative selection using a biotinylated antibody cocktail against CD8α, CD11b, CD45R, DX5, and Ter-119 followed by magnetic anti-biotin microbeads. Labeled cells were separated from CD4$^+$ T cells by application of a magnetic field. Purified T cells (3 x 10^5/well) were seeded into 96-well round-bottom plates

with purified $CD11c^+$ DCs (9 x 10^4/well). Synthetic OTII OVA peptide [KISQAVHAAHAEINEAG] was added to half of the cultures at a final concentration of 100 μg mL^{-1}. Cultures were maintained for 24 hours with [^{3}H]thymidine (1μCi) added for the last 10 hours. Response to OVA peptide was determined by subtracting background proliferation (no peptide) from specific, peptide-induced proliferation. The total antigen-specific (i.e., background subtracted) counts were divided by the number of OTII cells per well (obtained by flow cytometry, Figure 3.8 A) to determine the radioactive counts per cell. The proliferation index was calculated as the ratio of the response to OVA peptide in an experimental group to the response to OVA peptide in the PBS group.

3.5.6 Cell Sorting

To obtain sufficient numbers of DCs for antigen presentation and cytokine analysis, we injected C57BL/6 mice with a Flt3-ligand secreting tumor cell line to promote the expansion of DCs. 14 days after administration mice were sacrificed and the spleens were isolated. DCs were purified from the spleens by positive selection with anti-CD11c microbeads as described above and stained with FITC-conjugated anti-I-A^b and Cychrome-conjugated anti-CD8α. Cells were then sorted on a MoFlo fluorescence-activated cell sorter (Dakocytomaton) into $CD8\alpha^+$I-A^{b+} and $CD8\alpha^-$I-A^{b+} populations. The purity of each subset was 80% with approximately 6% cross-contamination. DCs from each subset were used in antigen proliferation assays as described above (section 3.5.5).

3.5.7 Adoptive Transfer and CFSE Labeling

Spleens from OTII mice were mechanically dissociated, filtered, washed 2x in PBS and then resuspended at 1 x 10^8 cells mL^{-1} in PBS. Cells were transferred to B6.Ly5.2/Cr mice by retro-orbital intravenous injection (200 μL/mouse). Alternatively, the cells were resuspended in RPMI (no FBS) at 5 x 10^7 cells mL^{-1} after being filtered and incubated with an equal volume of 30 μM CFSE in PBS to obtain a final CFSE concentration of 15 μM. Cells were incubated in a 37°C water-bath for 10 minutes and then washed 1x with 10% FBS/RPMI and 2x with PBS. CFSE-labeled cells were diluted to 1 x 10^8 cells mL^{-1} in PBS and injected into B6.Ly5.2/Cr.

3.5.8 Cytokine ELISAs

75-150 μL aliquots of supernatant were sampled from antigen presentation assays at 24, 48, and 72 hours. 75 μL aliquots were removed from the antigen rechallenge assays at 14 hours, prior to the addition of [^{3}H]thymidine. 25 μL of each supernatant were diluted 1:1 with PBS/1% BSA and analyzed in triplicate for IFN-γ, IL-10, and IL-4 using DuoSet ELISA reagents from R&D Systems. The lower limit of cytokine detection in these ELISAs was approximately 0.3 ng mL^{-1}.

3.6 References Cited

(1) Steinman, R. M., Hawiger, D., Nussenzweig, M.C. *Annu Rev Immunol.* **2003**, *21*, 685-711.

(2) Wang, H.; Griffiths, M. N.; Burton, D. R.; Ghazal, P. *Proc Natl Acad Sci U S A* **2000**, *97*, 847-852.

(3) Hawiger, D.; Inaba, K.; Dorsett, Y.; Guo, M.; Mahnke, K.; Rivera, M.; Ravetch, J. V.; Steinman, R. M.; Nussenzweig, M. C. *J Exp Med* **2001**, *194*, 769-779.

(4) Bonifaz, L.; Bonnyay, D.; Mahnke, K.; Rivera, M.; Nussenzweig, M. C.; Steinman, R. M. *J Exp Med* **2002**, *196*, 1627-1638.

(5) Mahnke, K., Qian, Y., Knop, J., Enk, A. *Blood* **2003**, *101*, 4862-4869.

(6) Haase, W. C., Seeberger, P.H. *Chemical Reviews* **2000**, *100*, 4349-4394.

(7) Ratner, D. M.; Adams, E. W.; Disney, M. D.; Seeberger, P. H. *Chembiochem* **2004**, *5*, 1375-1383.

(8) Appelmelk, B. J.; van Die, I.; van Vliet, S. J.; Vandenbroucke-Grauls, C. M.; Geijtenbeek, T. B.; van Kooyk, Y. *J Immunol* **2003**, *170*, 1635-1639.

(9) Park, C. G.; Takahara, K.; Umemoto, E.; Yashima, Y.; Matsubara, K.; Matsuda, Y.; Clausen, B. E.; Inaba, K.; Steinman, R. M. *Int Immunol* **2001**, *13*, 1283-1290.

(10) Caminschi, I., Lucas, K., O'Keefe, M., Hochrein, H., Laabi, Y., Brodnicki, T.C., Lew, A., Shortman, K., Wright, M *Molecular Immunology* **2001**, *38*, 365-373.

(11) Sallusto, F.; Cella, M.; Danieli, C.; Lanzavecchia, A. *J Exp Med* **1995**, *182*, 389-400.

(12) Kopp, E.; Medzhitov, R. *Curr Opin Immunol* **2003**, *15*, 396-401.

(13) Heath, W. R.; Belz, G. T.; Behrens, G. M.; Smith, C. M.; Forehan, S. P.; Parish, I. A.; Davey, G. M.; Wilson, N. S.; Carbone, F. R.; Villadangos, J. A. *Immunol Rev* **2004**, *199*, 9-26.

(14) Maldonado-Lopez, R.; Moser, M. *Semin Immunol* **2001**, *13*, 275-282.

(15) Inaba, K.; Pack, M.; Inaba, M.; Sakuta, H.; Isdell, F.; Steinman, R. M. *J Exp Med* **1997**, *186*, 665-672.

(16) Kearney, E. R.; Pape, K. A.; Loh, D. Y.; Jenkins, M. K. *Immunity* **1994**, *1*, 327-339.

(17) Pulendran, B.; Smith, J. L.; Jenkins, M.; Schoenborn, M.; Maraskovsky, E.; Maliszewski, C. R. *J Exp Med* **1998**, *188*, 2075-2082.

(18) Reis e Sousa, C.; Hieny, S.; Scharton-Kersten, T.; Jankovic, D.; Charest, H.; Germain, R. N.; Sher, A. *J Exp Med* **1997**, *186*, 1819-1829.

(19) Takahara, K.; Omatsu, Y.; Yashima, Y.; Maeda, Y.; Tanaka, S.; Iyoda, T.; Clausen, B. E.; Matsubara, K.; Letterio, J.; Steinman, R. M.; Matsuda, Y.; Inaba, K. *Int Immunol* **2002**, *14*, 433-444.

(20) Takahashi, K.; Donovan, M. J.; Rogers, R. A.; Ezekowitz, R. A. *Cell Tissue Res* **1998**, *292*, 311-323.

(21) Galustian, C.; Park, C. G.; Chai, W.; Kiso, M.; Bruening, S. A.; Kang, Y. S.; Steinman, R. M.; Feizi, T. *Int Immunol* **2004**, *16*, 853-866.

(22) Stambach, N. S.; Taylor, M. E. *Glycobiology* **2003**, *13*, 401-410.

(23) Taylor, M. E. *Biochem Soc Trans* **1993**, *21*, 468-473.

(24) Taylor, M. E.; Drickamer, K. *J Biol Chem* **1993**, *268*, 399-404.

(25) Aichele, P.; Brduscha-Riem, K.; Zinkernagel, R. M.; Hengartner, H.; Pircher, H. *J Exp Med* **1995**, *182*, 261-266.

(26) Perez, V. L.; Van Parijs, L.; Biuckians, A.; Zheng, X. X.; Strom, T. B.; Abbas, A. K. *Immunity* **1997**, *6*, 411-417.
(27) Fehervari, Z.; Sakaguchi, S. *Int Immunol* **2004**, *16*, 1769-1780.
(28) Groux, H.; O'Garra, A.; Bigler, M.; Rouleau, M.; Antonenko, S.; de Vries, J. E.; Roncarolo, M. G. *Nature* **1997**, *389*, 737-742.

Eddie W. Adams

Education:

Ph.D. Biological Chemistry	•January, 2005
Massachusetts Institute of Technology	•Thesis Advisor: Prof. Peter H. Seeberger
B.S., Biotechnology	•June, 1995
Rochester Institute of Technology	•Research Advisor: Prof. John P. Neenan

Professional Experience:

Quantum Dot Corporation •1999-2001
Research Scientist
Area of Specialization: Colloid Chemistry

Binax, Incorporated •1997-1999
Research Scientist
Area of Specialization: Immunoassay Development

Publications:

Ratner, D.M.; Adams, E.W.; Disney, M.D.; Seeberger, P.H. Tools for Glycomics: Mapping Interactions of Carbohydrates in Biological Systems. *ChemBioChem*, **2004**, *5*, 1375-1383

Adams, E.W.; Ratner, D.M.; Bokesh, H.R.; McMahon, J.B.; O'Keefe, B.R.; Seeberger, P.H. Oligosaccharide and Glycoprotein Microarrays as Tools in HIV-Glycobiology: A Detailed Analysis of Glycan-Dependent gp120/Protein Interactions. *Chem. Biol.*, **2004**, *11*, 875-881

Ratner, D.M.; Adams, E.W.; Su, J; O'Keefe, B.R.; Mrksich, M.; Seeberger, P.H. Probing Protein-Carbohydrate Interactions with Microarrays of Synthetic Oligosaccharides. *ChemBioChem*, **2004**, *5*, 379-382

Adams, E.W.; Ueberfeld, J; Ratner, D.M.; O'Keefe, B.R.; Walt, D.R.; Seeberger, P.H. Encoded Fiber-Optic Microsphere Arrays for Probing Protein-Carbohydrate Interactions. *Angew. Chem. Int. Ed.* **2003**, *42*, 5317-5320

Patents:

• Adams, E.W.; Bruchez, M.P. Patent # 6,649,138: Surface-Modified Semiconductive and Metallic Nanoparticles Having Enhanced Dispersibility in Aqueous Media, (November 18, 2003)

• Seeberger, P.H.; Ratner, D.M.; Adams, E.W. U.S. Provisional Application No. 10/9950, 701: Microarrays and Microspheres Comprising Oligosaccharides, Complex Carbohydrates, or Glycoproteins, (Filed September 2004)

• Hacohen, N; Adams, E.W.; Seeberger, P.H. Provisional Patent Application: Antigen-Carbohydrate Conjugates, (Filed July 2004)

Teaching Experience:

• MIT, TA, Principles of Chemical Science, Fall 2001

Honors:

• American Society for Engineering Education, NDSEG Graduate Fellowship, 2001-2004